A STUDY OF GAS SOLUBILITIES AND TRANSPORT PROPERTIES IN FUEL CELL ELECTROLYTES

Research Grant NGL 10-005-022

Tenth Semi-Annual Report

Period Covered: March 1, 1970 - August 31, 1970

ENGINEERING AND INDUSTRIAL EXPERIMENT STATION

College of Engineering

University of Florida

Gainesville

A STUDY OF GAS SOLUBILITIES AND TRANSPORT PROPERTIES IN FUEL CELL ELECTROLYTES

Research Grant NGL 10-005-022

Tenth Semi-Annual Report

Period Covered: March 1, 1970 - August 31, 1970

Prepared for

National Aeronautics and Space Administration
Washington, D. C.

October 30, 1970

R. D. Walker, Jr.

ENGINEERING AND INDUSTRIAL EXPERIMENT STATION

College of Engineering
University of Florida
Gainesville, Florida

Table of Contents

List of Tables

List of Figures

Symbols

C = concentration of reacting species, millimoles/liter

C_s = molarity of salt

D = diffusion coefficients, cm^2/sec

e_1 = partial molecular internal energy of solute

f = fugacity

f^o = fugacity in standard state

g_{ij} = radial distribution function for i-j pairs

h = Planck constant

$\bar{H}_1$ = partial molal enthalpy of solute

i_t = net diffusion current, μA

k = Boltzmann constant

k_s = salting coefficient

K_1^o = Henry constant of gas in pure water

m = mass flow rate of mercury, mg/sec

m_i = molecular mass of species i

$\tilde{n}$ = number of electrons involved in the reaction

N_i = number density (molecules/cc)

P = pressure

P^o = vapor pressure

P_c = critical pressure

R = gas constant

R_i = reduced diameter of i

$\bar{S}_1$ = partial molecular entropy of solute

S^E = excess entropy

t = drop time of the mercury electrodes, sec.

T = temperature

T_c = critical temperature

$\bar{v}_1$ = partial molecular volume of solute

$\bar{V}_1$ = partial molal volume of solute

$\bar{V}_s$ = partial molal volume of salt in solution

V_s = liquid molar volume of salt

x = mole fraction of electrolyte

x_1 = mole fraction of gas in electrolyte solution

x_1^o = mole fraction of gas in pure water

Z = total number of electrons in ion

α_1 = polarizability of solute molecule

β = compressibility of solution

β_o = compressibility of pure water

γ = activity coefficient

ϵ = energy parameter in Lennard-Jones potential

μ = viscosity

μ_1 = chemical potential of solute

μ_1^o = chemical potential of solute in standard state

μ_2 = dipole moment of water molecule

ν_i = valency of species i

ρ_1 = number of 1-molecules per unit volume

σ_i = core diameter of particle of type i

ϕ_{ij} = pair potential energy between particles i and j

ω = Pitzer acentric factor

$\Lambda_1 = \left(\frac{h^2}{2\pi m\ kT}\right)^{1/2}$

ζ = reduced number density

1.0 INTRODUCTION

Theoretical studies of the solubility of gases in electrolytes, based on the Percus-Yevick theory, have been made, following the extensive experimental studies of the solubilities of these systems. The theory predicts accurately the solubility and activity coefficients for both the salting-in and the salting-out systems.

Several problems were solved in the measurement of partial molal volume of gases in electrolytes. Results for a few measurements are reported in the pertinent section. Improvements on the theory for partial-molal volume were made, and comparison with experimental data shows favorable results.

Diffusion coefficients of oxygen in lithium hydroxide were measured using the dropping mercury electrode method for temperatures up to 60°C. Measurement at higher temperatures presented severe problems. In the case of the theoretical studies, a hard sphere kinetic theory has been developed. This theory gives fair prediction on the diffusion coefficients of gases in electrolytes.

An extensive literature survey was made on the physical properties of the ternary system K_2CO_3 - KOH - H_2O. Even though the volume of work on such properties as solid-liquid equilibrium, electrical conductivity, solubility and absorption of CO_2 in this system is significantly large, relatively little work has been done on the liquid-vapor equilibrium. To remedy this situation, experimental measurements of the vapor pressure using the isopiestic method were performed. The feasibility of using an empirical mixing rule was also investigated.

2.0 DIFFUSION OF OXYGEN IN LITHIUM HYDROXIDE SOLUTION

Measurements have been made, using the polarographic method, on the diffusion coefficients of oxygen in lithium hydroxide solution over the lithium hydroxide concentration range of 0.0 wt % to saturation, and temperatures from 25°C to 60°C.

2.1 Material

Lithium hydroxide pellets with purity of 95.5% were used. Degassed distilled water prepared by distilling deionized water was used in preparing solutions. 0.1 N HCl solution was prepared from ampule of Acculate standard solutions.

Mercury used was of the dry, triple distilled grade.

2.2 Experimental

The polarographic method (1) consists of determining the current-voltage curve of electro-oxidizable or electro-reducible substances as they are electrolysed in a cell having an electrode consisting of mercury falling dropwise from a capillary tube.

In the present case, two plateaux were formed in such a current-voltage curve. The first one corresponding to the reduction of oxygen to hydrogen peroxide, which was further reduced to water in the second plateau. Only the first plateau current density was used for calculating the diffusion coefficient, because of the variation of drop time with voltage in the region of the second plateau.

2.2.1 Procedure

A Sargent S-29381 Electrolysis Cell, equipped with provision to bubble gas through the solution and also introducing a stream of gas above the solution, was used in the experiment. The cell was filled with lithium

hydroxide solution and submerged in a water bath, controlled to within ± 0.5°C. Oxygen, presaturated with water vapor was bubbled through the solution for 45 minutes. After this period, a stream of oxygen was passed through the gas phase above the solution to prevent the loss of oxygen from the solution. A clean dropping mercury electrode was then introduced into the solution. With the mercury dropping at a constant rate, the polarograph was turned on, and the resulting current-voltage curve recorded. The current corresponding to the maximum of the first plateau was used (after deduction of residual current) in the modified Ikovic equation, Equation (2-1) to calculate the diffusion coefficient.

$$i_t = 709\ \tilde{n}\ D^{1/2}\ C\ m^{2/3}\ t^{1/6} \left[1 + \frac{39\ D^{1/2}\ t^{1/6}}{m^{1/3}} \right] \qquad (2\text{-}1)$$

where i_t = net diffusion current in μA

$\tilde{n}$ = number of electrons involved in the reaction

D = diffusion coefficient, cm^2/sec

C = concentration of reacting species, millimole/liter

m = mass flow rate of mercury, mg/sec

t = drop time of the mercury electrode, sec

2.2.2 Measurement of Drop Time and Mass Flow-Rate of Mercury

In order to calculate D from the above equation we need to measure 'm' and 't'. These factors are functions of height of the mercury column, dimensions of the capillary, viscosity of solution and the applied voltage. Hence, 'm' and 't' were measured for each experiment under the same conditions as with measurement of diffusion current. The voltage used was kept at - 0.4 volt, which corresponds to the middle of the first

plateau. The time for twenty drops of mercury dropping into a small dipper was measured. The mercury collected was cleaned, dried and weighed, from which the factors 'm' and 't' were calculated. Irregular fluctuations in the current-voltage curves were observed at high temperatures. To stabilize this effect, the drop rate was increased at these temperatures. This instability was postulated to be due to the suction of solution into the capillary when the mercury retracts before a new drop begins to form. This suction effect will also dirty the electrode after being used for a length of time. Therefore, it is necessary to clean the capillary with 1:1 nitric acid, and rinse with distilled water before starting the experiment.

2.2.3 Measurement of Residual Current

The current measured in a polarogram consisted of the diffusion current and the residual current, which is the result of electrolytic conductivity. To measure the residual current, the solution in the electrolysis cell was stripped with nitrogen gas for 30 minutes, and the polarograph started as in the actual measurement. The residual current was taken as that corresponding to the maximum of the current-voltage curve at - 0.4 volt.

2.3 Results and Discussion

The measured diffusion coefficients of oxygen in lithium hydroxide solution are tabulated in Table 2-1 and also plotted in Figure 2-1.

Each point is the arithmetic mean of three repetitions. The experimental accuracy is estimated as $\pm$ 10%, $\pm$ 12% and $\pm$ 15% at 25°, 40° and 60°C respectively.

The diffusion coefficients of oxygen in water obtained by

Table 2-1

Diffusion Coefficients of Oxygen in Lithium Hydroxide Solutions

Values are reported as D x 10^5, cm^2/sec

Wt % LiOH	Temperature		
	25°C	40°C	60°C
2.0	1.75	2.91	
3.7			3.75
4.0	1.46	2.35	
5.8			3.24
6.0	1.16	1.93	
7.3			2.78
7.8	0.99	1.59	
10.4			1.99
10.7	0.74	1.19	

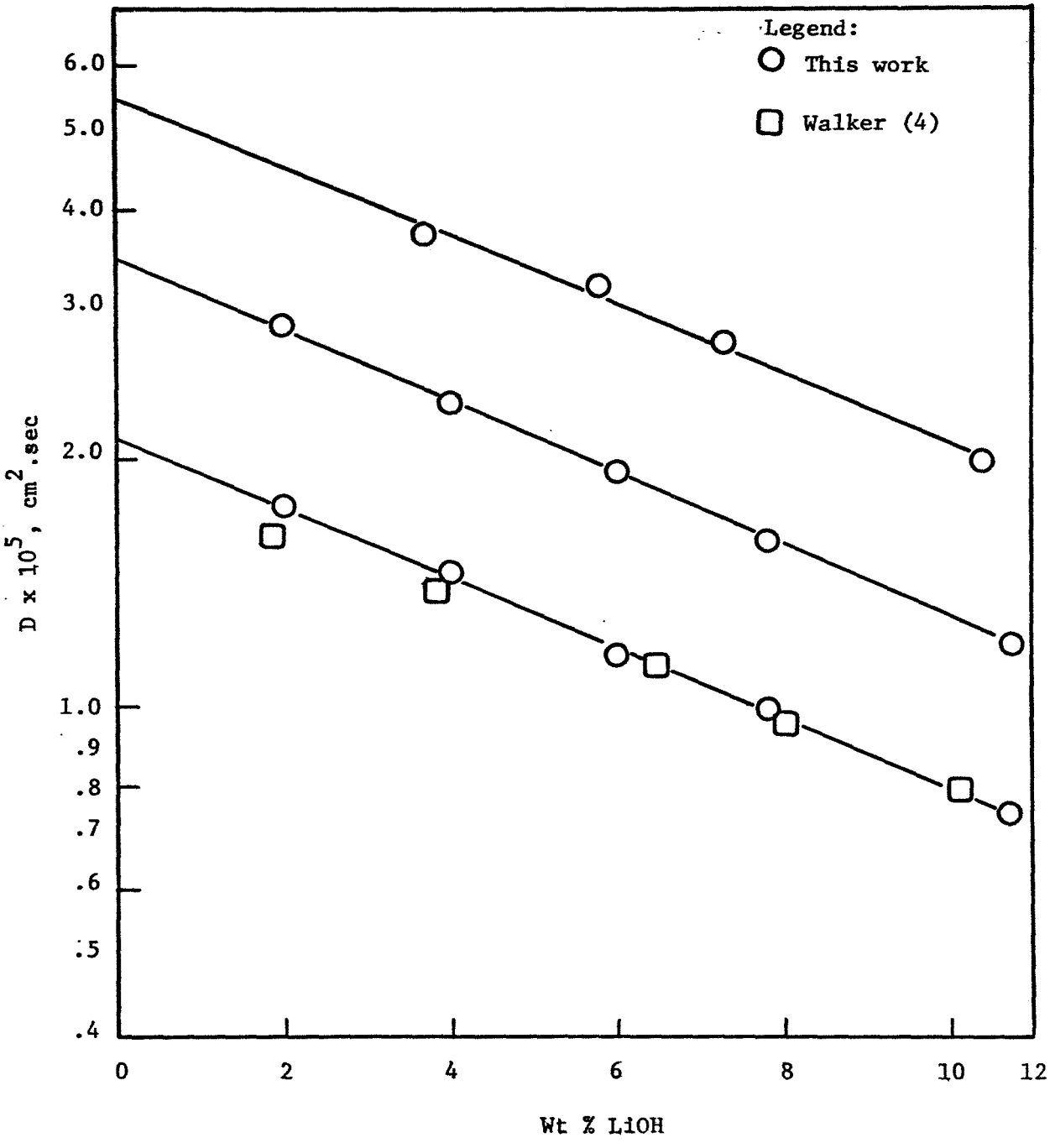

Figure 2-1. Diffusion Coefficients of Oxygen in LiOH Solutions

extrapolation were found to be 2.13×10^{-5}, 3.5×10^{-5} and 5.5×10^{-5} cm^2/sec at 25°, 40° and 60°C respectively. These data are in fairly good agreement with those of other workers, as can be seen from Table 2-2.

The modified Eyring theory prepared by Ratcliff and Holdcroft (2) predicts a linear relation between $\ell n\ D/D_o$ and $x/(1 - x + (\nu_1 + \nu_2)\ x)$. Figures 2-2, 2-3, 2-4 show plots of $\ell n\ D/D_o$ vs $x/(1 - x + (\nu_1 + \nu_2)\ x)$ for O_2 in LiOH solution at 25°, 40° and 60°C respectively. It can be seen that linearity was observed in all three cases.

The modified Eyring theory also predicts that, the product $D\mu/T$ is a constant for a particular concentration. It is shown in Table 2-3 that, within experimental error, the results satisfied this prediction.

In Figure 2-5, $\ell n\ D/T$ is plotted against $1/T$. Within experimental error these plots are linear. It should also be noted that slopes of these plots are nearly the same for each concentration, showing that the free energy of activation for oxygen in LiOH is nearly independent of concentration.

2.4 Comparison Between the Diffusion Coefficients of Oxygen in Lithium Hydroxide and Potassium Hydroxide Solutions.

In Figure 2-6, the diffusion coefficients of oxygen in lithium hydroxide are compared with those reported for KOH. The diffusion coefficients in LiOH are generally higher than those in KOH. On the other hand, the diffusion coefficients at infinite dilution for both electrolytes should be the same. In order to make a fair comparison between the two, we shifted the curves for one system (in this case we shifted the LiOH curves) parallelly until they coincided at zero electrolyte concentration with those of KOH. As can be seen from Figure 2-6, the diffusion coefficients

Table 2-2

Diffusion Coefficients of Oxygen in Water

Temperature, °C	D x 10^5, cm^2/sec	Reference
1.0	1.23	44
10	1.7	45
	1.82	44
15	1.51	46
	1.67	47
	1.78	46
	2.21	48
16	1.87	49
17.5	2.45	44
18.2	1.99	50
20	1.76	46
	2.01	47
	2.22	46
	2.3	45
21.7	1.87	49
22	2.22	51
	2.25	52
25	1.87	53
	1.90	54
	1.90	4
	1.95	3
	2.0	2
	2.03	46
	2.07	55
	2.12	56
	2.13	This work
	2.19	57
	2.25	56
	2.41	59
	2.42	47
	2.55	46
	2.60	60

Table 2-2 (continued)

Temperature, °C	D x 10^5, cm^2/sec	Reference
30	2.8	45
37	3.0	61
40	3.0	2
	3.5	This work
	3.8	45
45	4.87	57
50	4.2	45
60	4.6	2
	4.7	3
	5.5	This work
	5.7	45
65	4.87	57
80	6.5	2

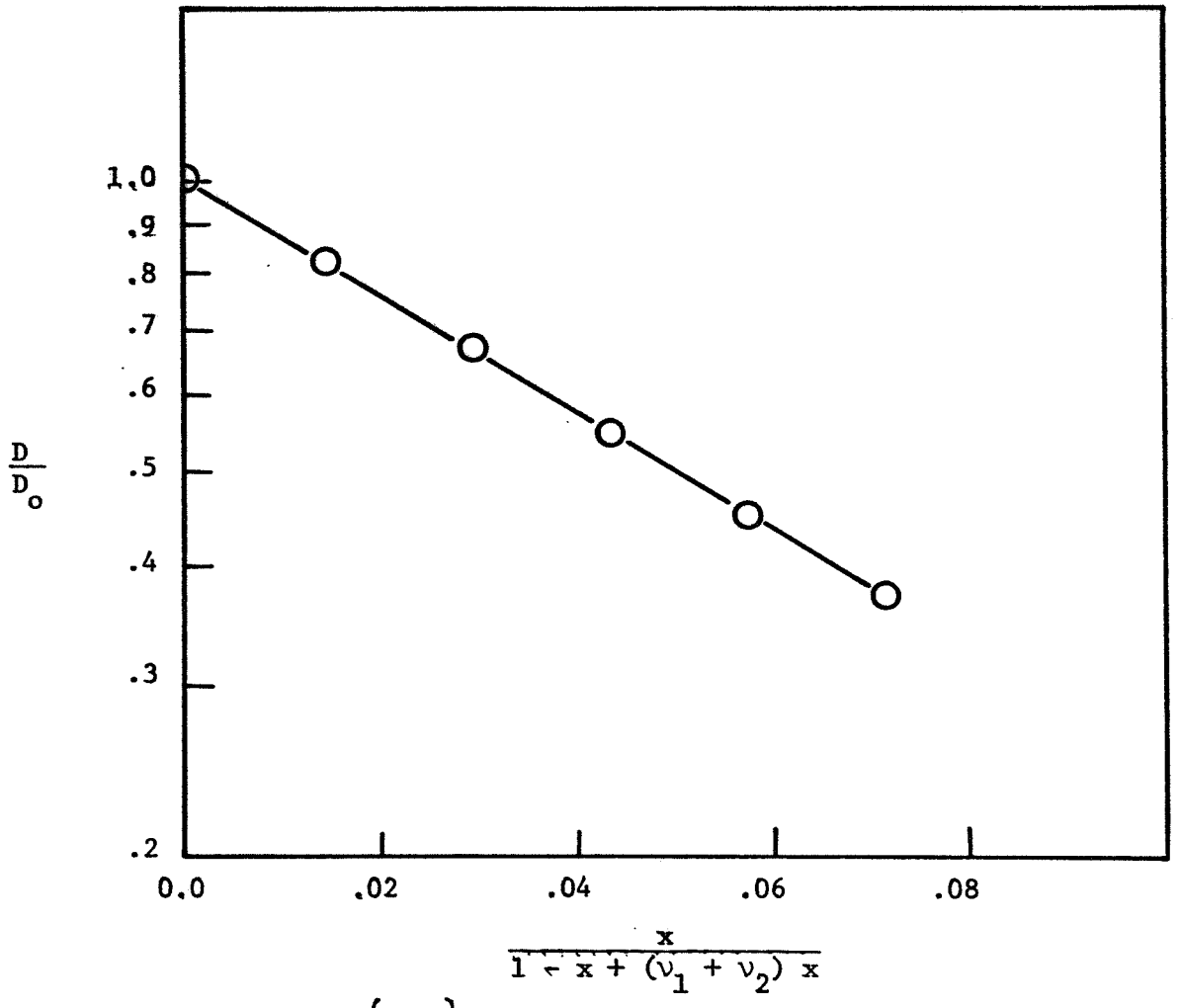

Figure 2-2. $\ell n \left\{ \frac{D}{D_o} \right\}$ vs. Species Fraction for Oxygen in LiOH at 25°C

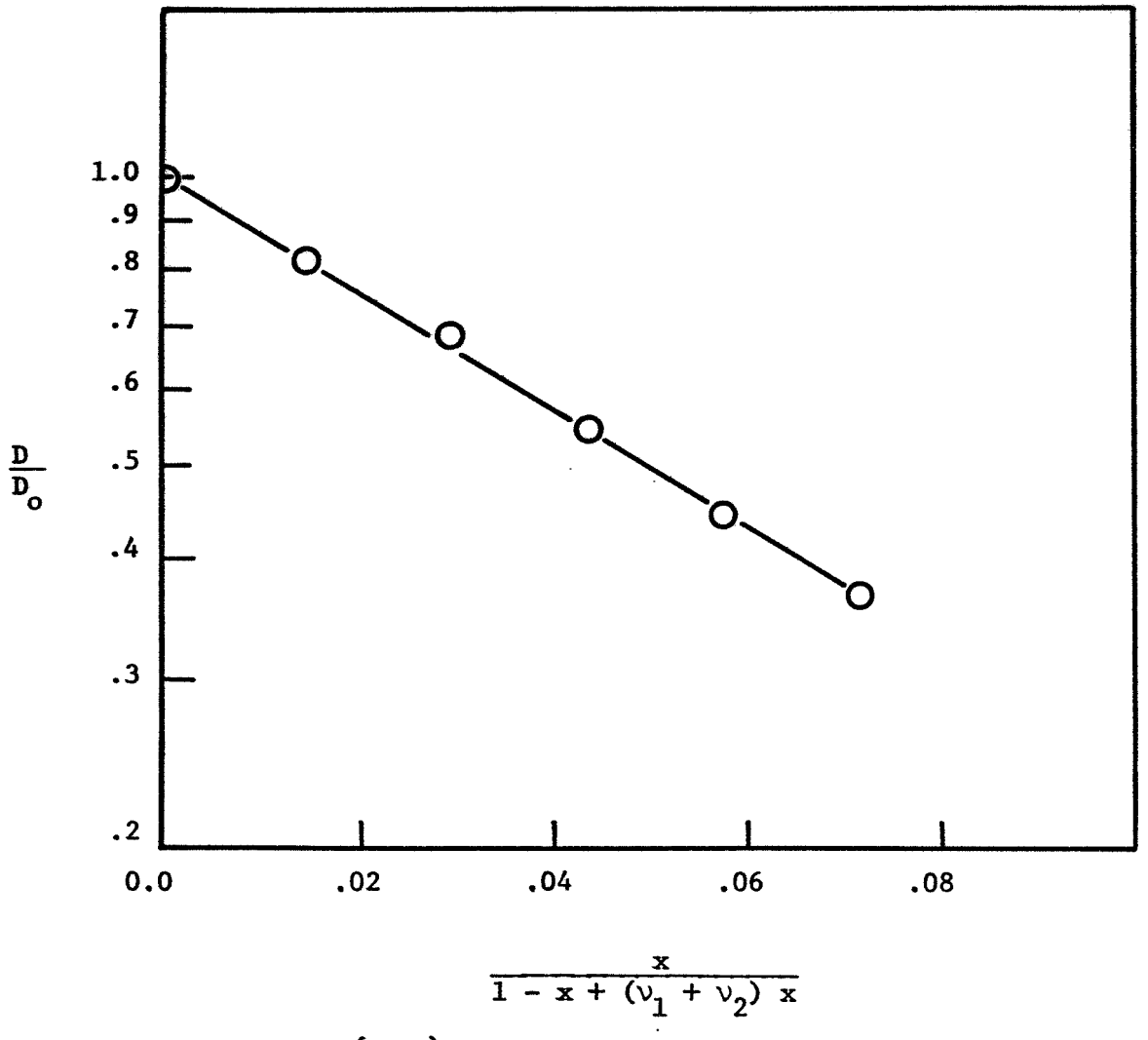

Figure 2-3. $\ln \left(\frac{D}{D_o} \right)$ vs. Species Fraction for Oxygen in LiOH at 40°C

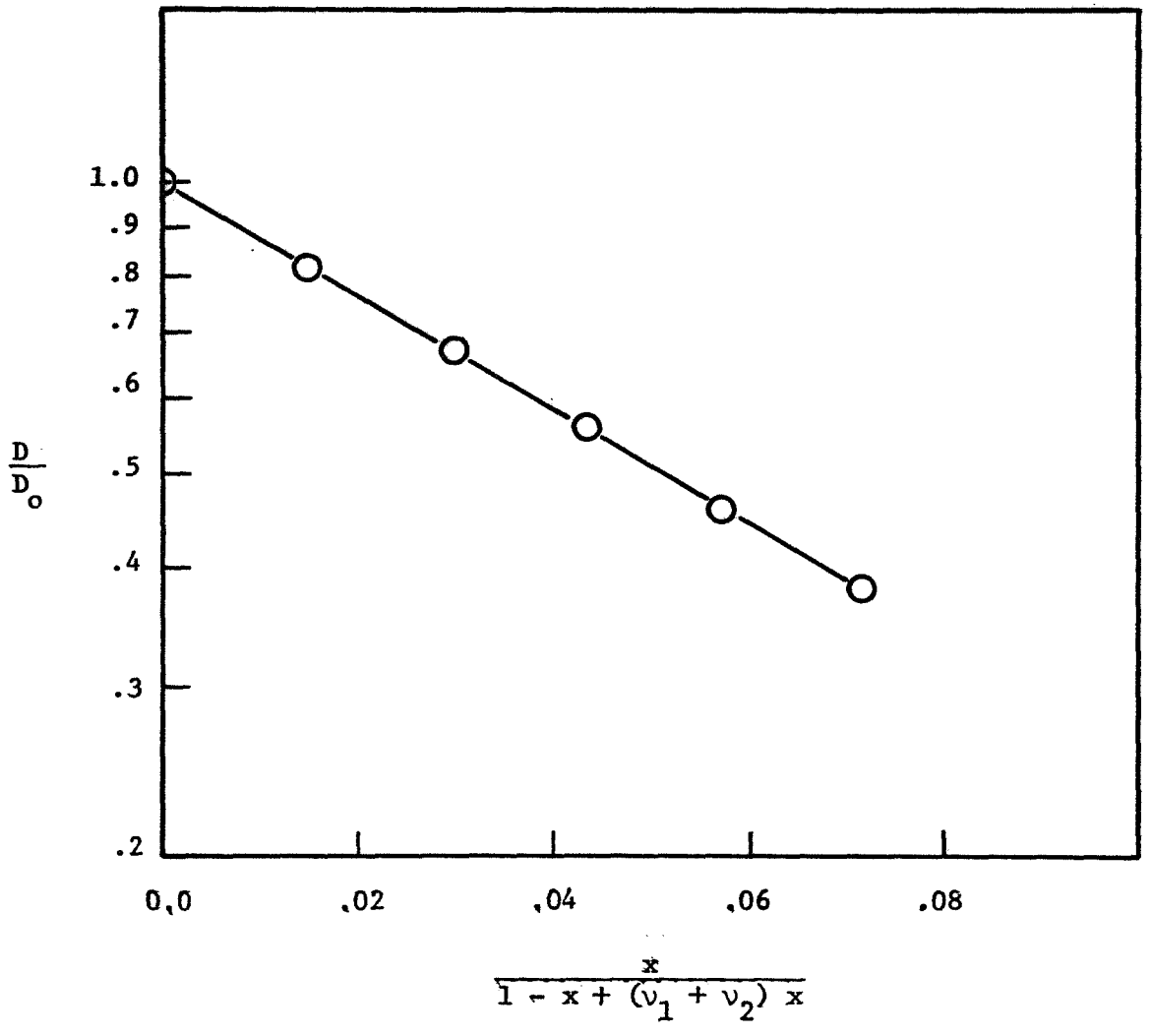

Figure 2-4. $\ell n \left(\frac{D}{D_o} \right)$ vs. Species Fraction for Oxygen in LiOH at 60°C

Table 2-3

($D\mu/T$) for Oxygen in Aqueous Lithium Hydroxide Solutions

Wt % LiOH	Temp. (°K)	$D \times 10^5$ (cm^2/sec)	$\mu \times 10^{2*}$ (g/cm sec)	$D\mu/T \times 10^9$ (g $cm/sec^2 °K$)
2	298	1.76	1.12	0.66
4	298	1.44	1.40	0.68
6	298	1.17	1.80	0.71
8	298	0.96	2.34	0.75
10	298	0.79	3.12	0.83
2	313	2.87	0.80	0.73
4	313	2.34	1.00	0.75
6	313	1.91	1.25	0.76
8	313	1.56	1.60	0.80
10	313	1.28	2.06	0.84
2	333	4.51	0.55	0.74
4	333	3.72	0.68	0.76
6	333	3.08	0.85	0.79
8	333	2.53	1.06	0.81
10	333	2.10	1.30	0.82

* Viscosity data taken from reference (3).

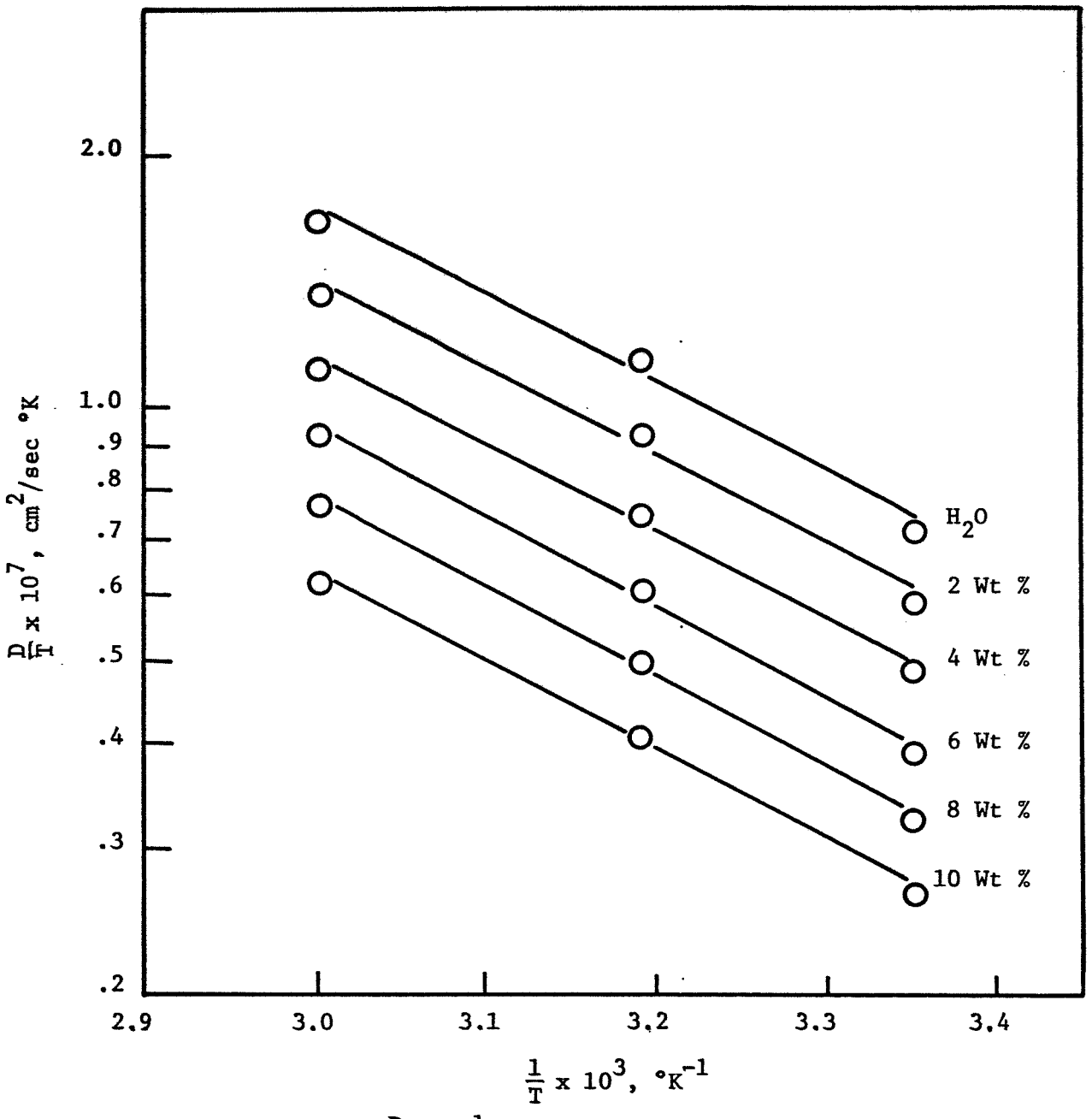

Figure 2-5. $\ell n \frac{D}{T}$ vs. $\frac{1}{T}$ for Oxygen in LiOH Solutions and Water

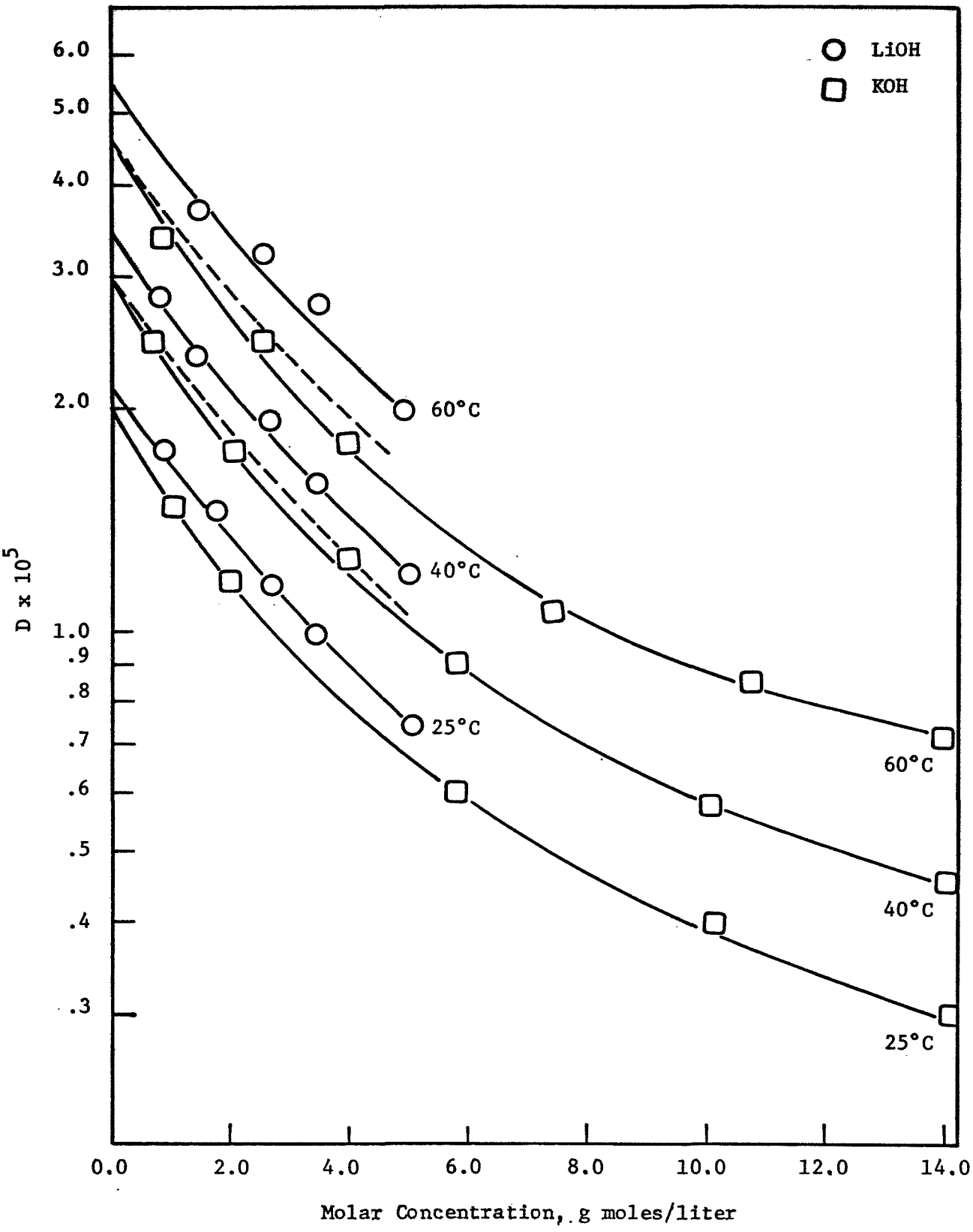

Figure 2-6. Comparison of the Diffusion Coefficients of Oxygen in LiOH to those in KOH

in both systems are within a few percent of each other. Since in the performance of fuel cells, we know that the diffusion process is the limiting factor, it can be concluded that LiOH is at best as good an electrolyte as KOH for use in fuel cells.

3.0 THERMODYNAMICS OF GAS-ELECTROLYTE SYSTEMS

In recent months we have made some promising advances in the theoretical aspects of the general problem of the thermodynamics of slightly soluble solutes in electrolyte solutions. Much of the work has been presented at the August 1970 AIChE meeting (5) and we review this work in section 3.1. Experimentally we are beginning to get data for the KOH system, however, this system seems to be especially difficult due to the low solubility of the gases in concentrated KOH solutions. Experimental results on O_2 in KOH and some discussion of determining the polarizabilities of complex salting-in ions is given in section 3.2.

3.1 Percus-Yevick Theory of Gas-Electrolyte Systems

In this section we have examined in some detail the general problem of the thermodynamics of low soluble solutes in electrolyte solutions. Perhaps the most interesting points of the theory as it is developed here are that we have used a new, more accurate equation of state for rigid sphere mixtures and the derivation of the resulting equations avoid the previously used Kirkwood coupling parameter method. Thus, the theory is easier to follow, is based more soundly on ideas from statistical mechanics, and is more readily amendable to further improvement. The systems used in comparing this modified theory have been primarily the alkali halides, the tetra-alkyl ammonium bromides and KOH.

3.1.1 Introduction

Consider a nonpolar solute 1 (such as oxygen) dissolved in a polar liquid solvent 2 (e.g. water). The chemical potential of the solute is

$$\mu_1 = \mu_1^o + RT \ln \frac{f_1}{f_1^o} \qquad (3\text{-}1)$$

If a salt is now added to the solution the fugacity f_1 will be changed. This change may be an increase (salting-out) or a decrease (salting-in), and is often a large effect. If the liquid phase is in contact with another phase (gas, liquid or solid) there will be a transfer of component 1 between phases until the chemical potential μ_1 is again equal in all phases.

A satisfactory theory for the thermodynamic properties of a nonpolar solute in such a solution should predict the changes in the solute fugacity that occur on changing the electrolyte concentration, type of ion, temperature and pressure. Previous theories have usually been electrostatic in nature. The theory of Debye and McAulay (6) provided expressions for dilute solutions, and a variety of attempts have been made to improve their theory (7-9). All of these approaches are closely similar and treat the solvent as a continuous dielectric medium containing ions and solute molecules. A quantitative test of these theories is difficult because they involve parameters which are not readily available. Moreover, these theories are unable to explain important qualitative aspects of observed behavior, such as salting-in. In view of the initial assumptions present in the electrostatic theories it is difficult to see how they can be significantly improved. The regular solution theory has been widely used as a framework for discussing gases dissolved in nonpolar liquids (10). The major assumption in this theory is that $S^E = 0$; such an assumption is not justified for the

systems studied here.

In this report we propose an approach based on a more recent statistical mechanical theory. Over the last 10 years significant advances have been made in the theory of liquids (11). When used to make calculations of liquid properties from first principles these theories usually give rather poor results, because the theoretical equation of state is related in a very sensitive way to the pair potential function. If experimental values of the density are used in the final equations, however, good results are obtained. Since density data is readily available for most systems of interest it is therefore possible to use the theory to predict other thermodynamic properties.

The approach proposed makes use of the analytic solution to a modified Percus-Yevick equation for rigid spheres by dividing the potential function into a rigid core plus an outer attractive part. It is not necessary to assume $S^E = 0$. However, approximations are necessary to evaluate contributions from the attractive potential. Similar approaches based on the scaled particle theory have been used by Pierotti (12), Shoor and Gubbins (13) and Masterton and Lee (14) for other systems. The final equations are simple to use.

3.1.2 Classical Thermodynamics

We label the solute as component 1, water as component 2, and electrolyte species (ions) as 3, 4, ... m. Usually we shall assume the electrolyte to be completely dissociated to yield just two ionic species (3 and 4). Extensions to multivalent salts and partially dissociated species are an obvious extension. For gas-liquid equilibrium

$$f_1^G = f_1^L \qquad (3\text{-}2)$$

The standard state chosen for the solute is the hypothetical pure liquid referred to the solute at infinite dilution in water, so that

$$f_1^G = f_1^L = K_1^o \gamma_1 x_1 \qquad (3\text{-}3)$$

Assuming an ideal gas phase and a partial pressure of 1 atm., the solubility x_1 is

$$x_1 = \frac{1}{K_1^o \gamma_1} = \frac{x_1^o}{\gamma_1} \qquad (3\text{-}4)$$

The activity coefficient γ_1 usually obeys the Setchenow equation:

$$\log_{10} \gamma_1 = \log_{10} \left(\frac{x_1^o}{x_1} \right) = k_s C_s \qquad (3\text{-}5)$$

where k_s is the salting coefficient. The salting coefficient is defined in the limit of infinite dilution of salt; however, Eq. (3-5) usually holds for salt concentrations up to several molar. From Eq. (3-4) and (3-5) it is seen that for salting-in systems $\gamma_1 < 0$ and $k_s < 0$, whereas salting-out corresponds to $\gamma_1 > 0$ and $k_s > 0$.

3.1.3 Theory

We wish to obtain a general equation for the chemical potential from some fundamental statistical mechanical considerations. Having the chemical potential as a function of temperature, pressure and composition then completely describes the thermodynamics of any system. The theory is developed in more detail in Appendix A and we give just the results

needed here.

All species in the mixture are assumed to exhibit pairwise additivity and spherical symmetry and interact via a cut-off Lennard-Jones potential as shown below:

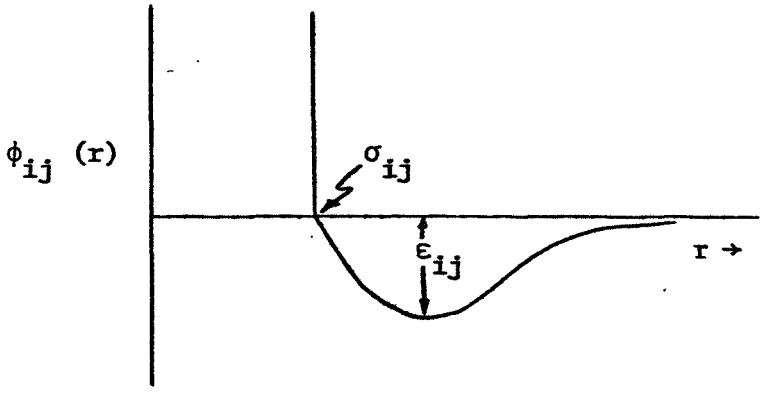

This potential can be written as the sum of a hard repulsive part and a soft attractive part as:

$$\phi_{ij}(r) = \phi^{h}_{ij}(r) + \phi^{s}_{ij}(r) \qquad (3\text{-}6)$$

where

$$\begin{aligned} \phi^{h}_{ij}(r) &= \infty && r \leq \sigma_{ij} \\ &= 0 && r > \sigma_{ij} \end{aligned} \qquad (3\text{-}7)$$

$$\begin{aligned} \phi^{s}_{ij}(r) &= 0 && r \leq \sigma_{ij} \\ &= 4\,\varepsilon_{ij}\left[\left(\frac{\sigma_{ij}}{r}\right)^{12} - \left(\frac{\sigma_{ij}}{r}\right)^{6}\right] && r > \sigma_{ij} \end{aligned}$$

Using this potential together with the results of a modified Percus-Yevick hard sphere theory the general relation for the chemical potential then

becomes*:

$$\frac{\mu_1}{kT} = -\ln(1-\zeta_3) + \frac{\pi}{6}\frac{P^{ref.}}{kT}\sigma_1^3 + \frac{3\zeta_2}{(1-\zeta_3)}\sigma_1$$

$$+ \frac{3\zeta_1}{(1-\zeta_3)}\sigma_1^2 + \frac{9}{2}\frac{\zeta_2^2}{(1-\zeta_3)^2}\sigma_1^2$$

$$+ 3\left(\frac{\sigma_1\zeta_2}{\zeta_3}\right)^2\left[\ln(1-\zeta_3) + \frac{\zeta_3}{(1-\zeta_3)} - \frac{\zeta_3^2}{2(1-\zeta_3)^2}\right] \qquad (3\text{-}8)$$

$$- \left(\frac{\sigma_1\zeta_2}{\zeta_3}\right)^3\left[2\ln(1-\zeta_3) + \frac{\zeta_3(2-\zeta_3)}{(1-\zeta_3)}\right]$$

$$- \frac{32\pi}{9kT}\sum_{j=1}^{m}\rho_j\varepsilon_{1j}\sigma_{1j}^3 - \frac{4\pi\rho_2\mu_2^2\alpha_1}{3\sigma_{12}^3}$$

where $\zeta_n = \frac{1}{6}\pi\sum_{j=1}^{m}\rho_j\sigma_j^n$

σ_i is the hard sphere diameter of species i, component 1 is the dissolved gas, component 2 is water, P is the pressure, μ_2 is the dipole moment of water and α_1 is the solute gas polarizability.

---

*See Appendix A for details of derivation.

The relation for the partial molal volume is given by

$$\bar{V}_1 = kT\,\beta \left\{ 1 + \frac{\zeta_3}{(1-\zeta_3)} + 3\,\frac{\zeta_2}{(1-\zeta_3)^2}\,\sigma_1 \right.$$

$$+ 3\,\frac{\zeta_1}{(1-\zeta_3)^2}\,\sigma_1^2 + 9\,\frac{\zeta_2^2}{(1-\zeta_3)^3}\,\sigma_1^2 \qquad (3\text{-}9)$$

$$\left. - \left(\frac{\zeta_2\,\sigma_1}{(1-\zeta_3)} \right)^2 \left[\frac{2\,\zeta_3}{(1-\zeta_3)} + \zeta_2\,\sigma_1 \right] \right\} + \frac{\pi}{6}\,\sigma_1^3$$

$$- \frac{4\,\pi}{3}\,\beta \left\{ \frac{8}{3} \sum_{j=1}^{m} \rho_j\,\varepsilon_{1j}\,\sigma_{1j}^3 + \frac{\rho_2\,\mu_2^2\,\alpha_1}{\sigma_{12}^3} \right\}$$

where β is the isothermal compressibility and is given in the appendix.

The salting coefficient is calculated from the relation

$$k_s = \frac{1}{C_s} \log_{10} \gamma_1 \qquad (3\text{-}10)$$

where $\ln \gamma_1$ is obtained from the theory as:

$$\ln \gamma_1 = \frac{\mu_1 - \mu_1^w}{kT} + \ln \sum_{j=1}^{m} \left(\frac{\rho_j}{\rho_w} \right) \qquad (3\text{-}11)$$

where the superscript w refers to pure water.

3.1.4 Determination of Molecular Parameters

In order to calculate the thermodynamic properties of nonpolar

solutes in electrolyte solutions from the above modified P-Y theory a knowledge of the molecular parameters σ and ε/k and experimental densities is necessary.

To lend some consistency to the determination of these parameters for the solute molecules, the recent results of Tee, Gotoh and Stewart (15) for smoothed Lennard-Jones potential parameters from second virial coefficient data were used. Knowing only critical constants for the nonpolar molecule the molecular parameters can be determined from:

$$\sigma = \left(\frac{T_c}{P_c} \right)^{1/3} [2.4380 + 1.7282\ \omega] \qquad (3\text{-}12)$$

$$\varepsilon/k = T_c\ [0.7500 - 0.5709\ \omega] \qquad (3\text{-}13)$$

Table 3-1 shows the results for the solutes used in this study. Parameters for water were determined by the method used by Pierotti (16), and are shown in Table 3-2.

The ionic parameters are more difficult to determine. Shoor and Gubbins (13) and Masterton and Lee (14) have assumed crystal diameters as the size parameter for ions. Other than convenience and availability, there is no apparent reason to assume that this is the proper size parameter to use for ions in solution.

We have, therefore, undertaken an extensive study of all available gas-alkali halide electrolyte systems data to determine the ionic diameters in solution more accurately. It was found that the diameters so determined were consistently about 4% higher than their corresponding

Table 3-1

Solute Parameters

Solute	σ (Å)	ε/k (°K)	$\alpha \times 10^{24}$ (cm^3)
He	2.570	10.80	0.204
Ne	2.883	33.4	0.83
Ar	3.567	113.7	1.63
Kr	3.818	157.3	2.46
H_2	2.960[c]	37.6[c]	0.79
N_2	3.901	91.8	1.76
O_2	3.604	114.2	1.60
CH_4	3.958	141.6	2.60
C_2H_6	4.847	210.7	4.47
C_3H_8	5.577	245.3	6.29
C_4H_{10}	6.258	270.1	8.24[a]
SF_6	5.903	192.3	6.21[b]
C_6H_6	6.354	352.6	9.89

(a) Calculated by method of Denbigh (17)

(b) T. M. Reed, J. Phys. Chem., 59, 428 (1955).

(c) T. M. Reed and K. E. Gubbins, "Applied Statistical Mechanics" McGraw-Hill, to be published.

Table 3-2

Parameters for Ions and Water

Ion	σ (Å)	ε/k (°K)	$\alpha \times 10^{24}$ cm^3 [(a)]
Li^+	1.24	48.3	0.031
Na^+	1.98	90.5	0.179
K^+	2.76	165.2	0.83
F^-	2.86	139.5	1.04
Cl^-	3.75	243.1	3.66
Br^-	4.07	313.0	4.77
I^-	4.48	391.0	7.10
OH^-	3.20	167.2	1.83
$(CH_3)_4N^+$	4.98	258.0	8.93[b]
$(C_2H_5)_4N^+$	6.03	277.7	16.69[b]
$(C_3H_7)_4N^+$	6.82	281.5	24.45[b]
$(C_4H_9)_4N^+$	7.74	227.3	32.21[b]
H_2O	2.76	85.3	-

(a) Landolt-Bornstein, "Zahlenwerte und Funktion aus Physik-Chemie-Astronomie-Geophysik-Technik," Vol. I, Part 1, 1950.

(b) Calculated by bond polarizabilities method of Denbigh (17).

crystal diameter values. It is, therefore, advisable to use a slightly increased crystal diameter as the proper size parameter for ions when using the MPY theory. Table 3-2 shows the values of ionic σ that were used in this study. The values for the tetra-alkyl ammonium ions were calculated using the relation

$$\sigma^{+} = 1.04\ \sigma^{crystal} \qquad (3\text{-}14)$$

This relation appears to be generally valid for all simple spherically symmetric ions. Ions such as OH^{-} do not appear to obey this simple law and Table 3-2 shows the value we have used for OH^{-}.

The energy parameter ε/k was determined from Mavroyannis-Stephen theory for dispersion interactions and gives

$$\varepsilon = 3.146 \times 10^{-24}\ \frac{\alpha^{3/2}\ Z^{1/2}}{\sigma^{6}} \qquad (3\text{-}15)$$

No polarizability measurements are available for the tetra-alkyl ammonium ions; for these ions values of α were estimated from the bond contribution method of Denbigh (17) and are included in Table 3-2.

3.1.5 Test of Theory: Salting-Out Systems

The theory was tested for most alkali halides and the KOH system for which data were available; results are shown in Table 3-3 for the salts LiCl, NaCl and KI. Also included in this table are the results given by the McDevit-Long internal pressure theory (7). This theory does not proceed from statistical mechanical foundations, but assumes that the effect of the solute molecule is to modify the ion-water interaction by

Table 3-3

Salting Coefficients (at Infinite Dilution of Salt)

for Salting-Out Systems

	LiCl			NaCl			KI		
Solute	Obs.	P-Y	M^c-L	Obs.	P-Y	M^c-L	Obs.	P-Y	M^c-L
		Eq. (26)	Eq. (30)						
He	.050[c]	.077	.026	.082[b]	.095	.036	.083[c]	.082	.016
Ne	.059[c]	.085	.087	.097	.105	.078	.080[c]	.089	.035
Ar	.096[c]	.094	.083	.133[c]	.117	.117	.108[c]	.088	.048
Kr	.116[c]	.096	.135	.146[c]	.120	.187	.120[c]	.086	.065
H_2	.076[a]	.087	.066	.114[a]	.108	.090	.081[d]	.090	.040
N_2	.095[d]	.116	.118	.121[d]	.119	.162	.100[d]	.116	.073
O_2	.100[a]	.095	.108	.141[a]	.144	.149	--	--	--
CH_4	.097[d]	.106	.122	.127[d]	.132	.167	.097[d]	.099	.075
C_2H_6	.124[d]	.126	.186	.162[d]	.158	.255	.101[d]	.115	.115
SF_6	.145[c]	.180	.257	.195[c]	.227	.353	.145[c]	.182	.159
C_6H_6	.141[a]	.132	.304	.198[a]	.170	.426	.049[c]	.112	.187

(a) Long, F. A. and W. F. McDevit, Chem. Rev., 51, 119 (1952).

(b) Conway, B. E., J. E. Desnoyers, and A. C. Smith, Phil. Trans. Roy. Soc. London A256, 389 (1964).

(c) Morrison, T. J. and N. B. B. Johnstone, J. Chem. Soc., 1955, 3655 (1955).

(d) Morrison, T. J. and F. Billett, J. Chem. Soc., 1952, 3819 (1952).

occupying volume in the solution. The theory is only applicable to small nonpolar solutes. It gives a limiting value for k_s:

$$k_s = \frac{\bar{V}_1 \ (V_s - \bar{V}_s^o)}{2.3 \ RT \ \beta_o} \qquad (3\text{-}16)$$

The term V_s (liquid molar volume of salt) is often difficult to obtain. In principle, the McDevit-Long theory is capable of predicting both salting-out and salting-in; the latter case corresponds to $V_s > \bar{V}_s^o$. However no systematic study of this has been made, because of the difficulty of obtaining V_s. From Table 3-3 it is seen that the two theories give similar results for small solutes, but that the McDevit-Long theory fails for large solute molecules.

Unlike the McDevit-Long theory, the present approach is able to predict the concentration dependence of the solute activity coefficient, in addition to the infinite dilution behavior. Tables 3-4 and 3-5 show the results for the KOH system. Figure 3-1 shows a typical result; the KOH system provides a rather rigorous test of the theory because of the high salt solubility and the strong salting-out nature of the ions. The present theory gives excellent results up to the highest concentrations. Two comparisons with electrostatic theories are also included. The theory of Debye and McAulay (6) was the first attempt at such a theory, and is the one on which later theories are based. It gives values of γ_1 that are much too low at high concentrations (by a factor of 50 for 50 wt % KOH). The more recent electrostatic theory of Conway et al. (18) gives good agreement for dilute electrolyte solutions, but fails completely at higher concentrations since it predicts negative solubilities. The

Table 3-4

Salting Coefficients (At infinite dilution) for KOH

k_s

	Debye-McAulay	Conway	P-Y	Expt'l.
H_2	0.039	0.094	0.147	0.129
O_2	0.065	0.108	0.176	0.180
Ar	0.049	0.099	0.166	0.179
CH_4	0.73	0.112	0.187	0.197

Table 3-5

Predicted and Experimental Values of $\ell n\ (\gamma_1 K_1^o)$ for KOH Solutions

Solute	Wt % KOH											
	0 %		10 %		20 %		30 %		40 %		50 %	
	Exp.	Theor.	Exp.	Theor.	Exp.	Theor.	Exp.	Theor.	Exp.	Theor.	Exp.	Theor.
H_2	11.17	11.05	11.85	11.76	12.41	12.59	13.17	13.56	14.13	14.67	15.2	16.04
O_2	10.66	10.64	11.50	11.44	12.46	12.41	13.54	13.58	14.73	14.94	16.07	16.66
Ar	10.62	10.57	11.38	11.36	12.30	12.32	13.40	13.47	14.63	14.81	-	-
CH_4	10.58	10.48	11.46	11.37	12.49	12.45	13.65	13.79	15.10	15.32	-	-
SF_6	12.38	11.44	13.88	12.96	15.58	14.87	17.52	17.25	-	-	-	-

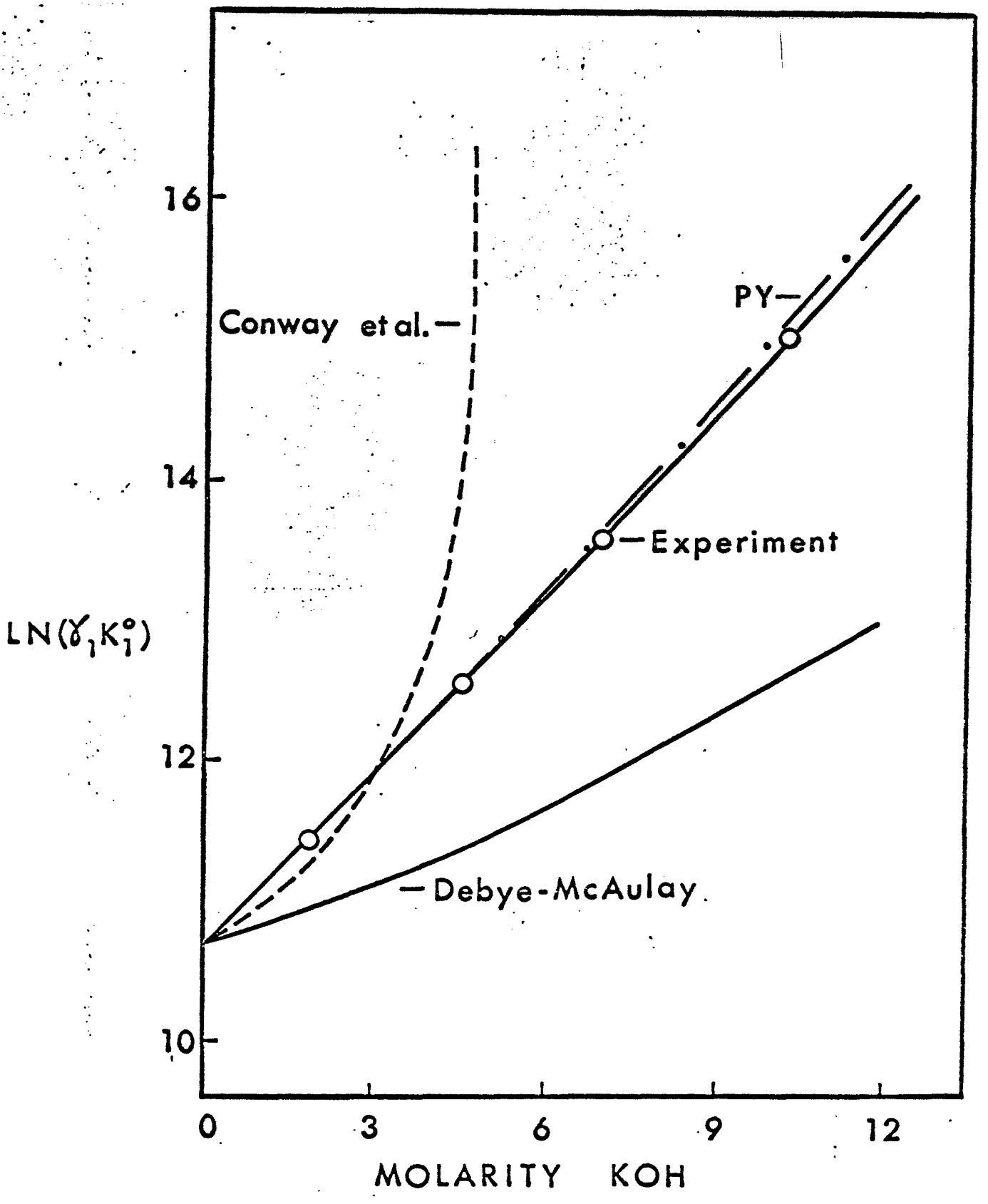

Figure 3-1. Activity Coefficients for Salting-Out System - Oxygen in KOH at 25°C.

McDevit-Long theory predicts results that are very close to those of the Debye-McAulay theory, and are therefore not included in Figure 3-1. (In Figure 3-1 the present theory has also been used to predict K_1^o, whereas the other theories assume an experimental value for this quantity.)

3.1.6 Test of Theory: Salting-In Systems

Typical of salting-in systems are hydrocarbon solutes dissolved in aqueous solutions of tetra-alkyl ammonium salts. The tetra-alkyl ammonium ions are capable of producing quite large effects; thus the solubility of benzene in a 4M tetra-alkyl ammonium bromide solution is about 140 times greater than in pure water (19).

No satisfactory theoretical explanation of these effects is available. Bockris *et al*. (20) attempted to account for salting-in by taking specific account of nonpolar interactions in the previously proposed electrostatic theories; their theory is qualitatively capable of predicting salting-in, but does not predict numbers of the correct order. Moreover, their theory contains parameters which are difficult to evaluate. The McDevit-Long theory is capable of predicting salting-in if $V_s > \bar{V}_s^o$; however, V_s is difficult to evaluate, and predictions are usually of incorrect order of magnitude (21). Other theories (e.g. the Debye-McAulay) fail to predict even the qualitative feature of salting-in.

Figure 3-2 compares theory and experiment for the methane tetramethyl ammonium bromide system. Although the present theory is an improvement over that of McDevit and Long, the prediction still leaves something to be desired; the Debye-McAulay theory is seen to incorrectly predict salting-out.

Table 3-6 compares experimental salting coefficients with the present theory. Although the theory predicts salting-in for these systems

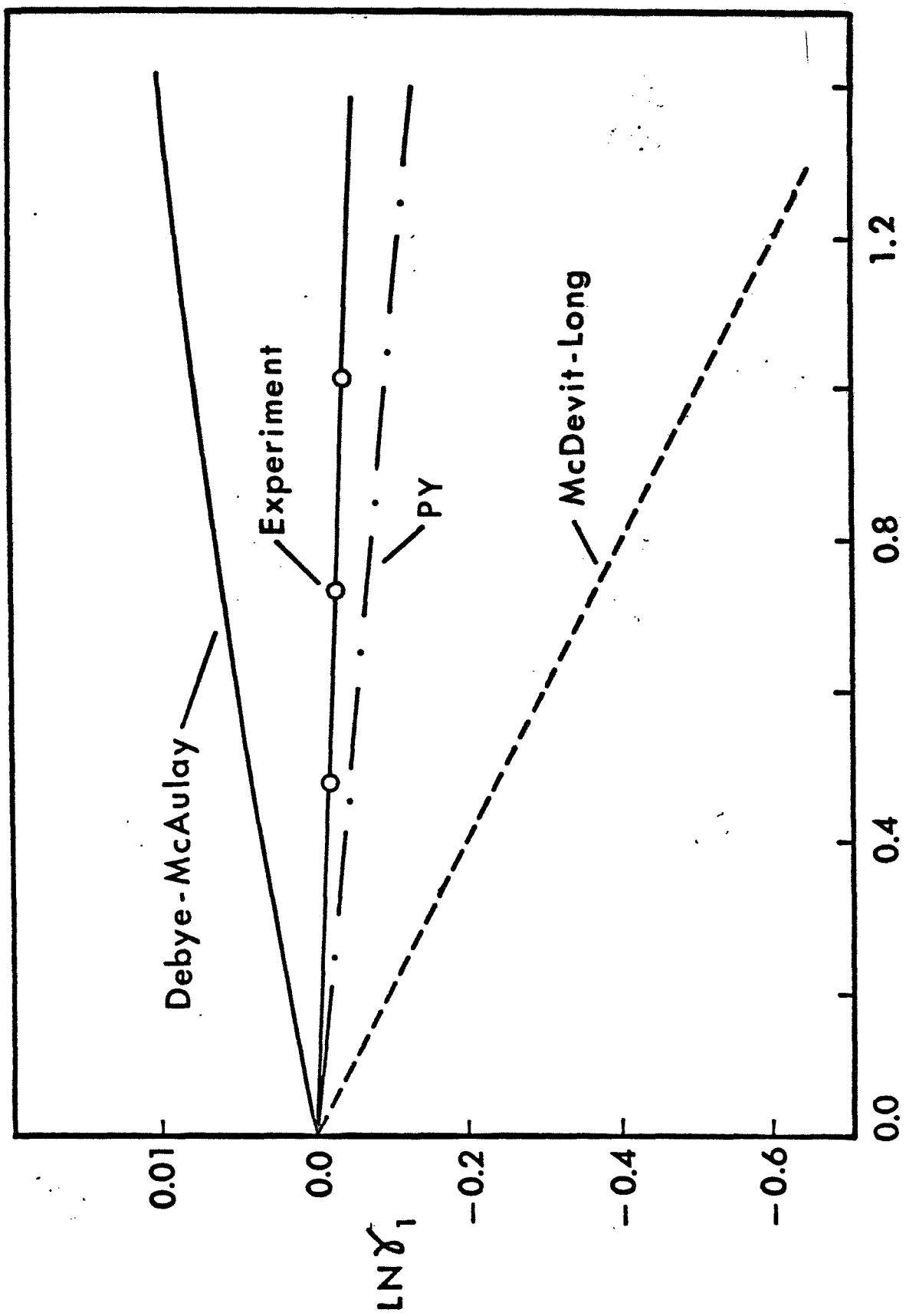

Figure 3-2. Activity Coefficients for Salting-In System - CH_4 in $(CH_3)_4NBr$ at 25°C.

Table 3-6

Salting Coefficients at Infinite Dilution of Salt for Salting-In Systems. (Experimental data taken from W. Wen and J. H. Hung, J. Phys. Chem., 74, 170 (1970))

Solute	$(CH_3)_4NBr$		$(C_2H_5)_4NBr$		$(C_3H_7)_4NBr$		$(C_4H_9)_4NBr$	
	Theory	Expt.	Theory	Expt.	Theory	Expt.	Theory	Expt.
CH_4	-.034	-.017	-.100	-.049	-.194	-.082	-.102	-.096
C_2H_6	-.026	-.040	-.078	-.117	-.162	-.141	+.016	-.155
C_3H_8	-.009	-.059	-.041	-.158	-.111	-.187	+.154	-.248
$n\text{-}C_4H_{10}$	+.016	-.074	+.013	-.168	-.032	-.227	+.331	-.286

the quantitative agreement is poor in most cases. The salting-in increases (a) as the size of the tetra-alkyl ammonium ion increases, and (b) as the size of the solute molecule increases. The theory does not predict either trend satisfactorily. In general, the predictions become poorer as the sizes of anions and solute increase.

The reason for the poor performance of the theory in these cases can be seen from an examination of Eq. (3-11) and the assumptions made in evaluating the term μ_1. In general, the hard sphere contribution to μ_1 and $\ell n \sum (\rho_j/\rho_w)$ in Eq. (3-11) are positive numbers, whereas the soft contribution in μ_1^s, given as the last two terms of Eq. (3-8) is negative. The positive terms are given by the theory with good accuracy (13); several approximations were introduced to obtain μ_1^s, however. For salting-out systems the positive terms in Eq. (3-11) dominate the μ_1^s term to produce positive values of $\ell n\ \gamma_1$; thus the errors in calculating μ_1^s term are not too serious. In the case of salting-in systems, however, the positive and negative terms in Eq. (3-11) are of similar magnitude; because of the resulting cancellation of terms, $\ell n\ \gamma_1$ is sensitive to errors in calculating μ_1^s. Thus, improvements in predictions for these systems must come from an improvement in the theory for the μ_1^s term. A study of this aspect of the theory is now underway.

3.1.7 Partial Molal Properties

The partial molal heat of solution, $\Delta\bar{H}_1$, provides a quantitative measure of the temperature dependence of μ_1 and is given by

$$\frac{\partial\ \ell n\ (\gamma_1\ K_1^o)}{\partial\ T} = -\frac{\Delta\bar{H}_1}{RT^2} \qquad (3\text{-}17)$$

Figure 3-3 shows a typical comparison of theoretical and predicted values of $\Delta\bar{H}_1$. In general the theory predicts values above those found experimentally. This was attributed to the assumption of rigid core particles. The real particles do not possess rigid cores, and the "effective rigid core diameter" might be expected to decrease as the temperature is raised because of the increase in molecular kinetic energy. To test this the calculation of $\Delta\bar{H}_1$ was repeated, allowing σ_i for each of the molecules and ions involved to decrease by 0.01 Å over a temperature range of 60°C. (This particular figure of 0.01 Å was suggested by calculations of σ_2 for water reported by Pierotti (12) at two temperatures.) The resulting improvement is shown in Figure 3-3 and indicates that the assumption of rigid cores leads to errors when one calculates the temperature dependence of thermodynamic properties.

A recent perturbation theory by Barker and Henderson (22) and the high temperature equation of state studies of Rowlinson have shown that the temperature dependence of the hard core can be adequately expressed as

$$d\ (T) = \int_0^{\sigma} \{1 - \exp(-\frac{\phi\ (r)}{RT}\ )\}dr \qquad (3\text{-}18)$$

Figure 3-3 shows this temperature dependence and it obeys quite closely the arbitrary values of temperature dependence that we have chosen. A study of the use of this equation for temperature dependent properties is now underway.

A quantitative measure of the pressure dependence of μ_1 is given by the partial molal volume (see Eq. (A-20)). The theory does an excellent job of predicting $\bar{V}_1$ for gases dissolved in pure water,

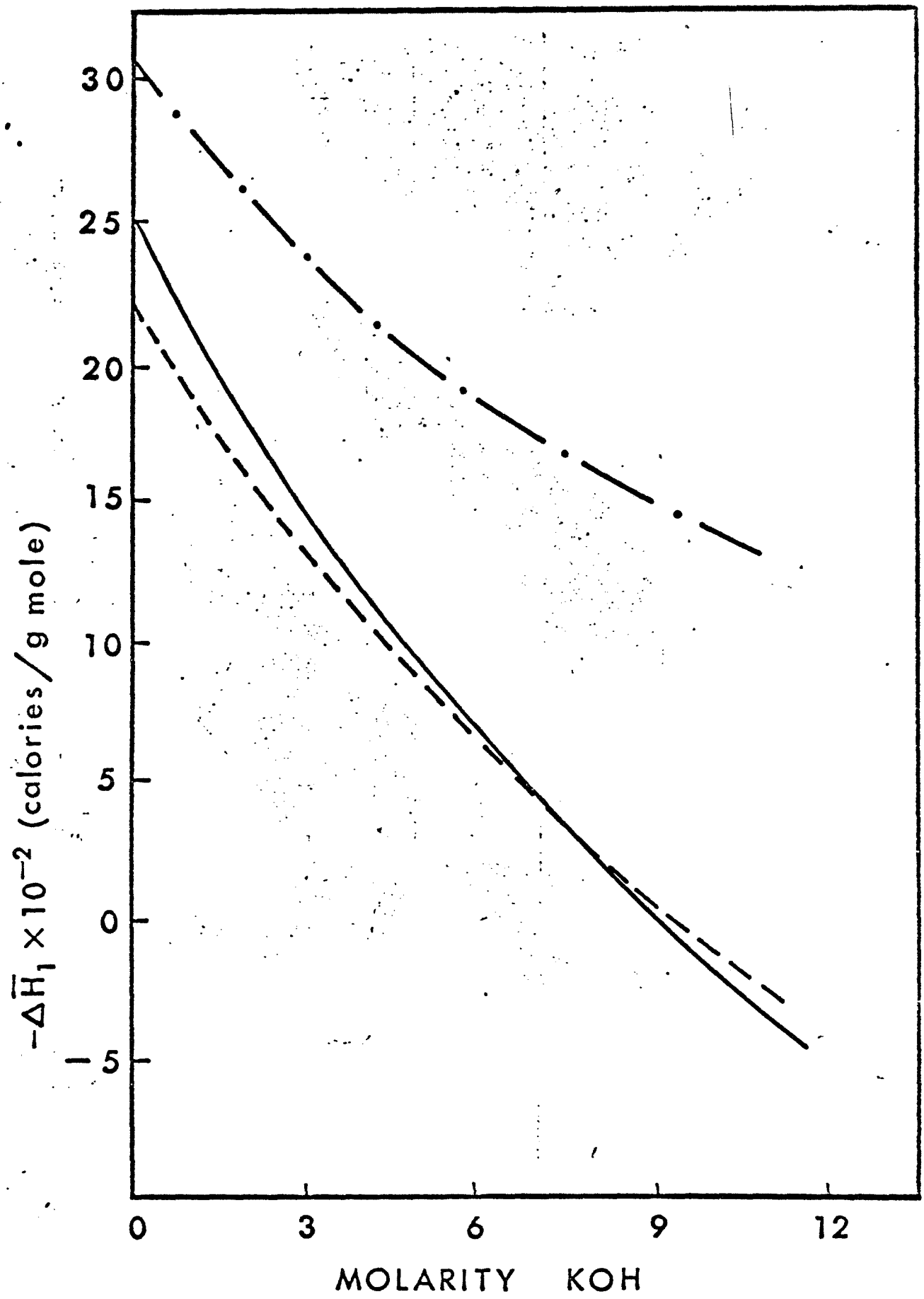

Figure 3-3. Partial Molal Heats of Solution for Oxygen in KOH at 25°C. ——— , Experiment; — • — Equations (3-17) and(A-10) σ Values; - - - Equations (3-17) and (A-10) with σ replaced by d(T) in calculating μ_1^h

using Eq. (3-9) and (A-24).

Figure 3-4 shows theoretically predicted partial molal volumes of methane in two salts. The theory predicts that $\bar{V}_1$ decreases with increasing salt concentration in the case of salting-out systems (e.g. CH_4/KOH), whereas it increases for salting-in systems (e.g. CH_4/Bu_4NBr). Except for the O_2 in KOH, results reported in the next section. No experimental values of $\bar{V}_1$ are available for electrolyte solutions at present, so that these predicted trends await experimental verification.

3.1.8 Conclusions

The theory satisfactorily predicts the concentration and pressure dependence of activity coefficients of nonpolar solutes dissolved in electrolyte solutions when salting-out occurs. In its present form the theory does not quantitatively predict the properties of salting-in systems, nor the temperature derivative of γ_1.

The principal advantage of the theory is that it is firmly based in statistical mechanics. Consequently the approximations involved are clearly defined and amenable to improvement. Current work involves (a) an effort to improve the prediction of $\Delta\bar{H}_1$ by studying the rigid core approximation, and (b) an effort to improve the description of salting-in systems by improving the calculation of μ_1^s.

3.2 Experimental Determinations of Partial Molal Volumes of Gases in Electrolyte Solutions

Some results on the experimental determinations of partial molal volumes of O_2 in KOH solutions have been obtained. Additionally, work on the determination of ion polarizabilities for salting-in systems is discussed.

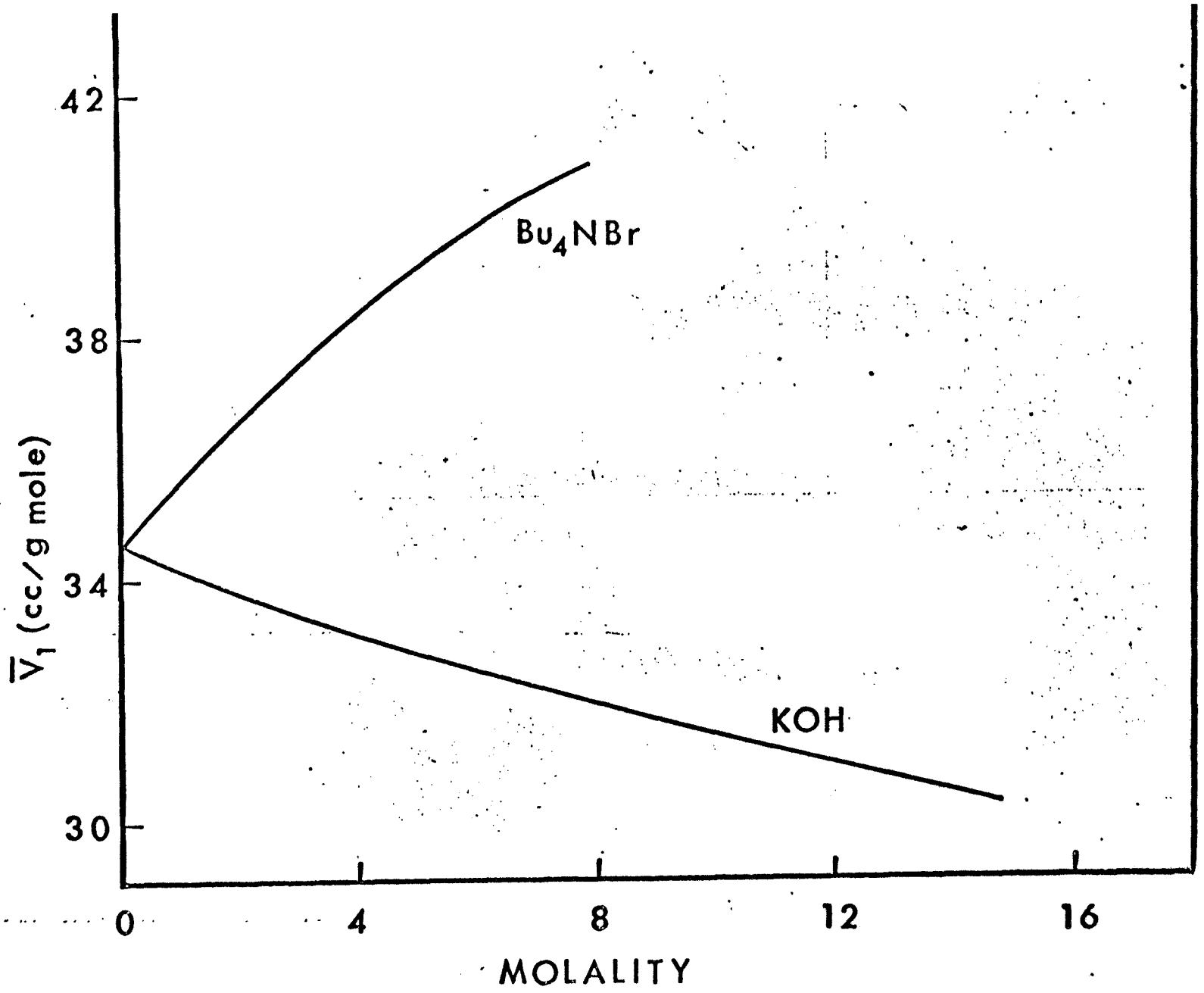

Figure 3-4. Calculated Values of Partial Molal Volume for CH_4 in KOH and $(C_4H_9)_4NBr$ Solutions at 25°C.

3.2.1 Partial Molal Volumes of O_2 in KOH

The experimental problems in the determination of $\bar{V}_1$ as discussed in the last report have made experimental progress slow. Figure (3-5) shows the results of $\bar{V}_1$ for KOH solutions. It is seen that for the salting-out system KOH $\bar{V}_1$ for O_2 decreases with increasing ionic concentration. This trend is what is theoretically predicted as well. However, we need to examine more salting-out systems before we can determine whether this is a general trend for all salting-out systems. We are presently trying to obtain data on the H_2-KOH system but it seems that a slight modification of the system will be necessary to accurately determine these values. Thereafter we hope to examine $\bar{V}_1$ of gases in the salting-in tetra-alkyl ammonium salts.

In the present development of the theory for $\bar{V}_1$ we have been using a theoretically predicted $\bar{V}_1$ which uses an equation for the isothermal compressibility, β, that is derived from a pure hard sphere theory. We have recently been examining equations for β based on a more realistic assumption for the equation of state. This modified equation of state is consistent with the other parts of the theory in that it is a first order equation. This equation for P is:

$$P = P^{h.s.} - \frac{16\pi}{g} \sum_{i=1}^{m} \sum_{j=1}^{m} \rho_i \rho_j \varepsilon_{ij} \sigma_{ij}^3 \qquad (3\text{-}19)$$

where as before $P^{h.s.}$ is the hard sphere equation of state.

$$P^{h.s.} = \frac{6kT}{\pi} \left[\frac{\zeta_o}{(1-\zeta_3)} + \frac{3\,\zeta_1\,\zeta_2}{(1-\zeta_3)^2} + \frac{3\,\zeta_2^3}{(1-\zeta_3)^3} - \frac{\zeta_3\,\zeta_2^3}{(1-\zeta_3)^3} \right.$$

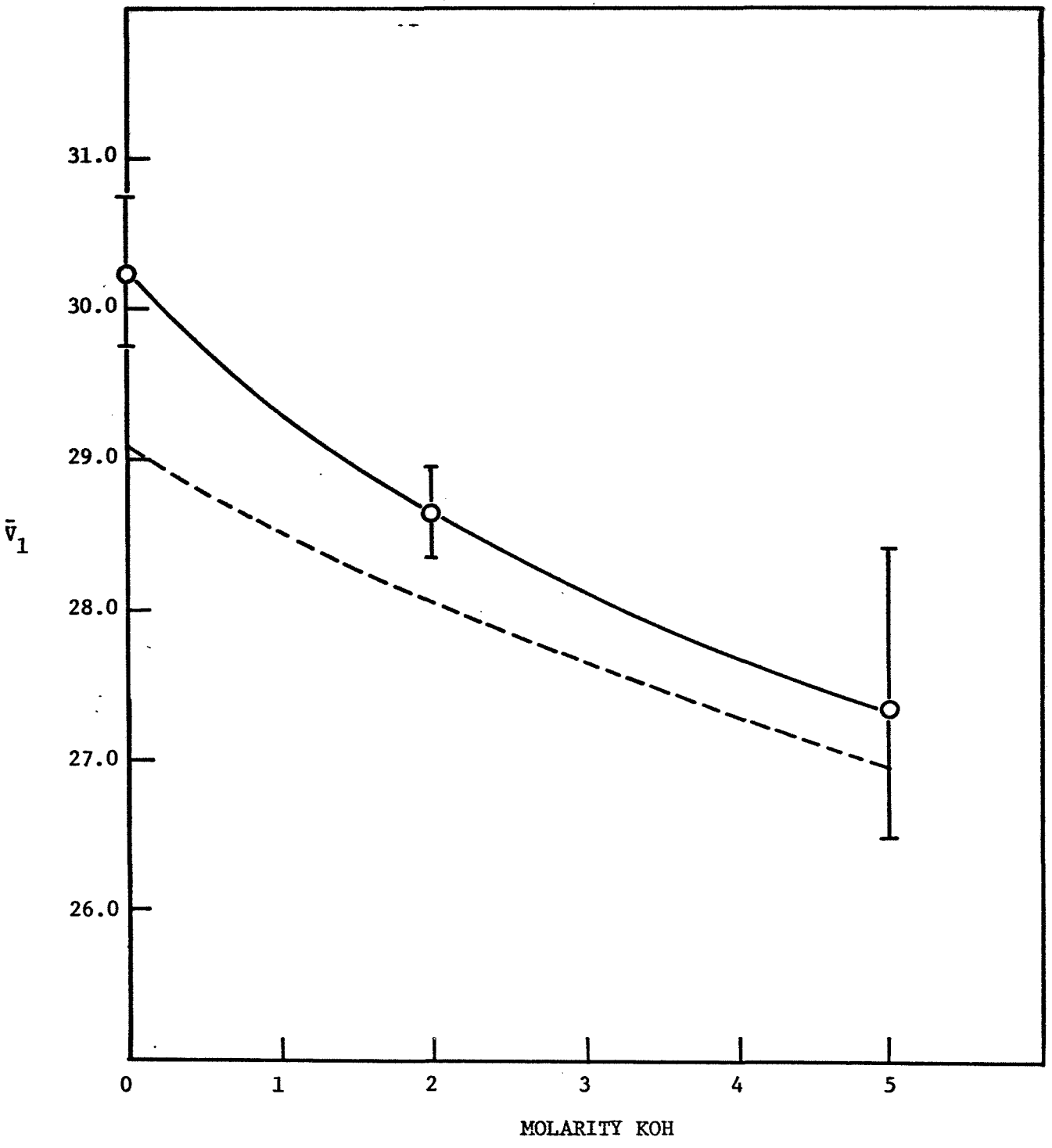

Figure 3-5. Partial Molal Volume of O_2 in KOH ——— Experimental Values
---- Theory.

An equation for the isothermal compressibility can then be derived from this equation of state and gives:

$$\beta = -\frac{1}{V}\left(\frac{\partial V}{\partial P}\right)_T = \frac{9\pi(1-\zeta_3)^4}{54\,kT\{\beta_{h.s.}\} - 32\pi^2 \sum_{i=1}^{m}\sum_{j=1}^{m} \rho_i \rho_j \varepsilon_{ij} \sigma_{ij}^3 (1-\zeta_3)^4} \tag{3-20}$$

where

$$\beta_{h.s.} = (1-\zeta_3)^2 \zeta_o + 6\zeta_1\zeta_2(1-\zeta_3) + 9\zeta_2^3 + \zeta_3^2\zeta_2^3 - 4\zeta_3\zeta_2^3$$

This equation when used in the theory for $\bar{V}_1$ gives theoretical results that appear to obey the concentration dependence of $\bar{V}_1$ quite well.

3.2.2 Polarizabilities of Salting-In Ions

As was described in the last report one of the difficulties in theoretically describing the thermodynamic behavior of the tetra-alkyl ammonium salts is that there exists no data on ionic polarizabilities for these salts. We have therefore, undertaken a project to determine these values experimentally. The initial data taken has shown that slight experimental errors tend to be magnified in the final values of α_i. Hence, we are recalibrating the Brice-Pheonix refractometer using a sensitive refraction cell with the hopes that our experimental error can be greatly reduced. We should have final results on the methyl, ethyl, propyl, butyl tetra-alkyl ammonium bromides within a few months. Having the values of α_i, we can then begin to study the other anomolous

behavior of these salts more closely, including using these salts as additives to strongly salting-out systems as a possible means of increasing the solubility.

4.0 THE HARD SPHERE KINETIC THEORY

The kinetic theory is derived from a consideration of the basic mechanism of molecular interactions. Such a theory was found to describe exactly the transport properties of dilute gas (23). Enskog (24) extended the kinetic theory to higher density for single component systems by modeling molecules which consisted of hard spheres and by correcting for the presence of position correlation by introducing the function $g(\sigma)$. Further development of this theory was hindered by the lack of knowledge of $g(\sigma)$. Recent publications of solution of the Percus-Yevick theory for $g(\sigma)$ (25-27) have revived the interest of many workers (28-30) on the kinetic theory.

4.1 Expression for Multicomponent Diffusion Coefficients

Tham and Gubbins (31), derived from the modified Boltzmann equation (Appendix B), an expression for multicomponent diffusion coefficients. Their expression is

$$\sum_{j\neq q} F_{ij}\, m_\ell\, D_{j\ell} = E_{im}\frac{P_\ell}{P_m} - E_{i\ell} \qquad (4\text{-}1)$$

$$(i,\ \ell = 1,\ \ldots\ \nu),\ \ell\neq m$$

where $$F_{ij} = -\sum_{\ell}\frac{n_i n_\ell g_{ij}\delta_{ij}}{n n_j \mathcal{D}_{i\ell}}(m_j m_i)^{-1/2} + \frac{n_i g_{ij}}{n m_j \mathcal{D}_{ij}}$$

$$\sum_{\ell}\frac{n_i n_\ell g_{i\ell}}{n n_q \mathcal{D}_{i\ell}}(m_q m_\ell)^{-1/2}\left[\left(\frac{m_\ell}{m_i}\right)^{1/2}\delta_{iq} - \delta_{\ell q}\right]$$

$D_{j\ell}$ = multicomponent diffusion coefficient of species j due to gradient of ℓ, in the mass average frame.

$$\mathcal{D}_{i\ell} = \frac{3}{8n\sigma_{i\ell}^2} \sqrt{\frac{\pi kT(m_i + m_\ell)}{(m_i m_\ell)}}$$

$$P_m = \sum_i (\delta_{im} + 2\rho b_{mi} g_{im} + \sum_k n_i \rho b_{ik} \frac{\partial g_{ik}}{\partial n_m})$$

$$= \sum_i E_{im}$$

m_ℓ = mass per molecule of species ℓ

n_i = number density of species i

$n = \sum_i n_i$

σ_i = hard sphere diameter of species i

$$\sigma_{i\ell} = \frac{\sigma_i + \sigma_\ell}{2} .$$

It is noted that, in the case where one component (component 1 for example) is infinitely dilute, then

$$D_{1j} = 0 \qquad \text{for } j \neq 1$$

also the diffusion coefficient in the mass average frame is equal to that in the volume average frame.

4.2 Calculation

The procedure used by Tham and Gubbins (31) for calculating

diffusion coefficient is to obtain hard sphere diameters for the dilute species (gas) and water from self-diffusion coefficient data (23), and using Pauling ionic radii for the ions. In the case of simple electrolytes, this method of calculation gives results in reasonable agreement with experimental results (2,32). Using the same set of parameters, unfortunately does not give as good an agreement for KOH and LiOH. This may be due both to the structure breaking nature and the hydration formation nature of KOH molecules in aqueous solution (33). Figures 4-1 and 4-2 show comparisons between experimental and calculated values using parameter shown in Table 3-1. The agreement for both cases is within experimental error.

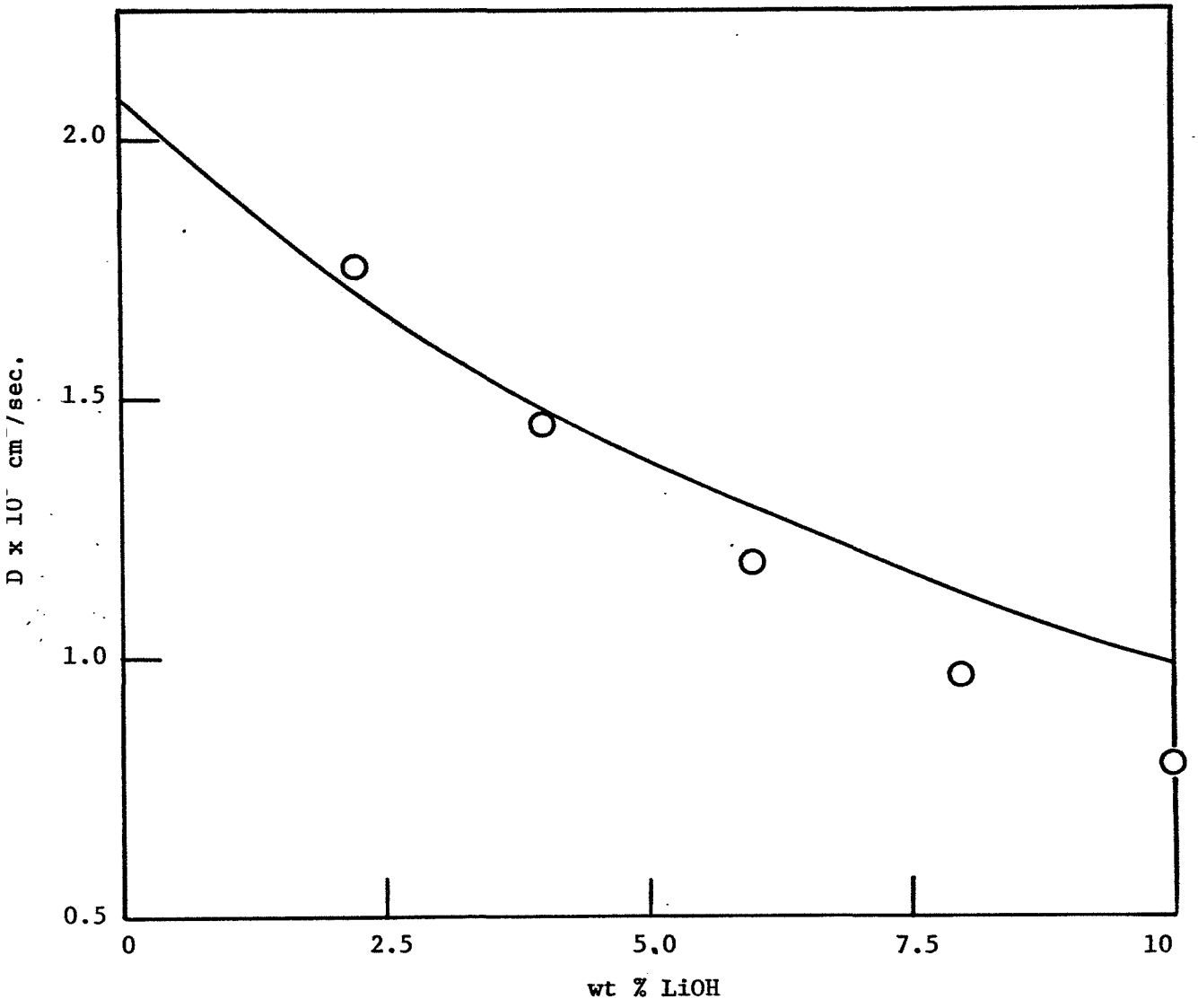

Figure 4-1. Diffusion Coefficients of Oxygen in Lithium Hydroxide Solution at 25°C. O experimental data. ——— Kinetic Theory.

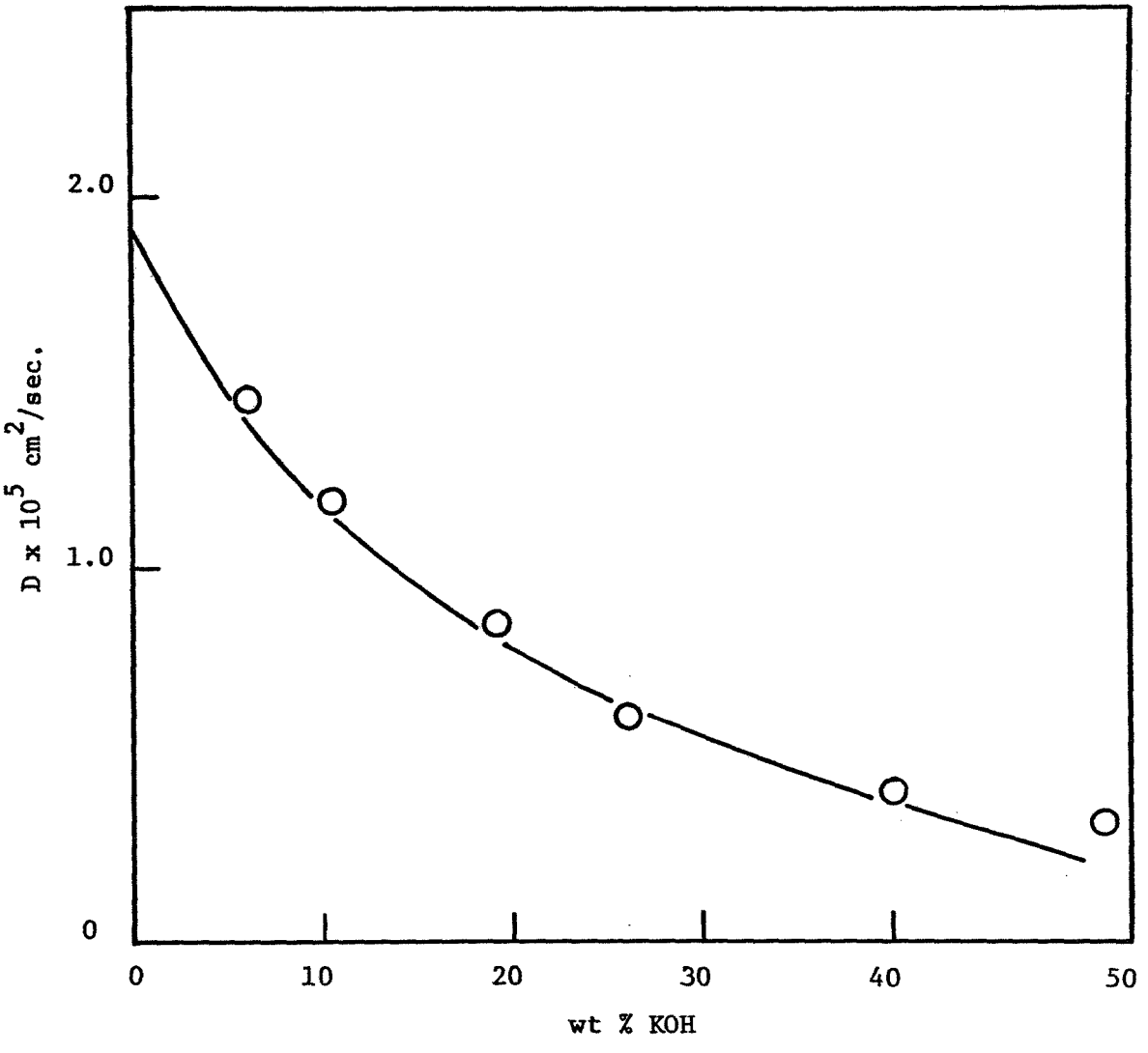

Figure 4-2. Diffusion Coefficients of Oxygen in Potassium Hydroxide Solution at 25°C. O Experimental Data. ——— Kinetic Theory.

5.0 VAPOR PRESSURE OF STRONG ELECTROLYTES

5.1 Binary System (K_2CO_3-H_2O, KOH-H_2O and LiOH-H_2O)

Experimental measurements of the vapor pressure of the systems KOH-H_2O, and LiOH-H_2O performed in this and other laboratories have been reported previously (34,35). These experimental data were used to fit the Antoine equation. The resultant parameters were also reported (34,36).

5.1.1 Antoine Parameter for K_2CO_3-H_2O

In the following, the vapor pressure data for K_2CO_3-H_2O system (37) was fitted by means of the Antoine equation

$$\log_{10} P = A - \frac{B}{C + T} \qquad (5\text{-}1)$$

where P is vapor pressure in mm Hg, T is the temperature in °C, and A, B, and C are constants that vary with K_2CO_3 concentration. The method described in reference 34 was used. Table 5-1 gives the values of A, B, and C which give the best fit to Eq. (5-1). The same problem, that of the smoothed Antoine constants not giving accurate vapor pressures, was encountered. Here the problem was somewhat aggravated by the fact that the vapor pressures were experimentally measured at only five concentrations and the rest were interpolated values.

Our belief is that the problem is two-fold: 1) the inaccuracy of the data, 2) the shortcomings of the Antoine model. Consequently, work will be undertaken to obtain better vapor pressure measurements through the use of an accurate monometer. Attempts will also be made at deriving a more suitable theoretical-empirical model for vapor pressures.

Table 5-1

Antoine Coefficients for K_2CO_3

$$\log_{10} P = A - \frac{B}{C + T}$$

Wt Pct	Molality	Temp Range	A	B	C
0	0	30°-80°	8.0657	1726.3	233
6.46	.5	30°-80°	8.0863	1741.2	234
12.14	1.0	30°-80°	8.2020	1814.3	240
17.17	1.5	30°-80°	8.2430	1842.3	242
21.65	2.0	30°-80°	8.2135	1831.2	241
25.68	2.5	30°-80°	8.1049	1772.8	236
29.31	3.0	30°-80°	8.3503	1925.0	248
32.60	3.5	30°-80°	8.4625	2002.2	254
35.60	4.0	30°-80°	8.6120	2102.2	261
38.34	4.5	30°-80°	8.5694	2082.5	259
40.86	5.0	30°-80°	8.8369	2264.1	272
43.19	5.5	30°-80°	8.8771	2298.6	274
45.33	6.0	30°-80°	9.1264	2475.5	286
52.51	8.0	30°-80°	11.0734	4014.2	375

Another source of data is that by Ravich et al. (38), who reported vapor pressure for K_2CO_3-H_2O system over a temperature range of 250° to 450°C and concentration up to 81 wt % K_2CO_3.

5.1.2 Dühring Plots

Tables 5-2 - 5-4 summarize the information we now have available on the KOH-H_2O, K_2CO_3-H_2O and LiOH-H_2O systems. The Dühring plot for KOH-H_2O was also given in Figure 5-1. Activity coefficients are available for the system KOH-H_2O (39). Work is planned to find methods to obtain the activity coefficients of the other electrolytes.

5.2 Ternary System K_2CO_3-KOH-H_2O

Experimental data for the vapor pressure of the ternary system K_2CO_3-KOH-H_2O are scarce. Recently, Kamino et al. (40) reported data for this system over a limited range of concentrations and temperatures. A few measurements on this system were also made in this laboratory using the isopiestic method. Table 5-5 summarizes all the data measured in this laboratory. Figures 5-2 to 5-5 give the Dühring plots for this system.

The number of variables involved in such measurement is large, hence the number of measurements one has to make will be enormous. At the present moment, in the lack of extensive experimental data it is desirable to study this problem from the theoretical point of view. The approach used is to calculate ternary vapor pressure from a knowledge of binary vapor pressure of the constituting substances. The model proposed is simple and plausible, and the results are quite encouraging.

5.2.1 Calculation of Ternary Vapor Pressure

Consider a non-ideal liquid solution in contact with a vapor

-- Table 5-2

Activity Coefficients of KOH

20°C

Wt %	Mole Fract	Molality	Molarity	Density	Activity Coefficient H_2O	Activity Coefficient KOH
4.72	.0157	.883	.876	1.041	.984	.751
9.09	.0311	1.782	1.759	1.086	.959	.831
16.66	.0603	3.563	3.453	1.163	.898	1.28
23.07	.0878	5.345	5.033	1.224	.804	2.02
28.57	.1138	7.128	6.522	1.281	.696	3.26
33.33	.1383	8.910	7.901	1.330	.596	5.23
37.50	.1615	10.693	9.156	1.370	.492	8.24
44.45	.2044	14.261	11.431	1.443	.315	19.3
50.00	.2430	17.822	13.322	1.495	.195	39.1
54.55	.2782	21.391	15.021	1.545	.125	72.8

40°C

4.72	.0157	.883	.867	1.031	.983	.744
9.09	.0311	1.782	1.744	1.077	.959	.807
16.66	.0603	3.563	3.420	1.152	.911	1.21
23.07	.0878	5.345	4.984	1.212	.807	1.83
28.57	.1138	7.128	6.461	1.269	.702	2.83
33.33	.1383	8.910	7.830	1.318	.604	4.36
37.50	.1615	10.693	9.076	1.358	.504	6.60
44.45	.2044	14.261	11.320	1.429	.336	14.3
50.00	.2430	17.822	13.197	1.481	.212	27.4
54.55	.2782	21.391	14.856	1.528	.137	51.6

60°C

4.72	.0157	.883	.861	1.023	.983	.711
9.09	.0311	1.782	1.731	1.069	.960	.787
16.66	.0603	3.563	3.393	1.143	.922	1.10
23.07	.0878	5.345	4.951	1.204	.809	1.60
28.57	.1138	7.128	6.410	1.259	.708	2.38
33.33	.1383	8.910	7.764	1.307	.611	3.53
37.50	.1615	10.693	8.996	1.346	.516	5.16
44.45	.2044	14.261	11.225	1.417	.358	10.5
50.00	.2430	17.822	13.099	1.470	.235	18.7
54.55	.2782	21.391	14.710	1.513	.154	32.3

-- Table 5-2

(Continued)

80°C

Wt %	Mole Fract	Molality	Molarity	Density	Activity Coefficient H_2O	Activity Coefficient KOH
4.72	.0157	.883	.852	1.012	.983	.681
9.09	.0311	1.782	1.714	1.058	.960	.735
16.66	.0603	3.563	3.361	1.132	.932	.980
23.07	.0878	5.345	4.897	1.191	.812	1.37
28.57	.1138	7.128	6.349	1.247	.713	1.69
33.33	.1383	8.910	7.675	1.292	.619	2.55
37.50	.1615	10.693	8.902	1.332	.529	4.01
44.45	.2044	14.261	11.106	1.402	.382	7.56
50.00	.2430	17.822	12.966	1.455	.263	12.6
54.55	.2782	21.391	14.564	1.498	.175	20.2

100°C

4.72	.0157	.833	.840	.998	.982	.623
9.09	.0311	1.782	1.684	1.040	.961	.686
16.66	.0603	3.563	3.310	1.115	.941	.868
23.07	.0878	5.345	4.815	1.171	.814	1.05
28.57	.1138	7.128	6.237	1.225	.718	1.42
33.33	.1383	8.910	7.544	1.270	.627	2.05
37.50	.1615	10.693	8.748	1.309	.542	3.00
44.45	.2044	14.261	10.916	1.378	.407	5.38
50.00	.2430	17.822	12.725	1.428	.296	8.38
54.55	.2782	21.391	14.292	1.470	.201	12.2

-- Table 5-3

Activity Coefficients of K_2CO_3

30°C

Wt %	Mole Fract	Molality	Molarity	Density	Activity Coefficient H_2O
6.46	.0089	.5	.493	1.0536	.9846
12.14	.0177	1.0	.974	1.1085	.9700
17.17	.0263	1.5	1.437	1.1563	.9563
21.65	.0348	2.0	1.884	1.2023	.9325
25.68	.0431	2.5	2.314	1.2452	.9081
29.31	.0513	3.0	2.725	1.2849	.8855
32.60	.0593	3.5	3.117	1.3212	.8620
35.60	.0672	4.0	3.494	1.3565	.8228
38.34	.0750	4.5	3.853	1.3889	.7856
40.86	.0826	5.0	4.196	1.4191	.7496
43.19	.0902	5.5	4.524	1.4478	.7155
45.33	.0975	6.0	4.836	1.4744	.6826
52.51	.126	8.0	5.957	1.5681	.5216

40°C

6.46	.0089	.5	.491	1.0500	.9858
12.14	.0177	1.0	.969	1.1026	.9711
17.17	.0263	1.5	1.431	1.1517	.9573
21.65	.0348	2.0	1.876	1.1973	.9335
25.68	.0431	2.5	2.305	1.2401	.9093
29.31	.0513	3.0	2.714	1.2796	.8864
32.60	.0593	3.5	3.102	1.3150	.8636
35.60	.0672	4.0	3.480	1.3511	.8255
38.34	.0750	4.5	3.837	1.3833	.7889
40.86	.0826	5.0	4.179	1.4135	.7542
43.19	.0902	5.5	4.506	1.4421	.7205
45.33	.0975	6.0	4.817	1.4686	.6892
52.51	.126	8.0	5.934	1.5621	.5291

Table 5-3

(Continued)

50°C

Wt %	Mole Fract	Molality	Molarity	Density	Activity Coefficient H_2O
6.46	.0089	.5	.489	1.0450	.9863
12.14	.0177	1.0	.964	1.0973	.9724
17.17	.0263	1.5	1.424	1.1462	.9586
21.65	.0348	2.0	1.867	1.1917	.9349
25.68	.0431	2.5	2.293	1.2344	.9114
29.31	.0513	3.0	2.702	1.2739	.8885
32.60	.0593	3.5	3.091	1.3101	.8659
35.60	.0672	4.0	3.464	1.3452	.8284
38.34	.0750	4.5	3.821	1.3775	.7939
40.86	.0826	5.0	4.162	1.4076	.7591
43.19	.0902	5.5	4.488	1.4363	.7267
45.33	.0975	6.0	4.798	1.4628	.6952
52.51	.126	8.0	5.912	1.5563	.5455

60°C

6.46	.0089	.5	.487	1.0400	.9860
12.14	.0177	1.0	.960	1.0920	.9730
17.17	.0263	1.5	1.418	1.1407	.9596
21.65	.0348	2.0	1.859	1.1862	.9368
25.68	.0431	2.5	2.283	1.2287	.9134
29.31	.0513	3.0	2.690	1.2683	.8910
32.60	.0593	3.5	3.079	1.3052	.8687
35.60	.0672	4.0	3.450	1.3394	.8322
38.34	.0750	4.5	3.805	1.3717	.7980
40.86	.0826	5.0	4.145	1.4018	.7637
43.19	.0902	5.5	4.470	1.4305	.7316
45.33	.0975	6.0	4.779	1.4570	.7012
52.51	.126	8.0	5.890	1.5505	.5456

Table 5-3

(Continued)

70°C

Wt %	Mole Fract	Molality	Molarity	Density	Activity Coefficient H_2O
6.46	.0089	.5	.484	1.0341	.9865
12.14	.0177	1.0	.954	1.0861	.9744
17.17	.0263	1.5	1.410	1.1347	.9615
21.65	.0348	2.0	1.849	1.1802	.9389
25.68	.0431	2.5	2.272	1.2228	.9162
29.31	.0513	3.0	2.677	1.2623	.8948
32.60	.0593	3.5	3.051	1.2993	.8733
35.60	.0672	4.0	3.435	1.3337	.8375
38.34	.0750	4.5	3.789	1.3658	.8043
40.86	.0826	5.0	4.127	1.3959	.7713
43.19	.0902	5.5	4.451	1.4246	.7406
45.33	.0975	6.0	4.759	1.4510	.7105
52.51	.126	8.0	5.867	1.5444	.5637

80°C

6.46	.0089	.5	.481	1.0281	.9880
12.14	.0177	1.0	.949	1.0800	.9753
17.17	.0263	1.5	1.403	1.1287	.9634
21.65	.0348	2.0	1.840	1.1742	.9422
25.68	.0431	2.5	2.261	1.2168	.9203
29.31	.0513	3.0	2.664	1.2563	.9001
32.60	.0593	3.5	3.051	1.2934	.8796
35.60	.0672	4.0	3.420	1.3276	.8467
38.34	.0750	4.5	3.772	1.3599	.8139
40.86	.0826	5.0	4.110	1.3900	.7829
43.19	.0902	5.5	4.433	1.4186	.7523
45.33	.0975	6.0	4.740	1.4450	.7238
52.51	.126	8.0	5.844	1.5383	.5822

Table 5-3

(Continued)

90°C

Wt %	Mole Fract	Molality	Molarity	Density	Activity Coefficient H_2O
6.46	.0089	.5	.478	1.0218	.9881
12.14	.0177	1.0	.932	1.0611	.9772
17.17	.0263	1.5	1.395	1.1227	.9649
21.65	.0348	2.0	1.831	1.1683	.9440
25.68	.0431	2.5	2.250	1.2109	.9232
29.31	.0513	3.0	2.652	1.2504	.9037
32.60	.0593	3.5	3.037	1.2875	.8837
35.60	.0672	4.0	3.404	1.3217	.8510
38.34	.0750	4.5	3.756	1.3540	.8204
40.86	.0826	5.0	4.093	1.3841	.7901
43.19	.0902	5.5	4.414	1.4127	.7615
45.33	.0975	6.0	4.720	1.4391	.7329
52.51	.126	8.0	5.821	1.5322	.5923

100°C

6.46	.0089	.5	.474	1.0140	.9877
12.14	.0177	1.0	.938	1.0677	.9749
17.17	.0263	1.5	1.388	1.1167	.9630
21.65	.0348	2.0	1.821	1.1623	.9428
25.68	.0431	2.5	2.239	1.2050	.9233
29.31	.0513	3.0	2.640	1.2445	.9043
32.60	.0593	3.5	3.024	1.2816	.8853
35.60	.0672	4.0	3.389	1.3159	.8533
38.34	.0750	4.5	3.740	1.3482	.8225
40.86	.0826	5.0	4.075	1.3783	.7929
43.19	.0902	5.5	4.396	1.4068	.7643
45.33	.0975	6.0	4.701	1.4332	.7364
52.51	.126	8.0	5.798	1.5262	.6169

-- Table 5-4

Activity Coefficients of LiOH

25°C

Wt %	Mole Fract	Molality	Molarity	Density	Activity Coefficient H_2O
1.90	.0143	.809	.809	1.0192	.9885
3.85	.0292	1.672	1.673	1.0406	.9789
6.45	.0492	2.879	2.877	1.0683	.9539
8.05	.0618	3.656	3.648	1.0852	.9478
10.10	.0779	4.692	4.668	1.1067	.9269

40°C

1.90	.0143	.809	.805	1.0144	.9881
3.85	.0292	1.672	1.665	1.0355	.9712
6.45	.0492	2.879	2.863	1.0629	.9586
8.05	.0618	3.656	3.629	1.0795	.9445
10.10	.0779	4.692	4.642	1.1006	.9131

60°C

2.40	.0181	1.027	1.014	1.0115	.9825
4.82	.0367	2.115	2.087	1.0372	.9715
6.45	.0492	2.879	2.839	1.0542	.9639
8.52	.0655	3.889	3.826	1.0754	.9515
10.20	.0787	4.743	4.655	1.0928	.9383

80°C

1.90	.0143	.809	.791	.9962	.9887
3.85	.0292	1.672	1.635	1.0173	.9709
6.45	.0492	2.879	2.858	1.0611	.9585
8.05	.0618	3.656	3.565	1.0605	.9527
10.10	.0779	4.692	4.561	1.0813	.9525

100°C

1.90	.0143	.809			.9770
3.85	.0292	1.672			.9417
6.45	.0492	2.879			.8834
8.05	.0618	3.656			.8441
10.10	.0779	4.692			.7844

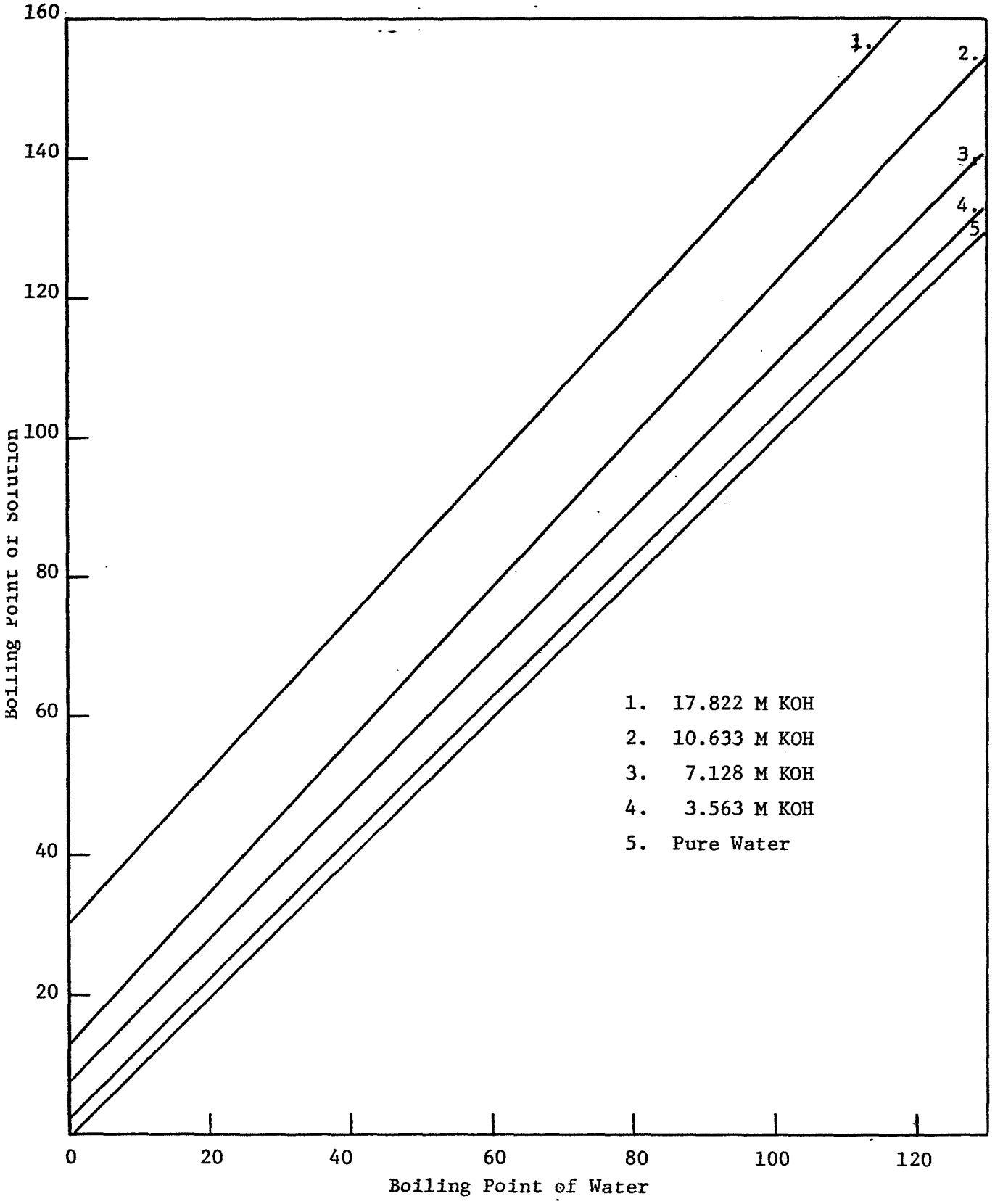

Figure 5-1. Dühring Plot for KOH-H_2O

Table 5-5

Vapor Pressure of Water Over KOH-K_2CO_3 Solutions

T = 25.00°C $\quad p^o_{H_2O}$ = 23.76 mm Hg

Wt. % KCl	Vapor Pressure, mm Hg	Wt. % KOH	Wt. % K_2CO_3	Wt. % H_2O	$U_{H_2O} = p/p^o$
25.14	14.77	19.96	0	80.04	0.62
25.05	14.78	18.94	0	81.06	0.62
25.16	14.77	18.74	0	81.26	0.62
25.04	14.78	20.21	4.62	75.17	0.62
25.23	14.76	20.22	4.69	75.09	0.62
25.00	14.78	19.32	6.56	74.12	0.62
25.99	14.66	20.92	5.22	73.86	0.62
25.88	14.67	20.34	5.08	74.68	0.62
26.94	14.53	27.05	8.93	64.02	0.61
26.79	14.55	26.74	8.69	64.57	0.61
26.92	14.53	27.30	9.51	63.19	0.61
27.44	14.46	26.46	10.29	63.25	0.61
27.59	14.43	32.84	12.19	54.97	0.61
28.03	14.37	30.52	13.14	56.44	0.60
27.80	14.40	31.79	13.85	45.64	0.61
28.51	14.30	31.06	13.69	44.75	0.60
28.11	14.36	32.26	12.66	44.92	0.61
27.46	14.45	32.08	13.85	45.93	0.61
25.76	14.69	30.76	17.75	48.51	0.62
28.71	14.27	30.99	18.40	49.39	0.60
30.88	13.97	30.02	16.78	46.80	0.59
28.99	14.24	30.95	18.44	49.39	0.60

All wt. % figures average of 3 experiments (not 3 aliquots).

Isopiestic method: KCl solution brought to equilibrium with KOH-K_2CO_3 solution, and final concentrations determined by titration. Vapor pressures taken from International Critical Tables.

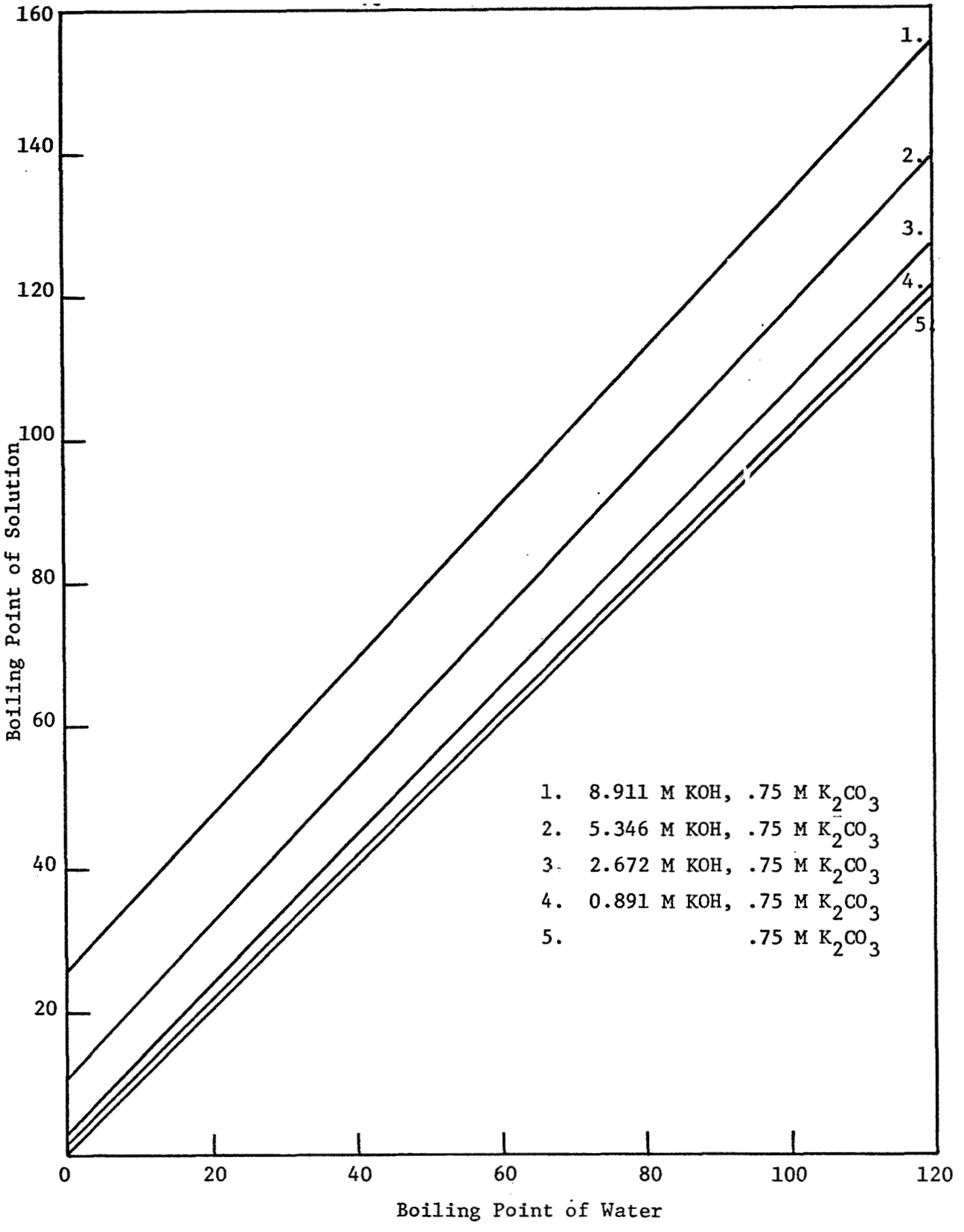

Figure 5-2. Dühring Plot for KOH-K_2CO_3-H_2O: 0.75 M K_2CO_3

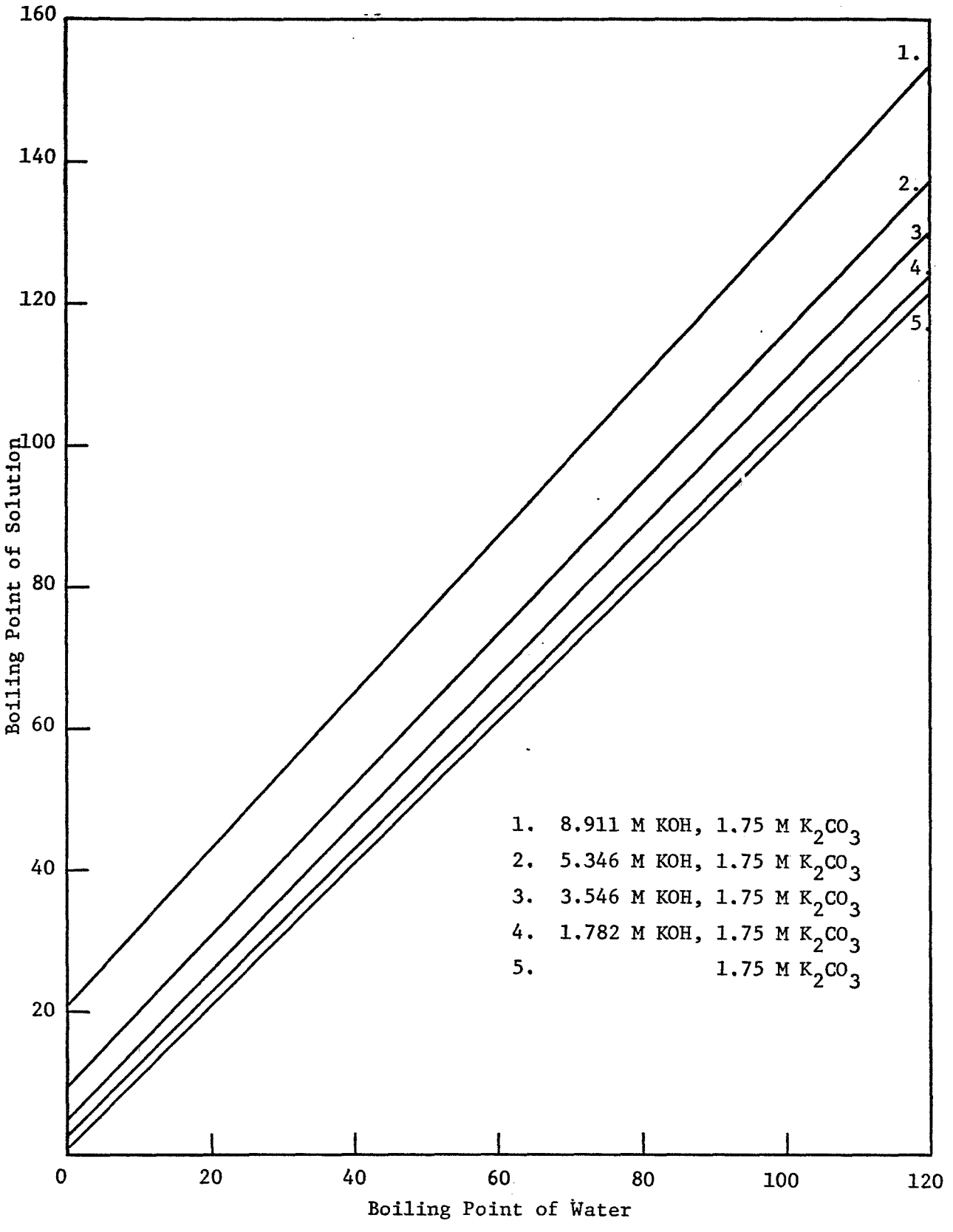

Figure 5-3. Dühring Plot for KOH-K_2CO_3-H_2O: 1.75 M K_2CO_3

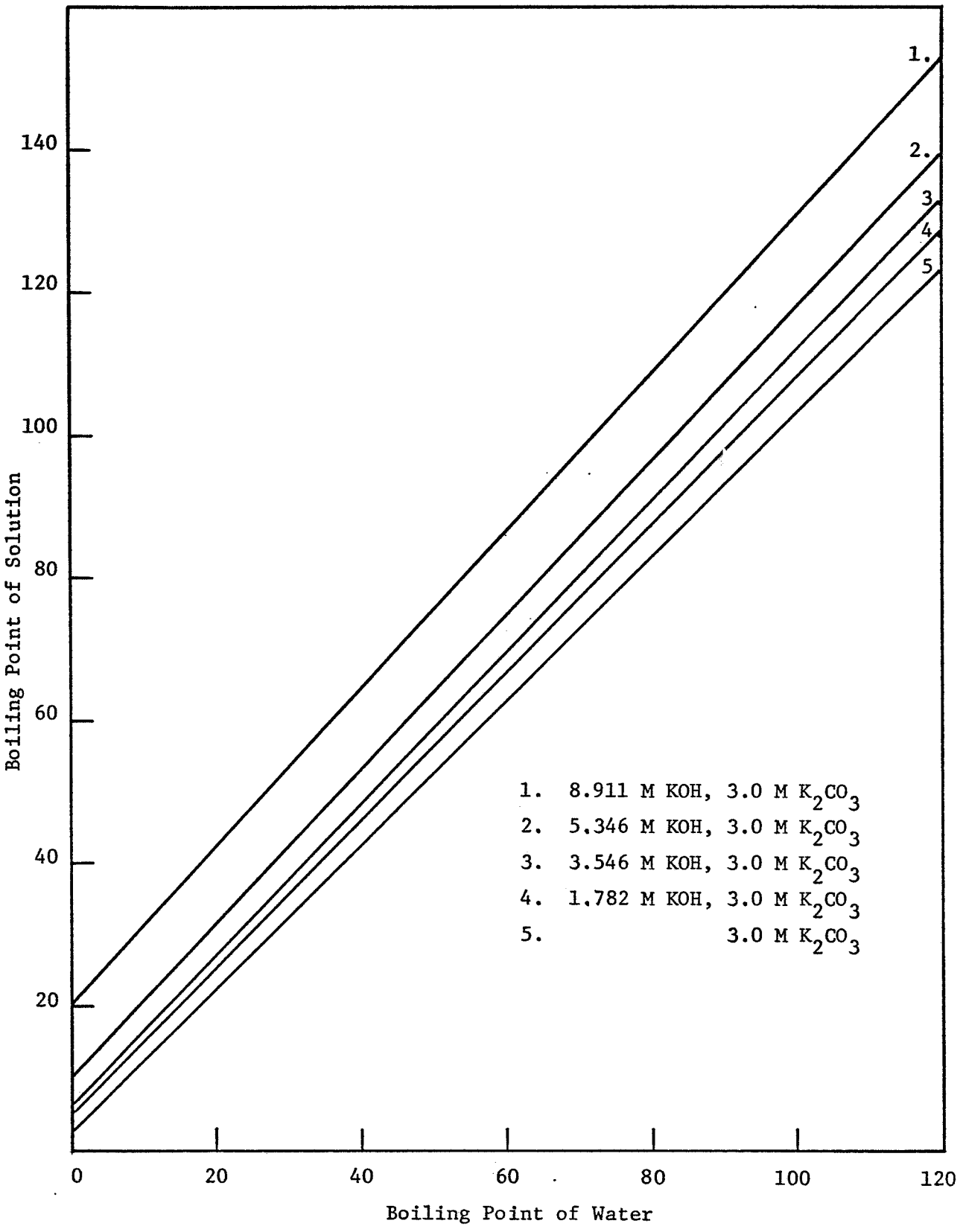

Figure 5-4. Dühring Plot for KOH-K_2CO_3-H_2O

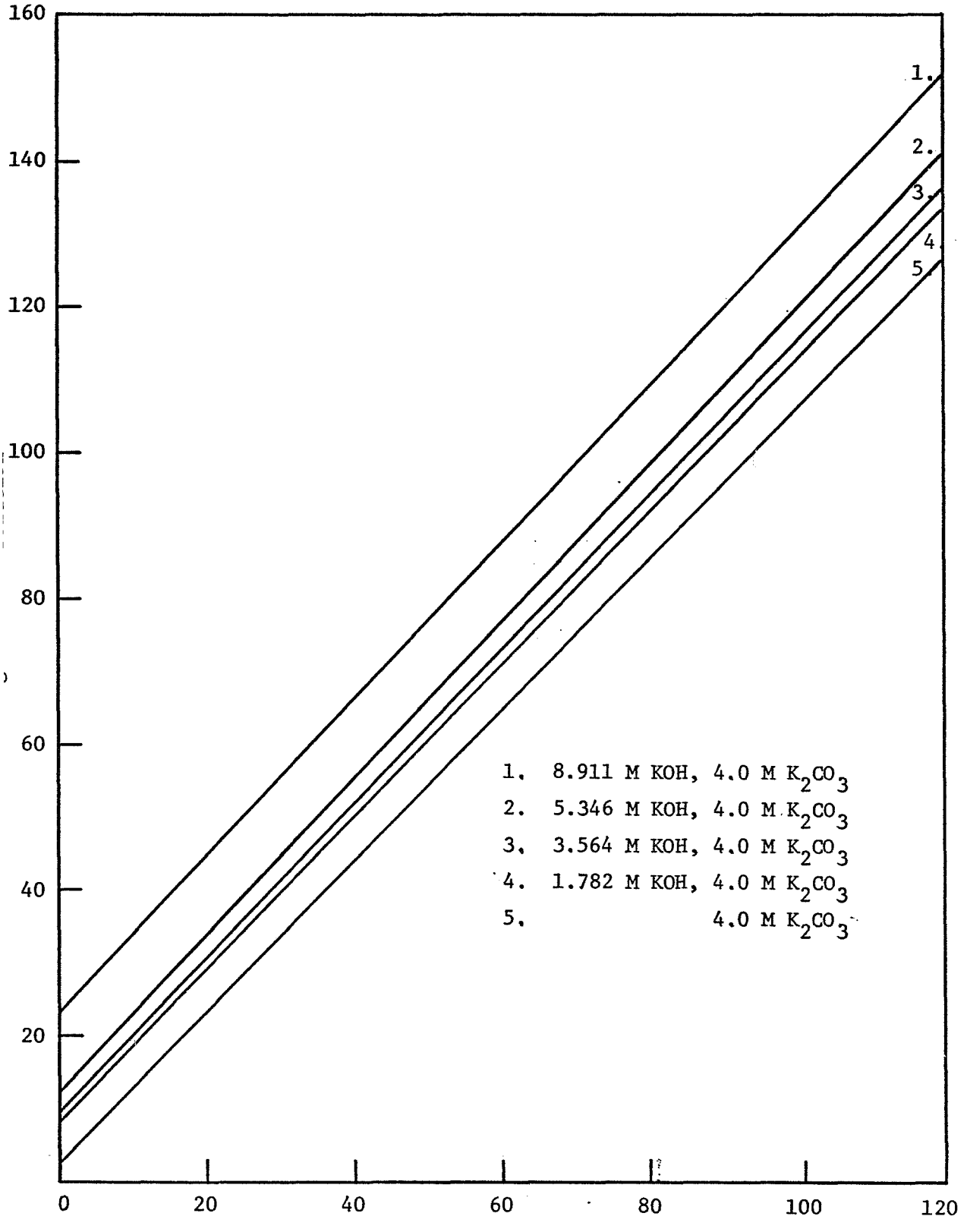

Figure 5-5. Dühring Plot for KOH-K_2CO_3-H_2O

phase. For any component i

$$f_i^G = f_i^L \tag{5-2}$$

where superscripts G and L refer to the gas and liquid phase and f_i is the fugacity of component i. In our region of interest, near atmospheric pressure, the gas phase is essentially ideal and

$$f_i^G = P_i \tag{5-3}$$

the fugacity can be replaced by the partial pressure. The fugacity in the liquid phase is given by

$$f_i^L = x_i \gamma_i f_i^s \tag{5-4}$$

where γ_i is the activity coefficient and f_i^s is the standard state fugacity. For water the standard state is pure liquid at the same temperature and pressure as the mixture, i.e. its pure component vapor pressure at the temperature of interest. Combining Equations (5-2), (5-3), and (5-4) with the above leads to

$$P_i = x_i \gamma_i P^o \tag{5-5}$$

where P^o is the pure component vapor pressure. Since in our systems, the solute is non-volatile, Eq. (5-4) also describes the total vapor

pressure of the solution.-

For a binary solution of water and non-volatile solute:

$$x_w = \frac{1000./18.015}{(1000./18.015) + m} \qquad (5\text{-}6)$$

where x_w is the mole fraction of water and m is the molality of the solute.

$$\gamma_w = \frac{P_w}{(x_w P^o)} \qquad (5\text{-}7)$$

describes the activity coefficient of water in the above binary solution where P_w is the partial pressure of the water above the solution, i.e. the vapor pressure of the solution.

It has been postulated that knowing the molalities and vapor pressures of two such binary solutions, the vapor pressure of their mixture could be predicted, thus allowing prediction of the vapor pressure of a ternary solution from the individual component solution vapor pressures (40).

$$P_3 = \frac{P_1 m_1 + P_2 m_2}{m_1 + m_2} \qquad (5\text{-}8)$$

where P_3 refers to the vapor pressure of the ternary solution, P_1 and P_2 to the vapor pressures of the two binary solutions, and m_1 and m_2 to their molalities. Putting this in terms of mole fractions and activity coefficients yields

$$\gamma_3 \, x_3 \, P^o = \frac{\gamma_1 x_1 m_1 P^o + \gamma_2 x_2 m_2 P^o}{m_1 + m_2} \qquad (5\text{-}9)$$

but

$$x_{w_3} = \frac{2 \, x_{w_1} x_{w_2}}{x_{w_1} + x_{w_2}} \qquad (5\text{-}10)$$

substituting Eq. (5-9) into Eq. (5-8) and solving for γ_3 yields

$$\gamma_3 = \frac{(x+Y)(\gamma_1 m_1 Y + \gamma_2 m_2 x)}{2xY(m_1 + m_2)} \qquad (5\text{-}11)$$

where: $x = \frac{1000}{18.015} + m_1$

$Y = \frac{1000}{18.015} + m_2$

thus giving the activity coefficient for water in a ternary solution as a function of the component binary solutions' activity coefficients and molalities. The following would be a more convenient form for those interested in vapor pressures of the ternary solutions directly.

$$\gamma_3 x_3 = \frac{\frac{1000.}{18.015} (\gamma_1 m_1 Y + \gamma_2 m_2 x)}{xY \, (m_1 + m_2)} \qquad (5\text{-}12)$$

thus the vapor pressure could be found by multiplying Eq. (5-11) by the pure component vapor pressure P^o.

Eq. (5-7) would have the most practical interest, while Eq. (5-11) should have some theoretical interest.

Sample Calculation

Mixture composition - 417.4 g K_2CO_3, 343.3 g KOH, 1000 g H_2O

m_1 = 417.4/138.2 = 3.02 moles/500 g => 6.04 molal K_2CO_3

m_2 = 343.3/56.1 = 6.12 moles/500 g => 12.24 molal KOH

P_1 = 93 mm Hg
P_2 = 55 mm Hg
} experimental

Using Eq. (5-8)

$$P_3 = \frac{(93)(6.04) + (55)(12.24)}{(6.04 + 12.24)} = 68.1 \text{ mm Hg}$$

experimental = 72 mm Hg

to find the activity coefficient of water on a ternary mixture from individual solution activity coefficient:

m_1 = 6.04	x_1 = .902	γ_1 = .691	Y = 67.75
m_2 = 12.24	x_2 = .819	γ_2 = .450	x = 61.55

Using Eq. (5-11)

$$\gamma_3 = \frac{(x + Y)(\gamma_1 m_1 Y + \gamma_2 m_2 x)}{2xY(m_1 + m_2)}$$

$$\gamma_3 = .528$$

This method has been shown accurate to individual component binary mixture concentrations of as high as 10 molal in KOH and 6 molal in K_2CO_3. Further studies will be undertaken to determine the full range of applicability.

One precaution must be taken when working with ternary solutions that are already mixed, the usual applicability. The molalities, m_1 and m_2, refer to the individual molalities before mixing. Thus, a solution which contained 6 gram moles KOH and 3 gram moles K_2CO_3 in 1000 grams of water would be treated as 12 molal in KOH and 6 molal in K_2CO_3 rather than 6 molal in KOH and 3 molal in K_2CO_3.

6.0 PHYSICAL PROPERTIES OF THE TERNARY SYSTEM: $KOH-K_2CO_3-H_2O$

6.1 Phase Equilibrium

6.1.1 Binary System: $KOH-H_2O$

The solid-liquid phase equilibria of $KOH-H_2O$ covering a significant range of concentrations were reported by several authors (41-45). The hydrates observed are $KOH.H_2O$ and $KOH.2H_2O_3$ while the latter present mainly at low temperatures, the former form of hydrate predominates above 25°C. The Eutectic is at 100.4°C and 85%.

Solvay (43), Vogel *et al*. (33), Mashovets *et al*. (45) and Merkel (46) reported vapor pressure for aqueous as well as molten $KOH-H_2O$. An attempt to fit experimental results by means of the Antoine equation was also reported by Walker (34).

6.1.2 Binary System: $K_2CO_3-H_2O$

The solid-liquid equilibrium for this system has been studied (47-53). The most extensive study is that of Carbonnel (48), who reported the complete phase diagram from -36° to +6°C and at 135°C (Normal boiling point of saturated K_2CO_3 solution). The hydrates formed are: $K_2CO_3.5H_2O$ below -5°C, $K_2CO_3.1.5H_2O$ between -6°C and 147°C. Between 147° and 153°C, a third hydrate, $K_2CO_3.0.5H_2O_3$ which has a very narrow domain was identified. The eutectic point is at -36.4°C, with 40.4% K_2CO_3. Hill's (53) conclusion that below -5°C, the hydrate is $K_2CO_3.6H_2O$ has been disputed by Carbonnel (48), who took pains to verify that the solid phase below -6°C is $K_2CO_3.5H_2O$ rather than $K_2CO_3.6H_2O$, using both the "Ensemble" method and the "Thermic" method.

Toshi et al. (54) also reported liquid-solid equilibrium data for 20, 30, and 40% K_2CO_3.

A brief discussion on the vapor pressure of this system is given in Chapter 4.

6.1.3 Ternary System: K_2CO_3-KOH-H_2O

The early report on the solid-liquid equilibrium data by Green et al. (55) and Itkina (56) are not in complete agreement with each other.

Recently, Carbonnel (48,57) reported data on this system at -22°, 30.7°C and from -60° to 140°C, Hostalek and Kasparova (58) studied this system for temperature range from 20° to 100°C; other investigators are Kamino and Miyaji (59) (from 0° to 90°C), and Klebanov and Pinchuk (60) (at 0°, 25° and 50°C). Comparison between data given by these authors, however, does not reveal any discrepancies. The hydrate observed confirmed those reported for the binary systems discussed above. The domain for the hydrate $K_2CO_3.0.5H_2O$ is again very narrow. It is observed that, the alkali KOH showed a very strong salting-out effect. Consequently, the concentration of K_2CO_3 decreases rapidly as KOH concentration increases. One interesting observation made by Kamino and Miyaji (59), is that the total potassium ionic concentration remains practically constant at a given temperature, in the saturated ternary solutions, and increases slightly with temperature. So far no explanation has been advanced Figure 6-1 shows a typical solid-liquid phase diagram, and Tables 6-1 - 6-4 give the experimental data reported.

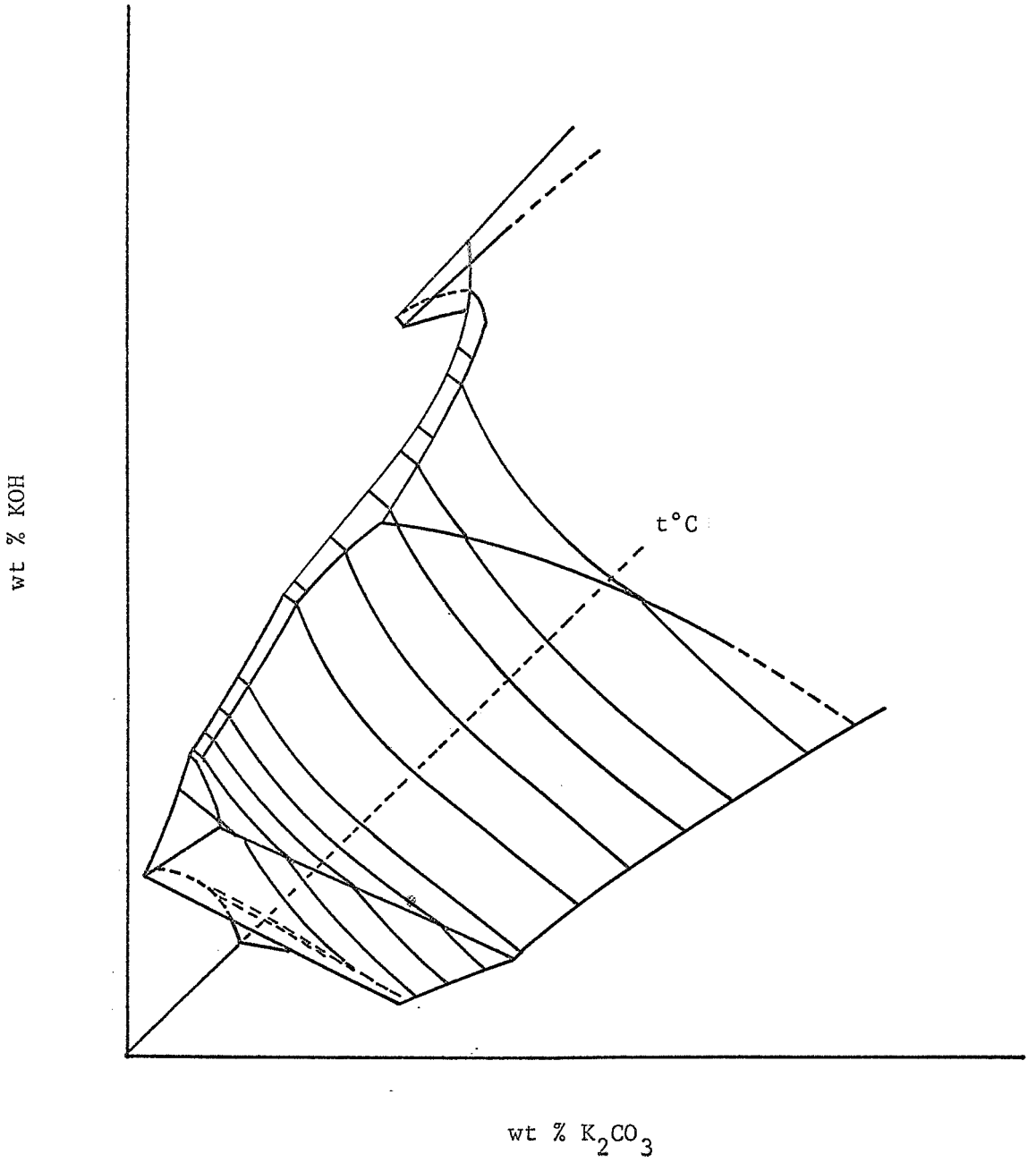

Figure 6-1. Solid-Liquid Phase Equilibrium for KOH-K_2CO_3-H_2O.

-- Table 6-1

Solid-Liquid Equilibrium for $KOH-K_2CO_3-H_2O$

Isotherm at 30.7°C

Solution Conc.	Liquid Phase Conc.	Solid Phase	Solution Conc.	Liquid Phase Conc.	Solid Phase
	53.31*	$K_2CO_3.1.5H_2O$	4.45	2.38	$K_2CO_3.1.5H_2O$
	0.00		53.50	55.03	
	43.00	"	5.13	2.40	$K_2CO_3 1.5H_2O$
	8.20		53.65	54.70	$KOH.2H_2O$
	40.76	"		2.38	"
	9.90			54.58	
53.04	31.80			2.37	"
10.06	17.44			54.60	
	31.93	"	6.47	2.39	"
	17.29		55.28	54.74	
53.00	30.40	"	0.73	1.90	$KOH.2H_2O$
10.75	18.80		58.53	54.93	
42.80	22.40	"	0.63	1.30	"
17.04	25.40		57.98	55.20	
53.89	18.10	"	0.72	0.84	"
13.50	29.20		56.07	55.63	
26.36	11.67	"	0.87	1.00	"
28.79	35.90		56.20	55.38	
31.98	9.66	"		0.00	"
26.52	37.77			56.50	
29.84	9.22	"	6.47	2.38	$K_2CO_3.1.5H_2O$
27.40	38.00		55.28	55.51	$KOH.1H_2O$
40.04	8.31	"	3.20	2.37	"
23.29	39.80		57.72	55.60	

* First figure represents wt % K_2CO_3, the second that of KOH.

-- Table 6-1

(Continued)

Solution Conc.	Liquid Phase Conc.	Solid Phase	Solution Conc.	Liquid Phase Conc.	Solid Phase
42.48	6.95	$K_2CO_3.1.5H_2O$		1.09	$KOH.1H_2O$
22.38	42.00			56.40	
	5.50	"	0.76	0.89	"
	44.00		59.25	56.62	
	5.30	"	0.63	0.68	"
	44.40		57.98	56.98	
8.08	2.50	"	0.72	0.00	"
50.30	53.85		58.86	56.66	
5.07	2.38	"		0.00	"
53.48	55.21			58.00	

-- Table 6-2

Solid-Liquid Equilibrium for K_2CO_3-KOH-H_2O:

Isotherm at 0.45°C

Solution Conc.	Liquid Phase Conc.	Solid Phase	Solution Conc.	Liquid Phase Conc.	Solid Phase
	51.25*	$K_2CO_3.1.5H_2O$	36.20	11.10	$K_2CO_3.1.5H_2O$
	0.00		22.00	33.60	
50.23	47.20	"	25.38	5.03	"
2.85	3.10		30.84	41.08	
47.96	42.15	"	30.32	2.84	"
6.04	6.95		29.78	44.84	
45.27	40.60	"		2.36	"
7.48	8.39			46.10	
45.10	37.86	"	30.21	2.31	"
8.88	10.35		30.71	46.75	
40.43	31.55	"	4.00	1.89	$K_2CO_3.1.5H_2O$
12.83	15.70		48.67	47.70	$KOH.2H_2O$
	25.45	"		1.87	"
	20.42			47.60	"
40.22	23.86	"	0.85	1.25	$KOH.2H_2O$
15.88	21.83		51.80	48.00	
23.30	17.70	"		0.00	$KOH.2H_2O$
24.95	27.30			48.95	

* First figure represents wt % K_2CO_3, the second that of KOH

Table 6-3

Solid-Liquid Equilibrium for KOH-K_2CO_3-H_2O:

Isotherm at - 12°C

Solution Conc.	Liquid Phase Conc.	Solid Phase	Solution Conc.	Liquid Phase Conc.	Solid Phase
	47.70*	$K_2CO_3.5H_2O$	40.00	19.00	$K_2CO_3.1.5H_2O$
	0.00		16.85	25.30	
	42.90	"	30.55	7.00	"
	4.65		25.10	36.10	
46.22	41.50	"	39.00	4.70	"
4.24	6.00		23.00	40.20	
47.95	40.90	"		2.10	$K_2CO_3.1.5H_2O$
4.12	6.80			45.50	KOH.2 H_2O
45.09	40.33	"	5.71	2.07	"
5.40	7.32		49.20	45.50	
47.54	40.00	"	0.70	1.20	KOH.2 H_2O
5.04	8.10		51.67	46.20	
48.05	39.60	"		0.00	"
5.20	8.70			47.50	
42.10	30.80	"		20.90	Ice
9.85	11.80			0.00	
50.00	43.20	$K_2CO_3.1.5H_2O$	14.20	18.00	"
4.90	5.90		2.60	3.20	
45.10	36.45	"	14.83	17.17	"
9.32	11.30		3.40	3.91	
37.42	33.00	"	13.78	14.55	"
12.83	14.00		5.18	5.39	

* The first figure represents wt % K_2CO_3, the second that of KOH.

Table 6-3

(Continued)

Solution Conc.	Liquid Phase Conc.	Solid Phase	Solution Conc.	Liquid Phase Conc.	Solid Phase
39.16	31.34	$K_2CO_3.1.5H_2O$	11.05	12.10	Ice
13.38	15.20		6.06	6.60	
	31.30	"	6.30	8.30	"
	15.40		6.90	9.00	
36.17	30.80	"	3.42	4.84	"
14.00	15.80		7.42	10.36	
40.43	26.71	"		0.00	"
14.62	19.20			12.50	

Table 6-4

Solid-Liquid Equilibrium KOH-K_2CO_3-H_2O

Temp. (°C)	Saturated Liquid (wt %)		Solution Conc. (wt %)		Solid Phase
	KOH	K_2CO_3	KOH	K_2CO_3	
0	(00.0)	(51.35)	-	-	$K_2CO_3 \cdot 3/2\ H_2O$
	21.0	25.5	11.5	51.7	"
	45.0	3.6	23.7	41.0	"
	47.4	2.0	23.6	43.0	"
	48.1	2.2	50.3	6.6	$K_2CO_3 \cdot 3/2\ H_2O$ +$KOH \cdot 2\ H_2O$
	48.8	0.9	60.3	0.0	$KOH \cdot 2\ H_2O$
	48.7	0.9	60.3	0.0	"
20	(0.00)	(52.5)	-	-	$K_2CO_3 \cdot 3/2\ H_2O$
	0.0	52.6	-	-	"
	5.8	45.6	-	-	"
	9.9	40.2	8.6	46.6	"
	9.9	40.2	6.6	56.1	"
	15.7	33.2	-	-	"
	24.8	21.5	-	-	"
	29.1	17.4	-	-	"
	36.2	10.4	-	-	"
	45.6	4.1	22.1	44.7	"
	48.5	2.8	-	-	"
	52.2	2.3	42.5	20.7	$K_2CO_3 \cdot 3/2\ H_2O$ +$KOH \cdot 2\ H_2O$
	52.4	1.4	57.2	0.6	$KOH \cdot 2\ H_2O$
	(52.74)	(0.00)	-	-	"

Table 6-4

(Continued)

Temp. (°C)	Saturated Liquid (wt %)		Solution Conc. (wt %)		Solid Phase
	KOH	K_2CO_3	KOH	K_2CO_3	
40	(0.00)	(53.9)	-	-	$K_2CO_3 \cdot 3/2\ H_2O$
	0.0	53.9	-	-	"
	4.2	49.1	-	-	"
	9.5	42.4	6.0	52.5	"
	14.8	35.8	-	-	"
	26.9	22.1	-	-	"
	34.2	14.3	-	-	"
	42.9	6.0	-	-	"
	45.3	5.4	17.9	52.6	"
	53.8	3.4	21.1	52.1	"
	53.8	3.4	14.2	62.6	"
	56.0	2.5	38.9	29.2	$K_2CO_3 \cdot 3/2\ H_2O$ $+KOH \cdot H_2O$
	57.2	1.4	64.0	0.8	$KOH \cdot H_2O$
	(57.79)	(0.00)	-	-	"
60	(0.0)	(57.1)	-	-	$K_2CO_3 \cdot 3/2\ H_2O$
	6.3	48.5	-	-	"
	8.9	45.1	6.7	55.7	"
	13.9	39.1	-	-	"
	21.3	30.8	-	-	"
	34.2	16.5	-	-	"
	42.5	10.2	19.8	49.5	"
	52.0	5.6	19.3	54.9	"

Table 6-4

(Continued)

Temp. (°C)	Saturated Liquid (wt %)		Solution Conc. (wt %)		Solid Phase
	KOH	K_2CO_3	KOH	K_2CO_3	
60	56.6	4.4	14.9	61.0	$K_2CO_3 \cdot 3/2\ H_2O$ $+KOH \cdot H_2O$
	58.5	1.3	65.1	0.7	$KOH \cdot H_2O$
	(59.33)	(0.00)	-	-	"
80	(0.0)	(58.3)	-	-	$K_2CO_3 \cdot 3/2\ H_2O$
	5.6	51.5	-	-	"
	8.5	47.9	6.2	58.0	"
	12.5	43.1	-	-	"
	21.8	32.1	-	-	"
	37.0	17.0	-	-	"
	39.4	15.2	15.3	57.4	"
	42.3	12.9	-	-	"
	49.9	9.1	17.3	57.8	"
	49.9	9.1	9.0	70.5	"
	58.2	5.1	-	-	$K_2CO_3 \cdot 3/2\ H_2O$ $+KOH \cdot H_2O$
	61.1	1.2	67.5	0.5	$KOH \cdot H_2O$
	(61.44)	(0.00)	-	-	"

A study of the solid-liquid equilibrium for molten K_2CO_3-KOH system was made by Cohen-Adad et al. (61). Their results showed a polymorphique transformation of KOH at 242°C and also a eutectic of K_2CO_3-KOH with 22% K_2CO_3 was observed at 360°C. Diogenov (62) and Unzhakov (63) in their works observed a second transition of the KOH at 375°C. On the other hand Jaffray and Martin (64), reported two transitions for the carbonate at 410°C and 465°C respectively. However, they are second order phenomena.

Again the study of the ternary vapor pressure, by Walker and Kamino et al. is discussed in Chapter 4.

6.2 Electrical Conductivity

A study of the electrical conductivity of an electrolyte is essential for evaluating its potential as a fuel-cell electrolyte. Accurate measurement of this quantity is both desirable and important. A few measurements were reported on the binary systems of KOH-H_2O, K_2CO_3-H_2O and the ternary system K_2CO_3-KOH-H_2O.

6.2.1 Binary System: KOH-H_2O

Vogel et al. (33) and Klochko and Godina (65) studied the electrical conductivity of KOH-H_2O for a temperature range of 50° to 220°C and concentration range of zero to saturation. The results of both teams of investigators agreed closely for data at 150°C and 175°C, but their data disagreed at lower temperatures. Horne et al. (66,67) investigated the effect of pressure on the electrical conductance of KOH solution. Their results were found to agree with those of Hamann and Strauss (68) at high pressure, but there is considerable discrepancy at low pressure. As in all strong electrolytes, the

specific conductance of KOH solution first increase, then decrease with increase in pressure. The latter is due to the increasing viscosity of the solvent. In the case of KOH this decrease is less pronounced than other salts (66,68).

6.2.2 Binary System: K_2CO_3-H_2O

Krmoyan (69) studied the conductivity of K_2CO_3 solution, whereas Manelyan et al. (70) reported their experiments on the effect of temperature on the electrical conductivity on this system.

6.2.3 Ternary System: K_2CO_3-KOH-H_2O

Usanovich and Sushkevich (71) measured conductance of this ternary system at 25°, 50° and 97°C, with KOH concentration range from 18.86 to 41.59 wt %, and containing carbonate content from 0 to 31%. The results are given in Table 6-5 and Figures 6-2 - 6-6. It was found that addition of potassium carbonate in the alkali lowers the specific conductance of the solution. Similar explanation was given as in the study of the effect of pressure, addition of carbonate increase the viscosity (please refer to the section on viscosity) and the ionic concentration. The decrease in conductance is due to the fact that relative increase in the viscosity exceeds the rise in the ionic concentration.

6.3 Viscosity

The viscosity of a solution is usually studied with other physical properties. These data are usually used to describe the hydrodynamic of a system, to explain behavior in diffusivity, and thermal conductivity in these systems

Table 6-5

Electrical Conductivity of $KOH-K_2CO_3-H_2O$

Per cent KOH	Per cent K_2CO_3	$\underline{k}_{25°}$	$\underline{k}_{50°}$	$\underline{k}_{97°}$
	-	0.6042	0.8769	1.4143
	2.00	0.5893	0.8588	1.3815
18.86	9.76	0.5289	0.7864	1.2759
	21.50	0.4329	0.6612	1.1304
	25.97	0.3933	0.6134	1.0510
	-	0.6527	0.9637	1.5506
	3.54	0.6225	0.9240	1.3880
	6.26	0.5959	0.8912	1.4458
21.95	14.20	0.5233	0.7959	1.3329
	18.20	0.4789	0.7452	1.2590
	31.10	0.3457	0.5708	1.0420
	-	0.6753	1.0190	1.6741
	2.55	0.6460	0.9831	1.6300
26.37	7.19	0.6016	0.9156	1.5398
	13.40	0.5275	0.8199	1.4176
	30.87	0.3291	0.5665	1.0501
	-	0.6694	1.0072	1.7042
	2.41	0.6395	0.9689	1.6475
28.58	8.14	0.5693	0.8806	1.5176
	14.60	0.5089	0.8013	1.3980
	21.30	0.4115	0.6709	1.2120

Table 6-5

(Continued)

Per cent KOH	Per cent K_2CO_3	$k_{25°}$	$k_{50°}$	$k_{97°}$
	-	0.6660	1.0185	1.7625
	2.81	0.6308	0.9735	1.7055
31.45	9.20	0.5505	0.8665	1.5473
	11.47	0.5244	0.8340	1.4926
	19.35	0.4294	0.7032	1.3092
	-	0.6449	1.0093	1.7262
	1.05	0.6340	1.0082	1.6692
	2.08	0.6289	0.9927	1.6198
33.72	2.97	0.6127	0.9604	1.5479
	9.98	0.5113	0.8629	1.5258
	23.5	0.3611	0.6217	1.2123
	-	0.5596	0.9305	1.7315
	3.02	0.5237	0.8807	1.6601
41.59	7.00	0.4702	0.8023	1.5450
	11.47	0.4164	0.7258	1.4169
	12.50	0.3994	0.6998	1.3840

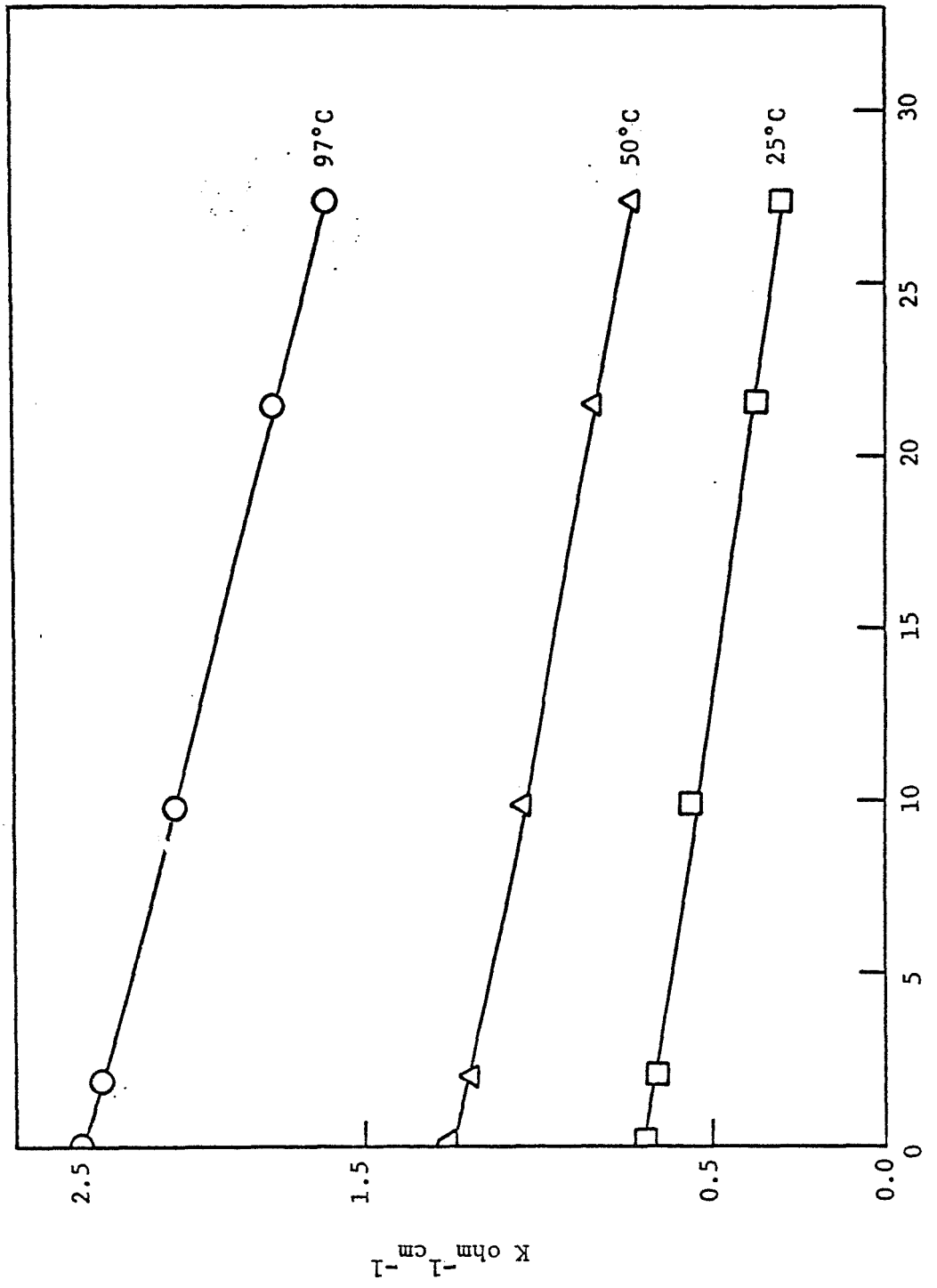

Figure 6-2. Conductivity of K_2CO_3-KOH-H_2O (18.86 % KOH)

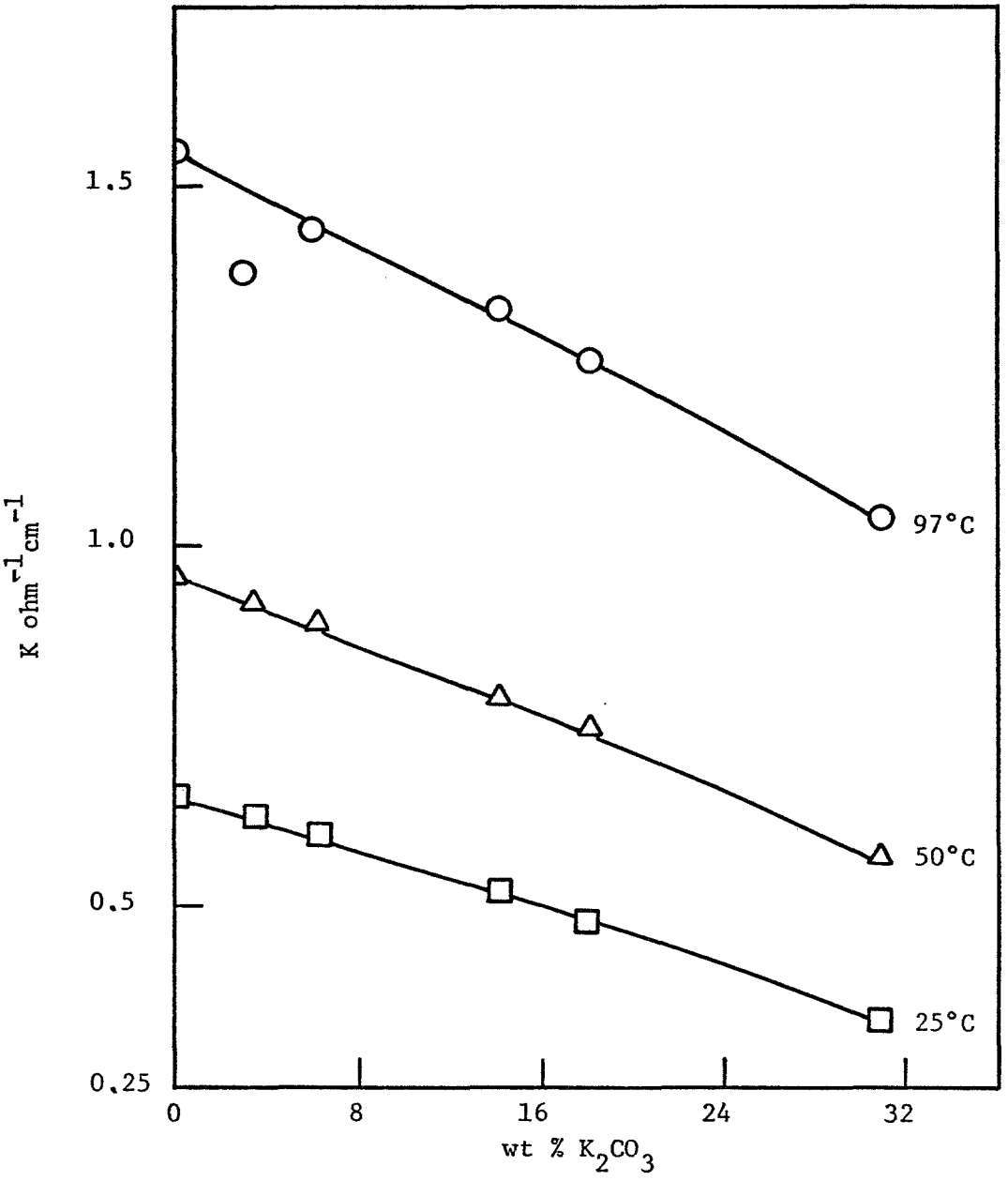

Figure 6-3. Conductivity of K_2CO_3-KOH-H_2O (21.95 % KOH)

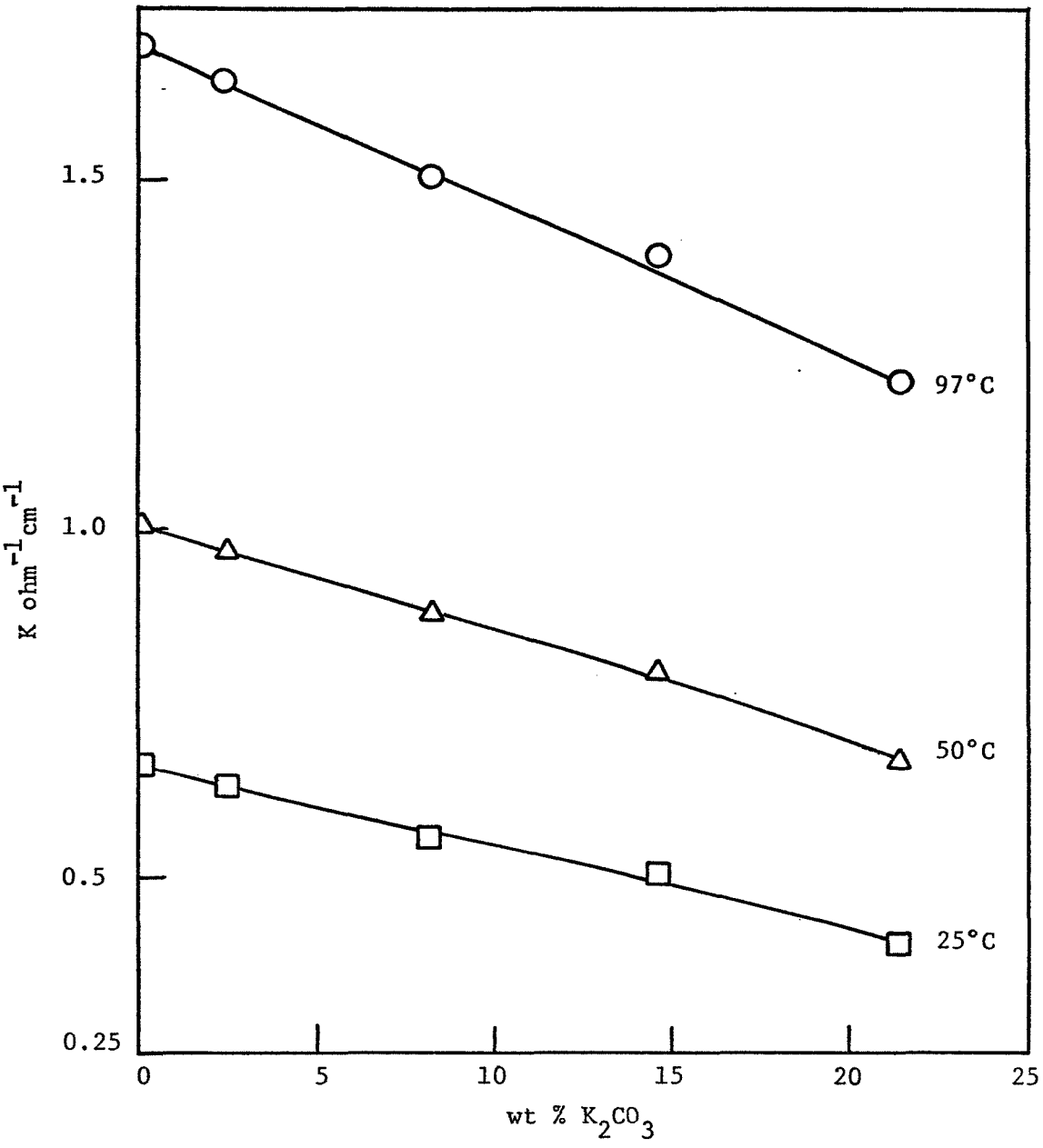

Figure 6-4. Conductivity of K_2CO_3-KOH-H_2O (28.58 % KOH)

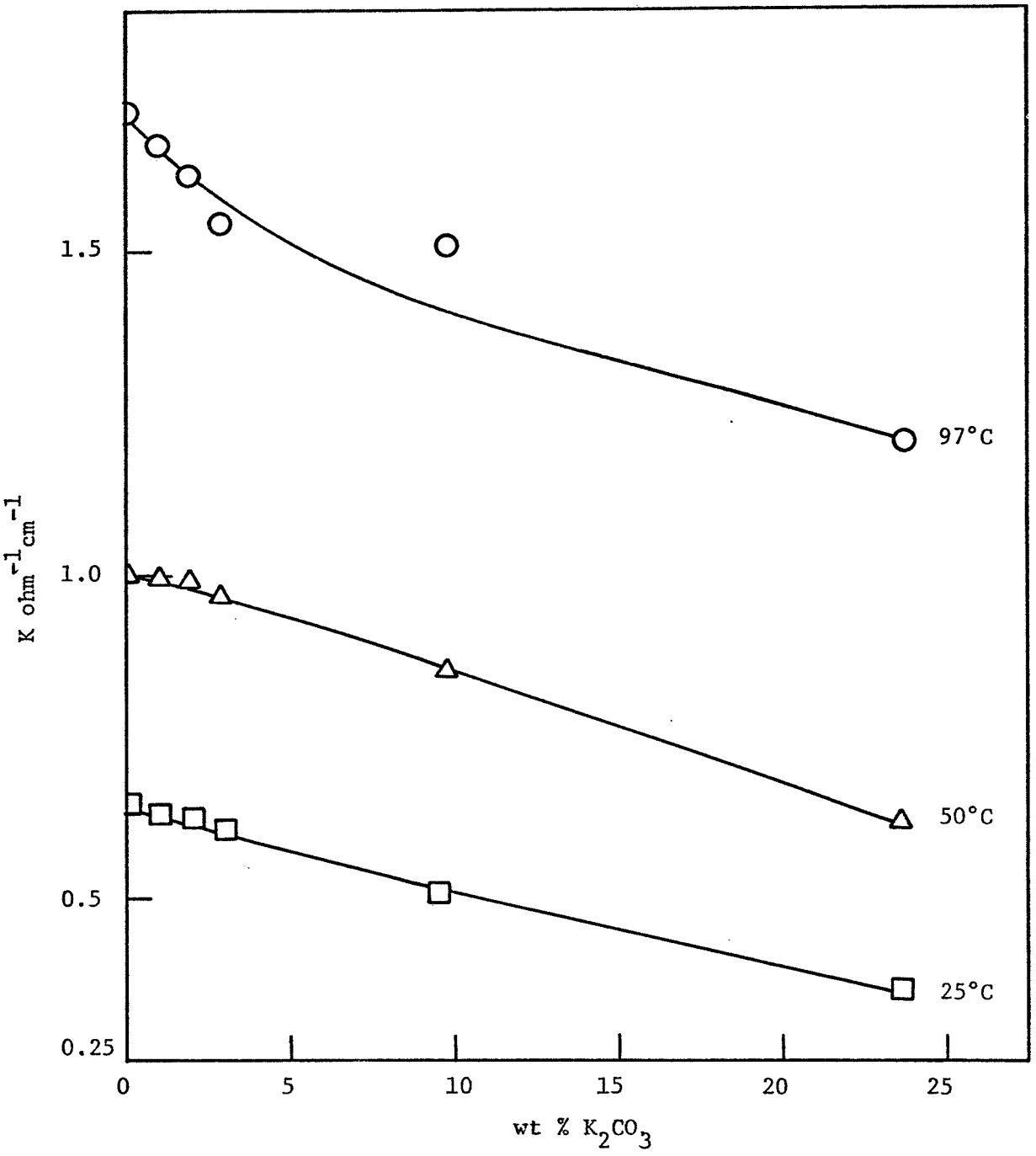

Figure 6-5. Conductivity of K_2CO_3-KOH-H_2O (32.72 % KOH)

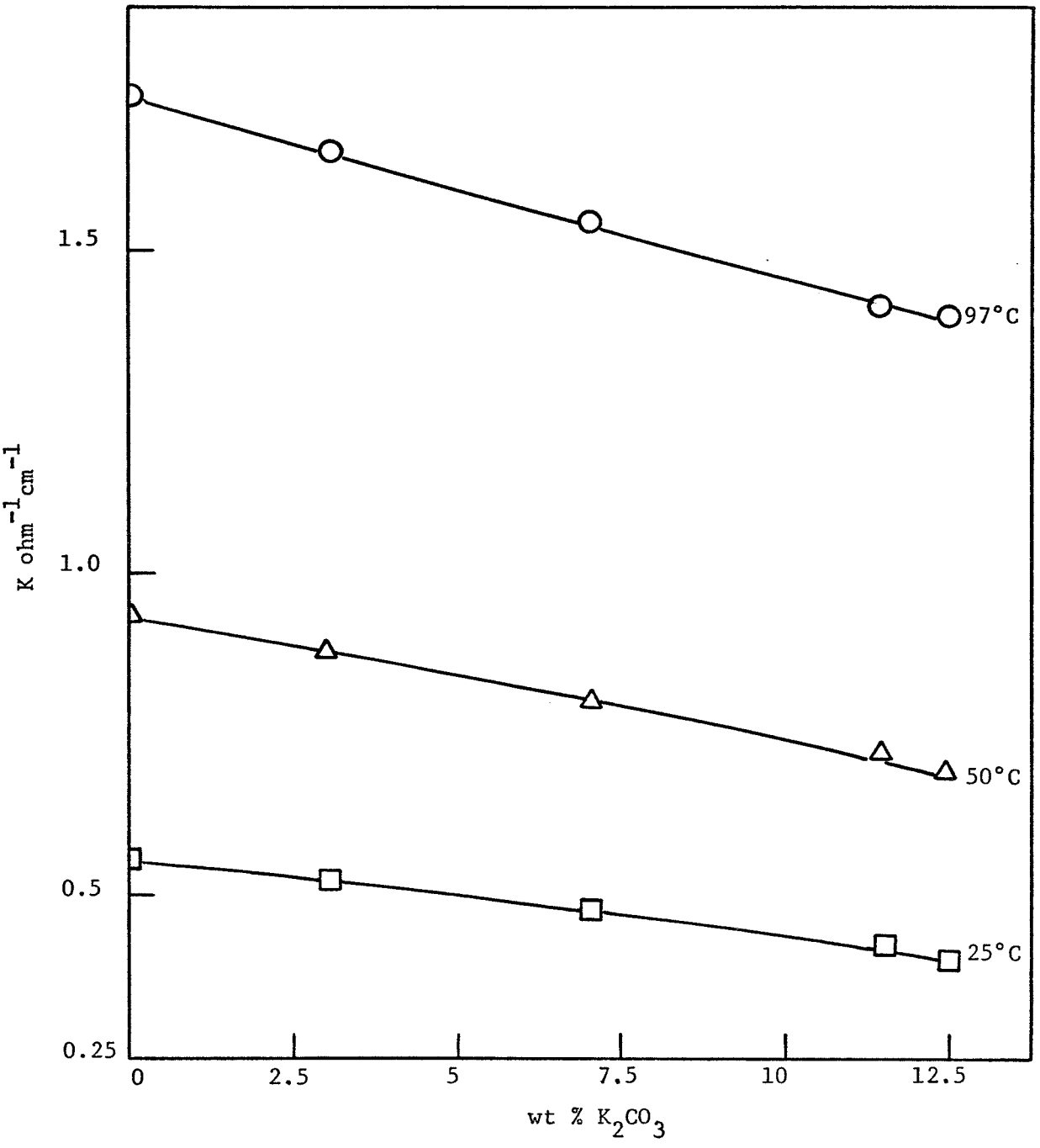

Figure 6-6. Conductivity of K_2CO_3-KOH-H_2O (41.59 % KOH)

Several authors have reported viscosity of KOH solution. Thus, Solvay (43) and Vogel et al. (45) measured viscosity over the complete liquid range (0 to 70 mole % KOH, and from 10° to 240°C). Other investigators on this subject are Hitchcock and McIlhenney (72), Lorenz (73) and a theoretical study by Good (74).

The viscosity of K_2CO_3 solution at 20°C was measured by Chesnokov (75).

Usanovich and Sushkevich (71) reported viscosity of the ternary system K_2CO_3-KOH-H_2O at 25° and 50°C, for 28.58 and 31.45% KOH and containing 0 to 21% K_2CO_3. The results of their experiment are given in Table 6-6 and Figures 6-7 and 6-8.

6.4 Absorption of Carbon Dioxide in Potassium Hydroxide and Potassium Carbonate Solutions

Absorption of carbon dioxide by scrubbing a gas mixture with an aqueous solution is an old problem in the industry. The excellent review by Sherwood (76) covers the period before 1937. Interest in this subject is ever increasing. The area of research covers the traditional study of mass transfer coefficients in packed columns, the study of the mechanism of chemical reaction in the solution, and the study of mechanism of physical transfer by means of various model and mathematical analyses.

6.4.1 Absorption in K_2CO_3 Solutions

The CO_2 rich gas is usually scrubbed either with methanol (Rectisol process), water, ethanolamine or hot potassium carbonate solution. The hot potassium carbonate process has several advantages over the others. Principally the advantage is in the reduction in

Table 6-6

Viscosity of $KOH-K_2CO_3-H_2O$

Wt % KOH	Wt % K_2CO_3	$\eta_{25°}$	$\eta_{50°}$
28.58	-	2.0975	1.2955
	2.41	2.2230	1.3570
	8.14	2.5916	1.5685
	14.6	3.0946	1.8229
	21.3	4.1209	2.3554
31.45	-	2.2786	1.3953
	2.81	2.5163	1.5254
	9.20	3.0707	1.8108
	19.35	4.1197	2.3506

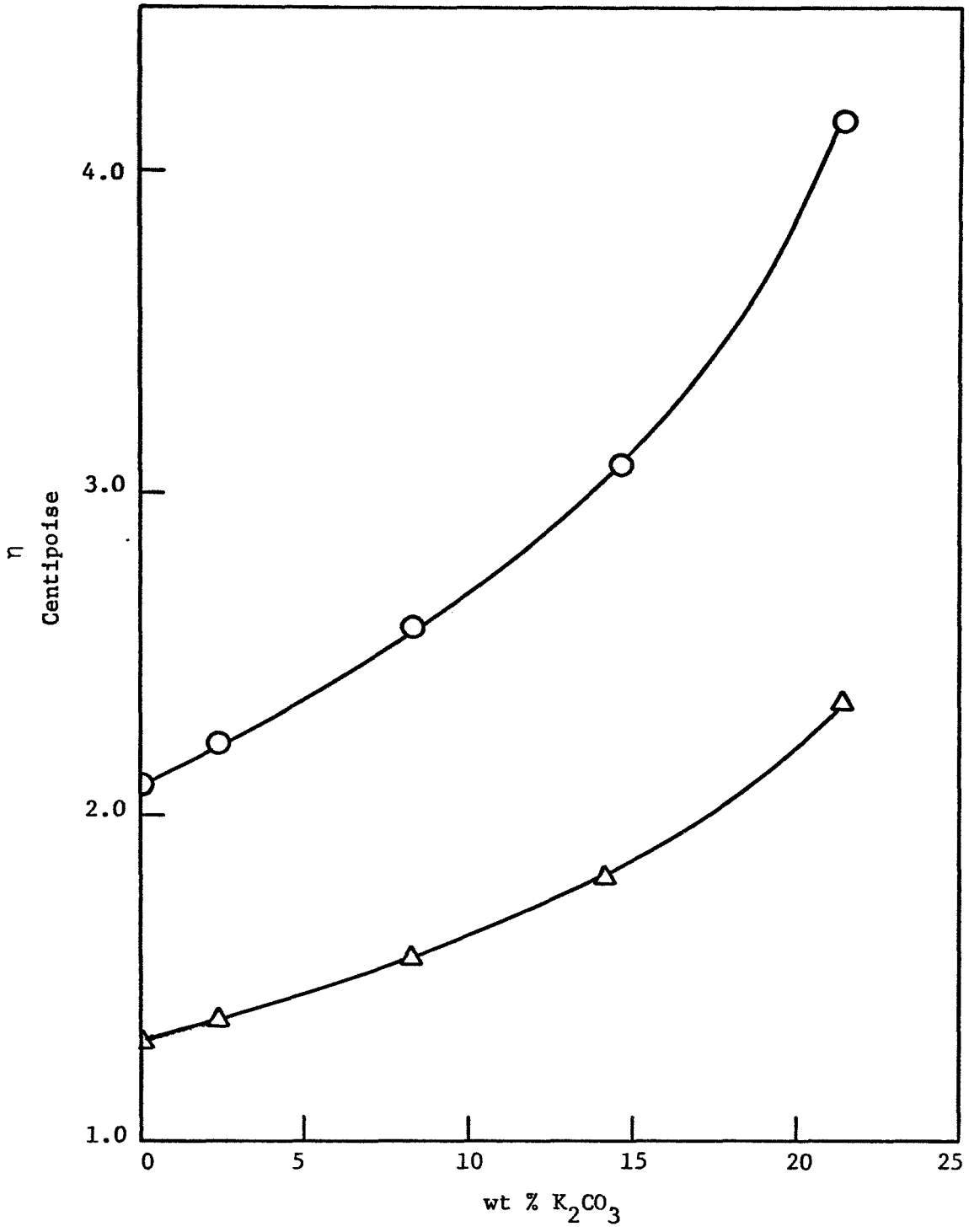

Figure 6-7. Viscosity of K_2CO_3-KOH-H_2O (28.58 % KOH)

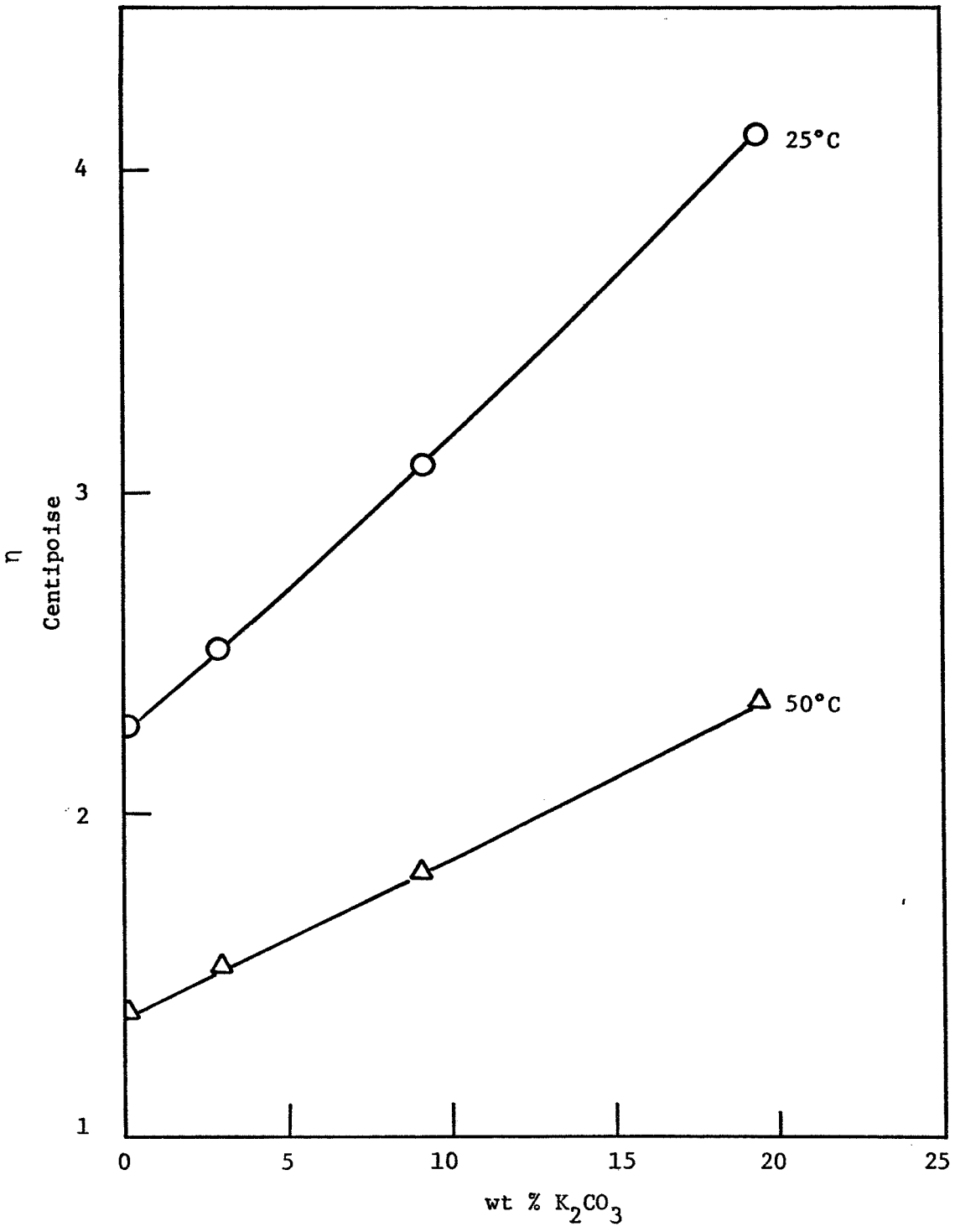

Figure 6-8. Viscosity of K_2CO_3-KOH-H_2O (31.45 % KOH)

operating and equipment costs for heating and cooling the gas mixtures (77-81). Benson et al. (82) reported pilot plant data for removal of CO_2 with hot K_2CO_3 solution. They compared the cost of operation and capital investment for both the ethanolamine and the potassium carbonate process. The latter process is found to be more economical. The main reduction is in the cooling, heating and solvent recovery system. Simultaneous removal of sulfide is also an asset of the carbonate process. These facts were confirmed by Palo and Armstrong (83) in commercial plant operation. They also pointed out some corrosion problems experienced in this process.

Very few equilibrium data for the system CO_2-K_2CO_3, which are essential for studying absorption processes, are reported. Benson et al. reported data for system with 40% equivalent K_2CO_3 and varying amounts of bicarbonate, for temperatures of 230°, 248°, 266°, and 284°F. Makranczy and Rusz (84) reported the absorption isotherm for the absorption of CO_2 in 5, 2 and 1 M K_2CO_3 solutions at 20°C, 50°C and 75°C. The pressure range is 1 atmosphere to 57 atmospheres. Figure 6-9 gives the gas-liquid equilibrium for this system at 40% K_2CO_3.

The early research (85-88) on the absorption in K_2CO_3 in packed columns was along the line of the traditional method of correlating overall mass transfer coefficients. These transfer coefficients were correlated with the physical properties and the dynamics of the system. Unfortunately, this system which involves chemical reaction, can not be treated as in the case of purely physical absorbing system.

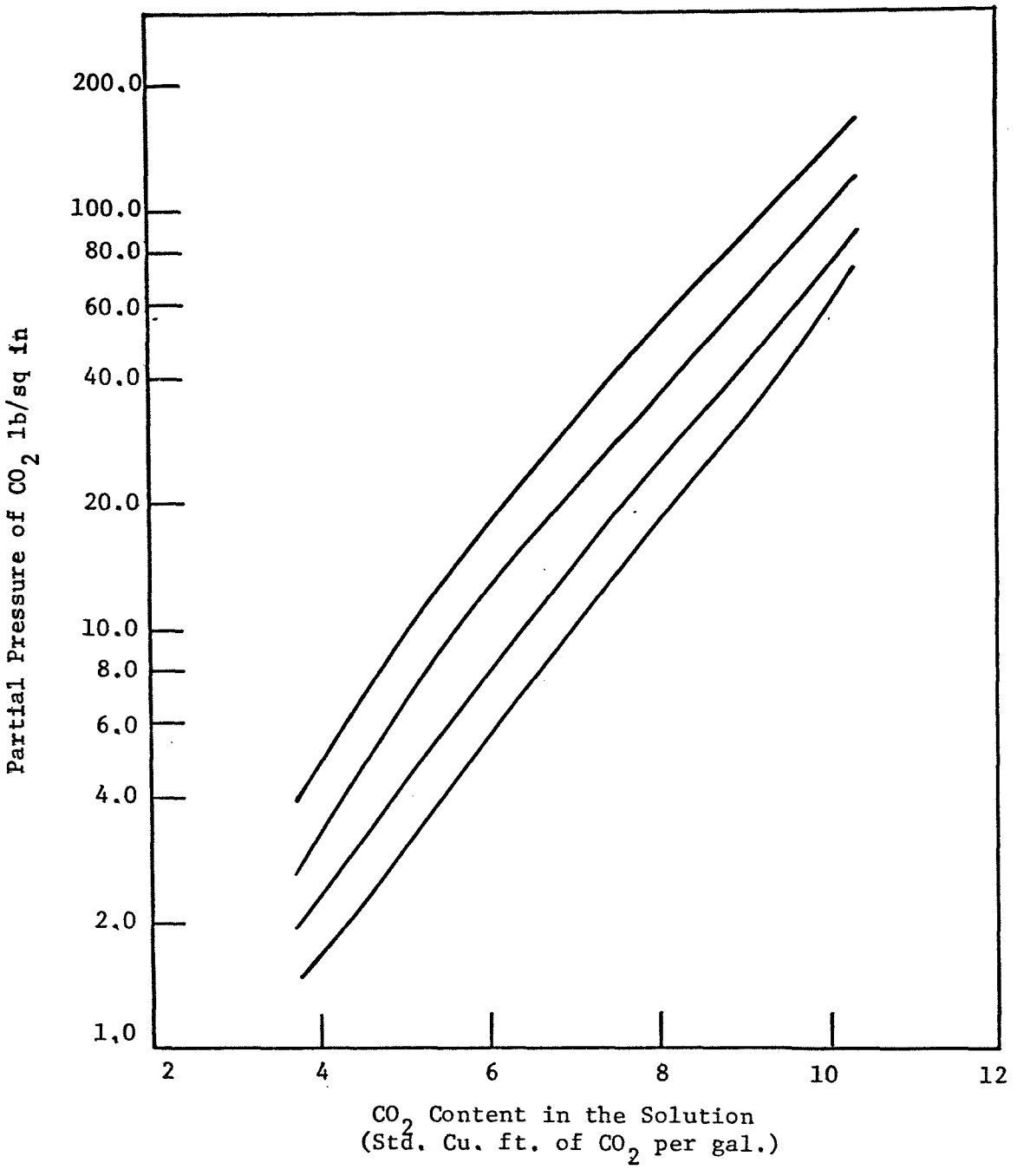

Figure 6-9. Equilibrium Pressure of CO_2 Over K_2CO_3 Solution (40% Equivalent K_2CO_3).

Consequently, it was observed that the Henry's law constant, which is an equilibrium property, was found to be a function of the flow velocities and a function of gas concentration (86).

Roper (87) studied the various factors which affect the absorption rate of carbon dioxide by potassium carbonate solutions in a Stephens-Morris disc column. The characteristics of the absorption carried out in the disc column were found to be similar to those of the absorption in packed towers with respect to the effect of the total solution concentration, percentage conversion to carbonates, liquid rate and temperature. This similarity opens up a possibility of experimentally determining the effect of chemical reactions in packed towers with the help of a small scale Stephens-Morris disc column (89).

Danckwerts (89) studied the mechanism of transfer in the light of the current theories, especially that of the Film model (90-93), and the Surface Renewal model (94). In the former model the rate of absorption is directly proportional to the diffusion coefficient D, while in the latter it is proportional to the square root of D. The mechanism of physical transfer proposed for these models are vastly different and the equations for the ratio R/R_o also differ. (R is rate of absorption with chemical reaction). However, the calculated values for this ratio are the same for both models for cases with first and second order reactions. Hence, from a practical point of view, it is not necessary to know the correct mechanism of absorption in order to predict the effect of reaction on absorption rates.

The reaction kinetics for the CO_2-K_2CO_3 reaction is known. When CO_2 is absorbed by a solution of K_2CO_3, the principal reaction is that between CO_2 and hydroxyl ions. In cases when $[CO_3^{=}]/[HCO_3^{-}]$ is uniform near the surface, the reaction can be considered as pseudo-first order. When this ratio is significantly less near the surface than in the bulk of the solution, the kinetic is more complicated. Similar studies were made by Nijsing (95) using a wetted wall column.

Danckwerts (89) pointed out that any of the theories which can adequately predict rate of physical absorption, can be used to describe the effect of chemical reaction on absorption rate in a packed column if the chemical kinetic is well known, otherwise this effect can be predicted by studying the reaction rate in a stirred tank or disc column which has the same K_L as the absorption column (96). Matsnyama (97) also made a similar type of analysis on this system.

Gianetto et al. (98-100), studied the absorption of CO_2 in K_2CO_3 by using the gas bubble method and the ring pump method, and the effect of chemical reaction reported.

6.4.2 Absorption in KOH Solutions

The study of absorption of CO_2 in KOH solution dates back to the ninteenth century. While Hatti's conclusion (101) that gas film resistance is the controlling factor was disputed by Jenny (102). Tepe and Dodge, also Spector and Dodge (104) from an experiment with counter current flow system concluded that the resistance in the gas film was significant but not predominent. The attempt to analyse the problem through processes that occur in the liquid phase was begun

by Brunner (105), and subsequent to this, Weber and Nilsson and also Davis and Crandall (106,107) extended and developed this analysis further.

Abandoning the traditional mass transfer coefficient method, Blum et al. (108), postulated that the rate of mass transfer is liquid phase limiting and that it is dependent on the chemical kinetics in addition to the fluid dynamics. In addition to the well known equations,

$$OH^- + CO_2 = HCO_3^- \qquad (6\text{-}1)$$

$$OH^- + HCO_3^- = HOH + CO_3^= \qquad (6\text{-}2)$$

a third equation was assumed to take place

$$CO_3^= + CO_2 + HOH = 2HCO_3^- \qquad (6\text{-}3)$$

The correlation of the rate of transfer with the ionic strength, concentration of ions and liquid flow rate lead to an expression which predicts the transfer rate very well. Again, it was found that the gas flow rate has little influence on the transfer rate.

In a recent paper, Danckwerts (89) analyzed the problem using the usual equations 6-1 and 6-2. It was found that the reaction rate is a very strong function of the concentration.

In all the studies of the mass transfer coefficient, it was

found that the transfer coefficient showed an initial increase with increase in normality of the KOH solution, until a maximum is reached between 1.5 to 2 N, whence further increase in normality caused the rate of transfer to decrease. This is due to the fact that when the caustic concentration increases, two counter acting effects result. On the one hand, the increase in viscosity and reduction in solubility and diffusion coefficient tends to reduce rate of transfer, on the other hand, the chemical reaction rate tends to increase with increase in concentration. Hence, a maximum rate is observed at some intermediate concentration.

Several other studies have been made on this system. Kobayashi et al. (109) studied the phenomenon taking place near the liquid interface in the absorption of CO_2 into stagnant KOH solution. The heat generated and the heat transfer process were also studied.

Hikita and Asai (110), studied transfer in wetted wall column for cases where there are ripples forming on the liquid surface and for cases where the ripples are eliminated by the addition of wetting agent. The results of the latter case conform with those predicted by the penetration theory. Due to the presence of turbulent current in cases where ripples are present, the penetration theory is found to be inadequate. Surprisingly, they found that the ratio R/R_o is the same as predicted by this theory, which is similar to the observation made by Danckwerts.

Nijsing et al. (111) studied the kinetics of the absorption of CO_2 in KOH solutions using both laminar jet and wetted wall methods.

The conclusion drawn is essentially similar to that of Danckwert (89). One can even consider this as an experimental proof of the validity of Dankwert's conclusion.

7.0 FUTURE PLANS

Since experimental measurements of vapor pressure of the ternary system KOH-K_2CO_3-H_2O are scarce, and the Isopiestic method does not seem to be applicable for temperatures higher than 25°C, a new technique is being explored, A differential manometer has been purchased and set up for such a purpose. This manometer is used to measure the difference in pressure between a solution of known vapor pressure and that of the solution to be measured. Preliminary measurements with this method give favorable results. It is therefore planned to measure the vapor pressure of the ternary system using the above-mentioned set up.

Measurements of diffusion coefficients of hydrogen in lithium hydroxide solutions using the stagnant microelectrode method will also be made. It is expected that slight modification on the existing technique will have to be made to ensure reproducibility.

Experimental and theoretical studies on the partial molal volume of gases dissolved in electrolytes (both salting-out and salting-in systems) will be continued for the next six months.

Appendix A

We wish to obtain a general equation for the chemical potential from fundamental statistical mechanical considerations. Assuming pair-wise additivity and spherical molecules with central interactions, an equation for μ_1 can be derived from the basic relation for pressure

$$p = kT \sum_{i=1}^{m} \rho_i - \frac{2}{3}\pi \sum_{i=1}^{m}\sum_{j=1}^{m} \rho_i\rho_j \int_0^{\infty} \frac{d\phi_{ij}(r)}{dr}\, g_{ij}(r,T,\rho_1\cdots\rho_m)\, r^3 dr \tag{A-1}$$

The Helmholtz free energy can be obtained from (A-1) and the classical thermodynamic relation

$$p = -\left(\frac{\partial A}{\partial V}\right)_{T,N_i} \tag{A-2}$$

and the chemical potential μ_1 is obtained from:

$$\mu_1 = \left(\frac{\partial A}{\partial N_1}\right)_{T,V,N_{j\neq i}} \tag{A-3}$$

The general relation for μ_1 then becomes:

$$\mu_1 = kT\ \ell n(\rho_1 \Lambda_1^3) + \frac{2}{3}\pi \left\{ \frac{\partial}{\partial N_1} \left[\sum_{i=1}^{m} \sum_{j=1}^{m} N_i N_j \int_{\infty}^{V} \frac{1}{v^2} \left[\int_0^{\infty} \frac{d\phi_{ij}}{dr}\, g_{ij}(r,T,\rho_1 \cdots \rho_m)\, r^3 dr \right] dv \right] \right\}_{T,V,N_{j\neq 1}} \tag{A-4}$$

In order to make use of some accurate analytical results for hard spheres we assume that the various species in the solution interact via a cut-off Lennard-Jones potential energy function.

$$\phi_{ij}(r) = \phi_{ij}^{h.s.}(r) + \phi_{ij}^{s}(r) \tag{A-5}$$

where $\phi_{ij}^{h.s.}(r)$ is the usual hard sphere potential and $\phi_{ij}^{s}(r)$ is a Lennard-Jones cut-off potential, the cut-off being taken at the value σ.

Using Eq. (A-5) in (A-4) causes the chemical potential to be divided into a hard and a soft contribution:

$$\mu_1 = kT\ \ell n(\rho_1 \Lambda_1^3) + \mu_1^h + \mu_1^s \tag{A-6}$$

where

$$\mu_1^h = -\frac{2}{3}\pi kT \left\{ \frac{\partial}{\partial N_1} \sum_{i=1}^{m} \sum_{j=1}^{m} N_i N_j \sigma_{ij}^3 \int_{\infty}^{V} \frac{1}{v^2} g_{ij}(\sigma_{ij};T,\rho_1 \cdots \rho_m)\, dv \right\}_{T,V,N_{j\neq 1}} \tag{A-7}$$

and

$$\mu_1^s = \frac{2}{3}\pi \left\{ \frac{\partial}{\partial N_1} \left[\sum_{i=1}^{m} \sum_{j=1}^{m} N_i N_j \int_{\infty}^{V} \frac{1}{v^2} \int_{0}^{\infty} \frac{d\phi_{ij}^s(r)}{dr} g_{ij}(r,T,\rho_1 \cdots \rho_m)\, r^3 dr\, dv \right] \right\}_{T,V,N_{j\neq 1}} \tag{A-8}$$

Using the general equation for the chemical potential in terms of the fugacity, μ_1^G can be written as

$$\mu_1^G = kT \ln \left\{ \frac{\Lambda_i^3}{kT} \right\} + kT \ln f_1^G \tag{A-9}$$

From the equality of the chemical potential in the gas and liquid phases, the activity coefficient can be written as:

$$\ln(K_1^o \gamma_1) = \frac{\mu_1^h}{kT} + \frac{\mu_1^s}{kT} + \ln\left\{ kT \sum_{j=1}^{m} \rho_j \right\} \tag{A-10}$$

The integral in the equation for μ_1^h can be solved analytically if an appropriate theoretical expression is available for $g_{ij}(\sigma_{ij},T,\rho_1 \cdots \rho_m)$, the value of the radial distribution function at contact. Lebowitz (112)

has solved the hard sphere mixture Percus-Yevick (P-Y) equations exactly. Using this result, Lebowitz and Rowlinson (113) have derived an expression for μ_1^h. A recent modification (114) of the Lebowitz result gives a value for $g_{ij}(\sigma_{ij},\rho_1\cdots\rho_m)$ which is in much better agreement with the molecular dynamics results of Alder (115,116) for all densities except those near the phase transition. This modified Percus-Yevick result (MPY) is:

$$g_{ij}(\sigma_{ij}\rho_1\cdots\rho_m) = \frac{1}{1-\zeta_3} + \frac{3\sigma_i\sigma_j}{(\sigma_i+\sigma_j)}\frac{\zeta_2}{(1-\zeta_3)^2} + 2\left[\frac{\sigma_i\sigma_j}{\sigma_i+\sigma_j}\right]^2\frac{\zeta_2^2}{(1-\zeta_3)^3} \tag{A-11}$$

where

$$\zeta_\ell = \frac{1}{6}\pi\sum_{j=1}^{m}\rho_j\sigma_j^\ell \tag{A-12}$$

Using the MPY result in equation (A-7) enables μ_1^h to be solved analytically. The result is:

$$\begin{aligned}\frac{\mu_1^h}{kT} = &-\ell n(1-\zeta_3) + \frac{\pi}{6}\frac{P}{kT}\sigma_1^3 + \frac{3\zeta_2}{(1-\zeta_3)}\sigma_1 + \frac{3\zeta_1}{(1-\zeta_3)}\sigma_1^2 + \frac{9}{2}\frac{\zeta_2^2}{(1-\zeta_3)^2}\sigma_1^2 \\ &+ 3\left[\frac{\sigma_1\zeta_2}{\zeta_3}\right]^2\left[\ell n(1-\zeta_3) + \frac{\zeta_3}{(1-\zeta_3)} - \frac{\zeta_3^2}{2(1-\zeta_3)^2}\right] \\ &- \left[\frac{\sigma_1\zeta_2}{\zeta_3}\right]^3\left[2\ell n(1-\zeta_3) + \frac{\zeta_3(2-\zeta_3)}{(1-\zeta_3)}\right]\end{aligned} \tag{A-13}$$

In order to calculate μ_1^s we must specify $\phi_{ij}^s(r)$ and the mixture radial distribution function for all values of r; not just at σ_{ij} as in the hard sphere case. The soft potential interaction $\phi_{ij}^s(r)$ is split into a nonpolar and polar part:

$$\phi_{ij}^s(r) = \phi_{ij}^{np}(r) + \bar{\phi}_{ij}^p(r) \tag{A-14}$$

The nonpolar part is assumed to be of the Lennard-Jones (6-12) kind

$$\begin{aligned} \phi_{ij}^{np}(r) &= 4\varepsilon_{ij}\left[\left(\frac{\sigma_{ij}}{r}\right)^{12} - \left(\frac{\sigma_{ij}}{r}\right)^{6}\right] \qquad \text{for } r \geq \sigma_{ij} \\ &= 0 \qquad\qquad\qquad\qquad\qquad\qquad\quad \text{for } r < \sigma_{ij} \end{aligned} \tag{A-15}$$

where the mixture potential parameters follow the usual mixing rules

$$\begin{aligned} \sigma_{ij} &= \frac{1}{2}(\sigma_i + \sigma_j) \\ \varepsilon_{ij} &= (\varepsilon_i\varepsilon_j)^{1/2} \end{aligned} \tag{A-16}$$

The polar interaction between the solute (1) and the solvent water (2) is assumed to be the angle-averaged polar-nonpolar molecule interaction and can be expressed as:

$$\bar{\phi}_{12}^p(r) = -\frac{\mu_2^2\alpha_1}{r^6} \tag{A-17}$$

where μ_2 is the dipole moment of water and α_1 is the polarizability of the solute 1.

The mixture radial distribution functions are not readily evaluated from any theory. As an approximation we assume that the solvent particles are uniformly distributed about the solute molecules so that

$$g_{1j} = 1 \qquad \text{for } r > \sigma_{1j} \tag{A-18}$$

Using equations (A-18), (A-17), (A-15) and (A-14) in equation (A-8) for μ_1^s gives:

$$\mu_1^s \simeq -\frac{32\pi}{9} \sum_{j=1}^{m} \rho_j \varepsilon_{1j} \sigma_{1j}^3 - \frac{4\pi\rho_2\mu_2^2\alpha_1}{3\sigma_{12}^3} \tag{A-19}$$

The partial molal volume of solute 1 in the electrolyte solution can be calculated from the well-known thermodynamic relation:

$$\bar{V}_1 = \left(\frac{\partial \mu_1}{\partial P}\right)_{T,n_j} \tag{A-20}$$

Differentiation of μ_1 using equations (A-19), (A-13) and (A-6) gives

$$\begin{aligned} \bar{V}_1 = kT\beta \Bigg\{ & 1 + \frac{\zeta_3}{1-\zeta_3} + 3\frac{\zeta_2}{(1-\zeta_3)^2}\sigma_1 + 3\frac{\zeta_1}{(1-\zeta_3)^2}\sigma_1^2 + 9\frac{\zeta_2^2}{(1-\zeta_3)^3}\sigma_1^2 \\ & - \left(\frac{\zeta_2\sigma_1}{1-\zeta_3}\right)^2 \left[\frac{2\zeta_3}{(1-\zeta_3)} + \zeta_2\sigma_1\right] \Bigg\} + \frac{\pi}{6}\sigma_1^3 \\ & - \frac{4\pi}{3}\beta \left\{ \frac{8}{3} \sum_{j=1}^{m} \rho_j \varepsilon_{1j} \sigma_{1j}^3 + \frac{\rho_2\mu_2^2\alpha_1}{\sigma_{12}^3} \right\} \end{aligned} \tag{A-21}$$

where β is the isothermal compressibility

$$\beta = -\frac{1}{V}\left(\frac{\partial V}{\partial P}\right)_{T,n_i} \tag{A-22}$$

In order to predict the compressibility an equation of state is necessary. We use the MPY equation for hard sphere mixtures (114).

$$\frac{P}{kT} = \frac{6}{\pi}\left\{\frac{\zeta_0}{1-\zeta_3} + \frac{3\zeta_1\zeta_2}{(1-\zeta_3)^2} + \frac{3\zeta_2^3}{(1-\zeta_3)^3} - \frac{\zeta_3\zeta_2^3}{(1-\zeta_3)^3}\right\} \tag{A-23}$$

Using this equation of state in (A-22), the compressibility of a mixture of hard spheres is given by:

$$\beta = \frac{\pi(1-\zeta_3)^4}{6kT\{(1-\zeta_3)^2\,\zeta_0 + 6\zeta_1\zeta_2\,(1-\zeta_3) + 9\zeta_2^3 + \zeta_3^2\zeta_2^3 - 4\zeta_3\zeta_2^3\}} \tag{A-24}$$

Use of equation (A-24) in the relation for the partial molal volume gives a relation for $\bar{V}_1$ consistent with the hard sphere MPY theory and for which no new parameters have been introduced.

Appendix B

The Multicomponent Hard Sphere Diffusion Equation

The approximations inherent in the Enskog form of the modified Boltzmann equation have been discussed in detail by several authors (117-120). The same considerations are valid for the multicomponent case. The principal assumptions are: (a) only binary collisions need be considered, (b) the molecular chaos assumption is valid, and (c) the nonequilibrium pair correlation function $g(\underline{r}, \underline{r} + \sigma\underline{k}; t)$ may be replaced by the local equilibrium value $g(\sigma)$. The last two approximations imply that the second order distribution function $f_{(2)}$ just prior to collision can be written in terms of the first order function as

$$f_{(2)}(\underline{r}_1,\underline{r}_2,\underline{v}_1,\underline{v}_2;t) = g(\sigma)\, f_{(1)}(\underline{r}_1,\underline{v}_1;t)\, f_{(1)}(\underline{r}_2,\underline{v}_2;t)$$

$$\text{for } |\underline{r}_1 - \underline{r}_2| = \sigma+$$

where σ is the rigid sphere diameter and $g(\sigma)$ is evaluated at the number density corresponding to the position of the point of contact. The molecular chaos approximation is the most serious one in the theory, and has been tested against molecular dynamics calculations by Dymond and Alder (121-122); they find that it may lead to errors of about 20% at higher densities.

For a rigid sphere mixture of ν components the modified Boltzmann equations are:

$$\frac{\partial f_i}{\partial t} + \underline{v}_i \cdot \frac{\partial f_i}{\partial \underline{r}} + \underline{x}_i \cdot \frac{\partial f_i}{\partial \underline{v}_i} = \sum_{j=1}^{\nu} \iint \left[g_{ij}(\underline{r} + \frac{1}{2}\sigma_{ij}\underline{k},\ \sigma_{ij})\ f_i'(\underline{r})\ f_j'(\underline{r} + \sigma_{ij}\underline{k}) \right.$$

$$\left. - g_{ij}(\underline{r} - \frac{1}{2}\sigma_{ij}\underline{k},\ \sigma_{ij})\ f_i(\underline{r})\ f_j(\underline{r} - \sigma_{ij}\underline{k}) \right] \sigma_{ij}^2 (\underline{w}_{ji} \cdot \underline{k})\ d\underline{k}\ d\underline{v}_j$$

$$i=1,2,\cdots\nu \qquad \text{(B-1)}$$

where f_i is the singlet distribution function for molecules of type i, $\underline{v}_i$ is molecular velocity, $\underline{x}_i$ is the external force per unit mass, $\underline{w}_{ji}$ is relative velocity between the i and j molecules, and $\underline{k}$ is the unit vector lying on a line joining the center of molecule j to molecule i at the moment of contact. The function $g_{ij}(\underline{r} + \frac{1}{2}\sigma_{ij}\underline{k},\ \sigma_{ij})$ is the local equilibrium radial distribution function, evaluated at the point of contact of the two rigid spheres, $(\underline{r} + \frac{1}{2}\sigma_{ij}\underline{k})$.

BI. INTEGRAL EQUATION FOR ϕ_i

As usual (123) we assume that the distribution functions g_{ij} and f_i are slowly varying in space so that we may expand these functions in a Taylor's series about $\underline{r}$, keeping only terms up to first order. When this is done and we put $f_i = f_i^{(o)}\ (1 + \phi_i)$ in Eq. (B-1) we get

$$\frac{\partial f_i^{(o)}}{\partial t} + \underline{v}_i \cdot \frac{\partial f_i^{(o)}}{\partial \underline{r}} + \underline{x}_i \cdot \frac{\partial f_i^{(o)}}{\partial \underline{v}_i}$$

$$= \sum_{j=1}^{\nu} \left\{ g_{ij}(\sigma_{ij})\, \sigma_{ij}^2 \iint f_i^{(o)}\, f_j^{(o)} (\phi_i' + \phi_j' - \phi_i - \phi_j)(\underline{w}_{ji} \cdot \underline{k})\, d\underline{k}\, d\underline{v}_j \right.$$

$$+ g_{ij}(\sigma_{ij})\, \sigma_{ij}^3 \iint f_i^{(o)}\, f_j^{(o)}\, \underline{k} \cdot \frac{\partial \ell n (f_j^{(o)'} f_j^{(o)})}{\partial \underline{r}} (\underline{w}_{ji} \cdot \underline{k})\, d\underline{k}\, d\underline{v}_j$$

$$\left. + \sigma_{ij}^3 \iint f_i^{(o)}\, f_j^{(o)}\, \underline{k} \cdot \frac{\partial g_{ij}(\sigma_{ij})}{\partial \underline{r}} (\underline{w}_{ji} \cdot \underline{k})\, d\underline{k}\, d\underline{v}_j \right\} \qquad \text{(B-2)}$$

In this equation ϕ_i represents the first order correction to $f_i^{(o)}$, and is a linear function of the first derivatives of number densities n_i, temperature T, and mass average velocity $\underline{v}_o$. The distribution function $f_i^{(o)}$ for the uniform steady state is

$$f_i^{(o)} = n_i \left(\frac{m_i}{2\pi kT} \right)^{3/2} e^{-m_i C_i^2 / 2kT} \qquad \text{(B-3)}$$

where $\underline{C}_i = \underline{v}_i - \underline{v}_o$ is the peculiar velocity. Using Eq. (B-3) in the left-hand side of Eq. (B-2) and in the second of the terms on the right gives:

$$f_i^{(o)} \left\{ \frac{1}{n_i} \frac{Dn_i}{Dt} - \left(\frac{3}{2T} - \frac{m_i C_i^2}{2kT^2} \right) \frac{DT}{Dt} + \frac{m_i}{kT} \underline{C}_i \underline{C}_i : \frac{\partial \underline{v}_o}{\partial \underline{r}} \right.$$

$$\left. + \underline{C}_i \cdot \left[\frac{1}{n_i} \frac{\partial n_i}{\partial \underline{r}} - \left(\frac{3}{2T} - \frac{m_i C_i^2}{2kT^2} \right) \frac{\partial T}{\partial \underline{r}} + \frac{m_i}{kT} \left(\frac{D\underline{v}_o}{Dt} - \underline{x}_i \right) \right] \right\}$$

$$= \sum_{j=1}^{\nu} \left\{ g_{ij}(\sigma_{ij}) \, \sigma_{ij}^2 \iint f_i^{(o)} \, f_j^{(o)} (\phi_i' + \phi_j' - \phi_i - \phi_j) (\underline{w}_{ji} \cdot \underline{k}) \, d\underline{k} \, d\underline{v}_j \right.$$

$$+ g_{ij}(\sigma_{ij}) \, \sigma_{ij}^3 \iint f_i^{(o)} \, f_j^{(o)} \, \underline{k} \cdot \left(\frac{2}{n_j} \frac{\partial n_j}{\partial \underline{r}} - \frac{3}{T} \frac{\partial T}{\partial \underline{r}} \right) (\underline{w}_{ji} \cdot \underline{k}) \, d\underline{k} \, d\underline{v}_j$$

$$+ g_{ij}(\sigma_{ij}) \, \sigma_{ij}^3 \iint f_i^{(o)} \, f_j^{(o)} \frac{m_j}{2kT^2} \underline{k} \cdot (C_j'^2 + C_j^2) \frac{\partial T}{\partial \underline{r}} (\underline{w}_{ji} \cdot \underline{k}) \, d\underline{k} \, d\underline{v}_j$$

$$+ g_{ij}(\sigma_{ij}) \, \sigma_{ij}^3 \iint f_i^{(o)} \, f_j^{(o)} \frac{m_j}{kT} \underline{k} \cdot \left[(\underline{C}_j' + \underline{C}_j) \cdot \frac{\partial \underline{v}_o}{\partial \underline{r}} \right] (\underline{w}_{ji} \cdot \underline{k}) \, d\underline{k} \, d\underline{v}_j$$

$$\left. + \sigma_{ij}^3 \iint f_i^{(o)} \, f_j^{(o)} \, \underline{k} \cdot \frac{\partial g_{ij}(\sigma_{ij})}{\partial \underline{r}} (\underline{w}_{ji} \cdot \underline{k}) \, d\underline{k} \, d\underline{v}_j \right\} \qquad \text{(B-4)}$$

The integrations involved in the last four terms on the right side of Eq. (B-4) can be evaluated using results proved in Section 16.8 of Chapman and Cowling, together with Eq. (B-3). In addition, the substantial time derivatives which appear on the left-hand side of Eq. (B-4) can be eliminated using the hydrodynamic equations:

$$\frac{Dn_i}{Dt} + n_i \frac{\partial}{\partial \underline{r}} \cdot \underline{v}_o = 0 \tag{B-5}$$

$$\frac{D\underline{v}_o}{Dt} - \underline{x}_i = -\frac{1}{\rho}\frac{\partial P}{\partial \underline{r}} - \sum_{j=1}^{\nu} \frac{\rho_j}{\rho} (\underline{x}_i - \underline{x}_j) \tag{B-6}$$

$$\frac{DT}{Dt} + \frac{2}{3nk} P \frac{\partial}{\partial \underline{r}} \cdot \underline{v}_o = 0 \tag{B-7}$$

where the pressure is given by:

$$P = \sum_{i=1}^{\nu} \sum_{j=1}^{\nu} n_i kT \, (1 + \rho b_{ij} g_{ij}) \tag{B-8}$$

When these two steps are carried out on Eq. (B-4) we obtain:

$$f_i^{(o)} \left\{ \left(1 + \frac{12}{5} \sum_{j=1}^{\nu} \rho b_{ij} g_{ij} \, M_{ij} M_{ji} \right) \left(\frac{m_i C_i^2}{2kT} - \frac{5}{2} \right) \frac{1}{T} \frac{\partial T}{\partial \underline{r}} \cdot \underline{C}_i \right.$$

$$+ \frac{m_i}{kT} \left(1 + \frac{4}{5} \sum_j M_{ji} \, \rho b_{ij} g_{ij} \right) \underline{C}_i^o \underline{C}_i : \frac{\partial \underline{v}_o}{\partial \underline{r}}$$

$$+ \frac{2}{3} \left(1 + 2 \sum_j M_{ji} \, \rho b_{ij} g_{ij} - \frac{P}{nkT} \right) \left(\frac{m_i C_i^2}{2kT} - \frac{3}{2} \right) \frac{\partial}{\partial \underline{r}} \cdot \underline{v}_o$$

$$\left. + \frac{n}{n_i} \underline{d}_i \cdot \underline{C}_i \right\} = \sum_{j=1}^{\nu} g_{ij} \sigma_{ij}^2 \iint f_i^{(o)} \, f_j^{(o)} (\phi_i' + \phi_j' - \phi_i - \phi_j) (\underline{w}_{ji} \cdot \underline{k}) \, d\underline{k} \, d\underline{v}_j \tag{B-9}$$

$$\text{where } \underline{d}_i = -\frac{\rho_i}{\rho nkT}\frac{\partial P}{\partial \underline{r}} - \frac{\rho_i}{\rho nkT}\sum_j \rho_j(\underline{x}_i - \underline{x}_j)$$

$$+ \sum_{j=1}^{\nu}\left\{\frac{n_i}{n}(\delta_{ij} + 2M_{ij}\,\rho b_{ij}g_{ij})\frac{1}{T}\frac{\partial T}{\partial \underline{r}} + \frac{1}{n}\left(\delta_{ij} + 2\rho b_{ji}g_{ij}\right.\right.$$

$$\left.\left. + \sum_{k=1}^{\nu} n_i \rho b_{ik}\frac{\partial g_{ik}}{\partial n_j}\right)\frac{\partial n_j}{\partial \underline{r}}\right\} \qquad \text{(B-10)}$$

$$b_{ij} = \frac{2}{3}\pi n_j\,\sigma_{ij}^3/\rho$$

$$M_{ij} = \frac{m_i}{m_i + m_j}$$

Eq. (B-9) and (B-10) are the multicomponent generalizations of Thorne's binary equations, (16.9,4) and (16.9,5) of Chapman and Cowling.

BII. SOLUTIONS OF INTEGRAL EQUATIONS

Since the right-hand side of Eq. (B-9) is linear in the gradients $\frac{\partial \ell nT}{\partial \underline{r}}$, $\frac{\partial \underline{v}_o}{\partial \underline{r}}$ and $\underline{d}_i$, we expect ϕ_i to be of the form:

$$\phi_i = -\underline{A}_i(\underline{W}_i)\cdot\frac{\partial \ell nT}{\partial \underline{r}} - \underline{\underline{B}}_i(W_i^2):\frac{\partial \underline{v}_o}{\partial \underline{r}} - n\sum_{h=1}^{\nu}\underline{C}_i^h\cdot\underline{d}_h \qquad \text{(B-11)}$$

where $\underline{W}_i = \underline{C}_i(m_i/2kT)^{1/2}$

Substituting this into Eq. (B-9) yields integral equations for the functions $\underline{A}_i$, $\underline{\underline{B}}_i$ and $\underline{C}_i^h$:

$$- \sum_{j=1}^{\nu} g_{ij}\, \sigma_{ij}^2 \iint f_i^{(o)}\, f_j^{(o)}\, (\underline{A}_i' + \underline{A}_j' - \underline{A}_i - \underline{A}_j)(\underline{w}_{ji} \cdot \underline{k})\, d\underline{k}\, d\underline{v}_j$$

$$= f_i^{(o)} \left(1 + \frac{12}{5} \sum_{j=1}^{\nu} \rho b_{ij} g_{ij}\, M_{ij} M_{ji}\right) \left(\frac{m_i C_i^2}{2kT} - \frac{5}{2}\right) \underline{C}_i \qquad \text{(B-12)}$$

and

$$- \sum_{j=1}^{\nu} g_{ij}\, \sigma_{ij}^2 \iint f_i^{(o)}\, f_j^{(o)}\, (\underline{\underline{B}}_i' + \underline{\underline{B}}_j' - \underline{\underline{B}}_i - \underline{\underline{B}}_j)(\underline{w}_{ji} \cdot \underline{k})\, d\underline{k}\, d\underline{v}_j$$

$$= f_i^{(o)} \left\{ \frac{m_i}{kT} \left(1 + \frac{4}{5} \sum_j M_{ji}\, \rho b_{ij} g_{ij}\right) \underline{C}_i^o \underline{C}_i \right.$$

$$\left. + \frac{2}{3} \left(1 + 2 \sum_j M_{ji}\, \rho b_{ij} g_{ij} - \frac{P}{nkT}\right) \left(\frac{m_i C_i^2}{2kT} - \frac{3}{2}\right) \underline{\underline{U}} \right\} \qquad \text{(B-13)}$$

and

$$- \sum_{j=1}^{\nu} \sum_{h=1}^{\nu} g_{ij}\, \sigma_{ij}^2 \iint f_i^{(o)}\, f_j^{(o)}\, (\underline{C}_i^{h'} + \underline{C}_j^{h'} - \underline{C}_i^h - \underline{C}_j^h) \cdot \underline{d}_h\, (\underline{w}_{ji} \cdot \underline{k})\, d\underline{k}\, d\underline{v}_j$$

$$= \frac{1}{n_i}\, \underline{d}_i \cdot \underline{C}_i f_i^{(o)} \qquad \text{(B-14)}$$

In connection with Eq. (B-14) it should be noted that the gradients $\underline{d}_i$ are not all independent (see below), so that it is not possible to equate terms for each of these gradients individually.

BII(i) Solution for $\underline{C}_i^h$. From Eq. (B-10) it follows that

$$\sum_i \underline{d}_i = 0 \tag{B-15}$$

Using this to eliminate the dependent gradient, $\underline{d}_k = -\sum_{i \neq k} \underline{d}_i$, in Eq. (B-14), and equating terms for individual gradients:

$$\sum_{j=1}^{\nu} g_{ij}\, \sigma_{ij}^2 \iint f_i^{(o)}\, f_j^{(o)} \{(\underline{C}_i^{h'} + \underline{C}_j^{h'} - \underline{C}_i^h - \underline{C}_j^h) - (\underline{C}_i^{k'} + \underline{C}_j^{k'} - \underline{C}_i^k - \underline{C}_j^k)\} (\underline{w}_{ji} \cdot \underline{k})\, d\underline{k}\, d\underline{v}_j = -\frac{1}{n_i} f_i^{(o)} (\delta_{ih} - \delta_{ik})\, \underline{C}_i \tag{B-16}$$

Expanding $\underline{C}_i^h$:

$$\underline{C}_i^h = C_{io}^h\, \underline{W}_i \tag{B-17}$$

Eq. (B-17) is substituted into (B-16), the equation multiplied by $\underline{W}_i$ and integrated over $\underline{v}_i$ to give:

$$\sum_j g_{ij} \{n_i n_j (C_{io}^h - C_{io}^k)[\underline{W}_i;\underline{W}_i]_{ij} + n_i n_j (C_{jo}^h - C_{jo}^k)[\underline{W}_j;\underline{W}_i]_{ij}\} = 3(\delta_{ih} - \delta_{ik}) \left\{\frac{kT}{2m_i}\right\}^{1/2} \tag{B-18}$$

The auxiliary condition yields the following relation among the $(C_{jo}^h - C_{jo}^k)$:

$$(C^h_{qo} - C^k_{qo}) = - \sum_{j \neq q} \frac{n_j m_j^{1/2}}{n_q m_q^{1/2}} (C^h_{jo} - C^k_{jo}) \qquad \text{(B-19)}$$

Using (B-19) in (B-18) gives:

$$\sum_{j \neq q} F_{ij} n_j \left[\frac{m_j kT}{2}\right]^{1/2} (C^h_{jo} - C^k_{jo}) = \delta_{ik} - \delta_{ih} \qquad \text{(B-20)}$$

$$(i,h=1,2,\cdots\nu)$$

where

$$F_{ij} = - \sum_{\ell} \frac{n_i n_\ell g_{i\ell} \delta_{ij}}{n\, n_j \mathcal{D}_{i\ell}} (m_j m_i)^{-1/2} + \frac{n_i g_{ij}}{n m_j \mathcal{D}_{ij}}$$

$$+ \sum_{\ell} \frac{n_i n_\ell g_{i\ell}}{n\, n_q \mathcal{D}_{i\ell}} (m_q m_\ell)^{-1/2} \left[\left[\frac{m_\ell}{m_i}\right]^{1/2} \delta_{iq} - \delta_{\ell q}\right]$$

and $\mathcal{D}_{i\ell}$ is the dilute gas binary diffusion coefficient:

$$\mathcal{D}_{i\ell} = \frac{3(m_i + m_\ell)kT}{16 m_i m_\ell n \Omega^{(1,1)}_{i\ell}}$$

The choice of q is arbitrary in general, and corresponds to the elimination of the mass flux for this component using the auxiliary condition.

BIII. MASS FLUX

There is no collisional contribution to the flux of mass, the entire flux being the kinetic part. The average peculiar velocity of j-molecules is

$$\langle \underline{C}_j \rangle = \frac{1}{n_j} \int f_j \underline{C}_j d\underline{v}_j$$

We now substitute Eq. (B-11) for ϕ_j, eliminate the dependent $\underline{d}_k$ by (B-15), and use the Sonine expansions and (B-17) up to the first term, to get

$$\langle \underline{C}_j \rangle = - \left(\frac{kT}{2m_j}\right)^{1/2} \left[\sum_{h \neq k} (C_{jo}^h - C_{jo}^k) n \, \underline{d}_h + a_{jo} \frac{\partial \ell n T}{\partial \underline{r}} \right] \qquad \text{(B-20)}$$

We now assume no external forces and mechanical equilibrium, so that $\underline{x}_j = 0$ and $\frac{\partial P}{\partial \underline{r}} = 0$. Using Eq. (B-10) for $\underline{d}_h$ in Eq. (B-20) gives:

$$\langle \underline{C}_j \rangle = - \left(\frac{kT}{2m_j}\right)^{1/2} \left\{ \sum_{h \neq k} (C_{jo}^h - C_{jo}^k) \sum_{\ell} \left[E_{h\ell} \frac{\partial n_\ell}{\partial \underline{r}} + n_h (\delta_{h\ell} + 2M_{h\ell} \, \rho b_{h\ell} g_{h\ell}) \frac{\partial \ell n T}{\partial \underline{r}} \right] + a_{jo} \frac{\partial \ell n T}{\partial \underline{r}} \right\} \qquad \text{(B-21)}$$

where $E_{h\ell} = \delta_{h\ell} + 2\rho b_{\ell h} g_{h\ell} + \sum_i n_h \rho b_{hi} \frac{\partial g_{hi}}{\partial n_\ell}$

However, in Eq. (B-21) the gradients of concentration are not all independent because they are related by the equation of state. From Eq. (B-8) with $\frac{\partial P}{\partial \underline{r}} = 0$,

$$\frac{\partial n_m}{\partial \underline{r}} = - \left\{ \sum_{\ell \neq m} \frac{P_\ell}{P_m} \frac{\partial n_\ell}{\partial \underline{r}} + \frac{1}{P_m} \sum_i \sum_\ell n_i (\delta_{i\ell} + 2M_{i\ell} \rho b_{i\ell} g_{i\ell}) \frac{\partial \ell n T}{\partial \underline{r}} \right\} \quad \text{(B-22)}$$

where $P_m = \sum_i \left(\delta_{im} + 2\rho b_{mi} g_{im} + \sum_k n_i \rho b_{ik} \frac{\partial g_{ik}}{\partial n_m} \right) = \sum_i E_{im}$

Eliminating the dependent concentration gradient from (B-21) using (B-22) gives:

$$\begin{aligned} \langle \underline{C}_j \rangle = & - \left(\frac{kT}{2m_j} \right)^{1/2} \sum_{\ell \neq m} \left\{ \sum_{h \neq k} (C_{jo}^h - C_{jo}^k) \left(E_{h\ell} - \frac{P_\ell}{P_m} E_{hm} \right) \right\} \frac{\partial n_\ell}{\partial \underline{r}} \\ & - \left(\frac{kT}{2m_j} \right)^{1/2} \left\{ a_{jo} + \sum_{h \neq k} (C_{jo}^h - C_{jo}^k) \sum_\ell \left[n_h (\delta_{h\ell} + 2M_{h\ell} \rho b_{h\ell} g_{h\ell}) \right. \right. \\ & \left. \left. - \frac{E_{hm}}{P_m} \sum_p n_p (\delta_{p\ell} + 2M_{p\ell} \rho b_{p\ell} g_{p\ell}) \right] \right\} \frac{\partial \ell n T}{\partial \underline{r}} \end{aligned} \quad \text{(B-23)}$$

The phenomenological equation for the mass flux is

$$\underline{J}_j = n_j m_j \langle \underline{C}_j \rangle = - \sum_{\ell \neq m} D_{j\ell} \, m_\ell \frac{\partial n_\ell}{\partial \underline{r}} - D_j^T \frac{\partial \ell n T}{\partial \underline{r}} \quad \text{(B-24)}$$

where $\underline{J}_j$ is the mass flux referred to the center of mass frame, $D_{j\ell}$ is the multicomponent diffusion coefficient on the center of mass frame, and D_j^T is the thermal diffusion coefficient on the center of mass frame. Comparing Eq. (B-23) and (B-24) gives the following equation for the diffusion coefficients:

$$D_{j\ell} = \frac{n_j m_j}{m_\ell} \left(\frac{kT}{2m_j}\right)^{1/2} \sum_{h\neq k} (C_{jo}^h - C_{jo}^k) \left(E_{h\ell} - \frac{P_\ell}{P_m} E_{hm}\right) \qquad \text{(B-25)}$$

In this equation $(C_{jo}^h - C_{jo}^k)$ is given by Eq. (B-20).

Equation (B-25) for the multicomponent isothermal diffusion coefficient can be simplified by using Eq. (B-20) to eliminate $(C_{jo}^h - C_{jo}^k)$. To do this, multiply Eq. (B-20) by $\left(E_{h\ell} - E_{hm} \frac{P_\ell}{P_m}\right)$ and sum over $h\neq k$, to get:

$$\sum_{j\neq q} F_{ij} n_j \left(\frac{m_j kT}{2}\right)^{1/2} \sum_{h\neq k} (C_{jo}^h - C_{jo}^k) \left(E_{h\ell} - E_{hm} \frac{P_\ell}{P_m}\right)$$

$$= \sum_{h\neq k} \left\{(\delta_{ik} - \delta_{ih}) \left(E_{h\ell} - E_{hm} \frac{P_\ell}{P_m}\right)\right\}$$

Using (B-25) to eliminate the sum over $h\neq k$ on the left-hand side gives

$$\sum_{j\neq q} F_{ij} m_\ell D_{j\ell} = E_{im} \frac{P_\ell}{P_m} - E_{i\ell} \qquad \text{(B-26)}$$

$$(i,\ell=1,\cdots\nu)$$

$$\ell\neq m$$

The choices of m and q are arbitrary; it is sometimes convenient to take m=q, but this is not always the case. In using (B-26) we note that

$$\sum_i F_{ij} = 0 \qquad j=1,2,\cdots\nu \qquad \text{(B-27)}$$

$$\sum_i \left(E_{im} \frac{P_\ell}{P_m} - E_{i\ell} \right) = 0 \qquad \ell=1,2,\cdots\nu \qquad \text{(B-28)}$$

References

1. Kolthoff, I. M., and Lingane, J. J., "Polarography", Interscience, New York (1952).

2. Ratcliff, G. A., and Holdcroft, J. G., Trans. Inst. Chem. Engrs. (London), 41, 315 (1963).

3. International Critical Tables 5, 15 (1929); Hitchcock, I., Ind. Eng. Chem. 29, 302 (1937).

4. Walker, R. D., Sixth Semi-Annual Report, February, 1969, NASA Research Grant, NGR 10-005-022.

5. Tiepel, E. W. and Gubbins, K. E., Technical paper presented at the National A.I.Ch.E. Meeting, August 1970, Denver, Colorado.

6. Debye, P. and McAulay, J., Z. Physik. 26, 22 (1925).

7. Long, F. A. and McDevit, W. F., Chem. Rev., 51, 119 (1952).

8. Harned, H. S. and Owen, B. B., "The Physical Chemistry of Electrolytic Solutions", 3rd Ed., Reinhold Publishing Corp., New York, N.Y., 1958; pp 80-88.

9. Conway, B. E., Ann. Rev. Phys. Chem. 17, 481 (1966).

10. Prauznitz, J. M., "Molecular Thermodynamics of Fluid-Phase Equilibria", Prentice-Hall, Englewood Cliffs, N. J. 1969 Chapter 8.

11. Temperley, H. N. V., Rowlinson, J. S., and Rushbrooke, G. S., (eds.), "Physics of Simple Liquids," North-Holland, Amsterdam, 1968.

12. Pierotti, R. A., J. Phys. Chem., 67, 1840 (1963).

13. Shoor, S. K. and Gubbins, K. E., J. Phys. Chem., 73, 498 (1969).

14. Masterton, W. L., and Lee, T. P., J. Phys. Chem., 74, 1778 (1970).

15. Tee, L. S., Gotoh, S. and Stewart, W. E., I. & EC Fundamentals, 5, 356 (1966).

16. Pierotti, R. A., J. Phys. Chem., 71, 2366 (1967).

17. Denbigh, K. G., Trans. Faraday Soc., 36, 936 (1940).

18. Conway, B. E., Desnoyers, J. E. and Smith, A. C., Phil. Trans. Roy. Soc., London, A256, 389 (1964).

19. Desnoyers, J. E., Peltier, G. E. and Joliceur, C., Can. J. Chem., 43, 3232 (1965).

20. Bockris, O'M. J., Bowler-Reed, J. and Kitchener, J. A., Trans. Faraday Soc., 47, 184 (1951).

21. Masterton, W. L., Lee, T. P. and Boyinton, R. L., J. Phys. Chem. 73, 2761 (1969).

22. Barker, J. A. and Henderson, D., J. Chem. Phys. 47, 4714 (1967).

23. Hirchfelder, J. O., Curtiss, C. F. and Bird, R. B., "Molecular Theory of Gases and Liquids", John Wiley and Sons, Inc., New York (1954).

24. Chapman, S. and Cowling, T. G., "The Mathematical Theory of Non-Uniform Gases", Cambridge Press 2nd edition (1953).

25. Wertheim, M., Phys. Review Letters 8, 321 (1963).

26. Thiele, E., J. Chem. Phys. 39, 474 (1963).

27. Lebowitz, J. L. and Rowlinson, J. S., J. Chem. Phys. 41, 133 (1964).

28. Jhunjhunwala, N., Boon, J. P., Frisch, H. L., and Lebowitz, J. L., Physica, 41, 536 (1969).

29. McLaughlin, E., J. Chem. Phys., 50, 1254 (1969).

30. McConalogue, D. J. and McLaughlin E., Molec. Phys. 16, 501 (1969).

31. Tham, M. K. and Gubbins, K. E., Technical paper presented at the National A.I.Ch.E. Meeting, August, 1970. Denver, Colorado.

32. Bhatia, K. K., M. S. Thesis, University of Florida (1965).

33. Vogel, W. M., Routsis, K. J., Kehrer, V. J., Landsman, D. A., and Tschinkel, J. G., J. C. E. D. 12, 465 (1967).

34. Walker, R. D., Third Semi-Annual Report, March, 1967. NASA Research Grant NGR 10-005-022.

35. Walker, R. D., Fifth Semi-Annual Report, May 1968. NASA Research Grant NGR 10-005-022.

36. Walker, R. D., Ninth Semiannual Report, November, 1970. NASA Research Grant NGR 10-005-022.

37. International Critical Tables, Vol. 4, McGraw-Hill Book Co., New York, N. Y. (1928).

38. Ravich, M. I. Borovaya, F. E. and Smernova, E. G., Zh. Neorg. Khim. 13, 1922 (1968).

39. Harned, H. S. and Owen, B. B., "The Physical Chemistry of Electrolytic Solutions", Reinhold, New York (1959).

40. Kamino, Y., and Masaaki, M., Denki Kagakn 36, 461 (1968).

41. Hooker Chemical Co., New York, Bulletin (1955).

42. Lang, E., Hooker Chemical Co., November, 1949.

43. Solvay Technical and Engineering Service Bulletin No. 15, published by Allied Chemical.

44. Cohen-Adad, R., Michand, M., Compt. Rend. 242, 2569 (1956).

45. Mashovets, V. P., Krumga, B. S., Debrou, I. A., and Matveena, R. P., Zh. Prikl. Khim. 38, 2342 (1965).

46. Merkel, F., Z. Ver Deut. Ing. 72, 113 (1928).

47. Marignac, Ann. Mines 12, 54 (1857).

48. Carbonnel, L., Rev. Chem. Minerale 1, 115 (1964).

49. Hill, A. E., and Miller, F. W., J. Am. Chem. Soc. 49, 669 (1927).

50. Forcrand, C. R., Acad. Sci. 148, 1732 (1909).

51. Poggiale, Ann. Chem. Phys. 9, 540 (1896).

52. Applebey and Leishman, J. Chem. Soc., 1605 (1932).

53. Hill, A. E., J. Am. Chem. Soc. 49, 968 (1927).

54. Toshi, J. S., Field, J. H., Benson, H. E. and Haynes, W. P., U. S. Bur. Mines. Rept. Invest. No. 5484 (1959).

55. Green, S. J. and Frattali, F. J., J. Am. Chem. Soc. 68, 1789 (1946).

56. Itkina, L. S., J. Appl. Chem., U.S.S.R. 26, 495 (1953).

57. Carbonnel, L., Bull. Soc. Chim., France 1990 (1959).

58. Hostalèk, Z., and Kasparova, S., Chem. Listy 50, 979 (1956).

59. Kamino, Y. and Miyaji, M., Denki. Kagaku 34, 914 (1966).

60. Klebanov, G. S. and Pinchuk, G. Ya., Zh. Prikl. Khim. 40, 2426 (1967).

61. Cohen-Adad, R. Michand, M., Said, J. and Rollet, A., Bull. Soc. Chim, France 356 (1960).

62. Diogenov, Kokl. Akad. Nauk. 78, 697 (1951).

63. Unzhakov, Dokl. Akad. Nauk. 87, 791 (1952).

64. Jaffray and Martin, C. R., J. Phys. Rad. 14, 553 (1953).

65. Klochko, M. A. and Godina, M. M. Russ. J. Inorg. Chem. 4, 964 (1959).

66. Horne, R. A., Banner, W. J. Sullivan, E. and Frysinger, G. R., J. Electrochemical Soc. 110, 1282 (1963).

67. Horne, R. A., Myers, B. R. and Frysinger, G. R., J. Chem. Phys. 39, 2666 (1963).

68. Hamann, D. and Strauss, W., Trans. Farad. Soc. 51, 1684 (1955).

69. Krmoyan, T. V., Inst. Organ. Khim., Evan 1957, 62-81 (Pub. 1962).

70. Manelyan, M. G., Kromoyan, T. V., Eganyan, A. G., and Kocharyan, A. M., Invest. Akak, Nauk. Armyan S.S.R. 9, 3 (1956).

71. Usanovich, M. I. and Sushkevich, T. I., J. Appl. Chem. U.S.S.R. 24, 657 (1951).

72. Hitchcock, L. B., McIlhenney, J. S., Ind. Eng. Chem. 27, 461 (1935).

73. Lorenz, M. R., Ph.D. dissertation, Rensselaer Polytechnic Institute, Troy, N. Y., 1960.

74. Good, W., Electrochimica Acta 12, 1031 (1967).

75. Chesnokov, N. A., Tr. Vses. Nanchu-Issled Inst. Metrol, 62, 44 (1962).

76. Sherwood, T. K., "Absorption and Extraction", New York, McGraw-Hill, 1937.

77. Mullowney, J. F., Oil and Gas J., February 10, 1958.

78. Zapfee, F., i.b.i.d., September 8, 1958.

79. Eichmeyer, A. G., Chemical Eng., August 25, 1958.

80. Graff, R. A., The Refining Engineer, May, 1958.

81. Buck, B. O. and Leitch, A. R. S., Proceed. Nat. Gasoline Association of America, April, 1958.

82. Benson, H. E., Field, J. H. and Haynes, W. P.,Chem. Eng. Prog. 52, 432 (1956).

83. Palo, R. O. and Armstrong, J. B., Proc. 33rd Ann. Meeting, Calif. Nat. Gasoline Association 59 (1958).

84. Makranczy, J. and Rusz, L., Veszpremi Vegyip Egyet Kozlem, A 10 (1-2), 37 (1966).

85. Hartmann, F. and Rock, G., Chim. Ingr. Tech. 37 (3), 214 (1965).

86. Plit, I. G., Zhur, Prick. Khim. 31, 186 (1958).

87. Roper, G. H., Chem. Engr. Sci. 4, 255 (1955).

88. Comstock, C. W. and Dodge, B. F., Industr. Engng. Chem. 29, 520 (1953).

89. Danckwerts, P. V., Pure and Appl. Chem. 10, 625 (1965).

90. Lewis, W. K. and Whitman, W. G., Ind. Eng. Chem. 16, 1215 (1924).

91. Hatta, S., Technol. Repts., Tohokn. Imp. U. 10, 119 (1932).

92. Hanratty, T. J., A.I.Ch.E. Journal, 2, 359 (1956).

93. Krevelan, D. W. van and Hoftijzer, P. J. Rec. Trav. Chim. Pay-Bas 67, 563 (1948).

94. Higbie, R., Trans. Am. Inst. Chem. Eng. 31, 365 (1965).

95. Nijsing, R. A. T. O., Proef. Tech. Hog. (1957).

96. Morris, G. A. and Jackson, J., Absorption Towers, London, Butterworth, 1951.

97. Matsnyama, T., Mem. Fac. Eng. Kyoto Univ. 15, 142 (1953).

98. Gianetto, A. and Demalde, P., Ann. Chim. (Rome) 53, 493 (1963).

99. Gianetto, A. and Demalde, P., i.b.i.d. 53, 521 (1963).

100. Gianetto, A. and Saracco, G. B., Ing. Chim. Ital. 2, 10 (1966).

101. Hatti, S., Technol. Repts. Tôhoku Imp. Univ., 8, 1 (1928-29).

102. Jenny, F. J., Thesis, Massachusetts Institute of Technology 1936.

103. Tepe, J. B., and Dodge, B. F., Trans. Am. Inst. Chem. Engrs., 39, 255 (1943).

104. Spector, N. A. and Dodge, B. F., i.b.i.d., 42, 827 (1946).

105. Brunner, E., Z. Phys. Chem. 47, 67 (1904).

106. Weber, H. C. and Nilsson, K., Ind. Eng. Chem. 18, 1070 (1926).

107. Davis, H. S. and Crandall, G. S., J. Am. Chem. Soc., 52, 3757 (1930).

108. Blum, H. A., Stutzman, L. F. and Dodds, W. S., Ind. and Eng. Chem. 44, 2969 (1952).

109. Kobayashi, T., Inone, H. and Yogi. S., Kogyo Kagaku Zasshi 70, 126 (1967).

110. Hikita, H. and Asai, S., Bull. Univ. Osaka Prefect. Ser. A 9, 81 (1961).

111. Nijsing, R. A. T. O., Hendriksz, R. H. and Kramers, H., Chem. Eng. Sci. 10, 88 (1959).

112. Lebowitz, J. L., Phys. Rev., 133, A895 (1964).

113. Lebowitz, J. L., and Rowlinson, J. S., J. Chem. Phys. 41, 133 (1964).

114. Mansoori, G. A., Carnahan, N. F., Starling, K. E., and Leland, T. W., J. Chem. Phys., in press.

115. Alder, B. J., and Wainwright, T. E., J. Chem. Phys. 33, 439 (1960).

116. Ree, F. H., and Hoover, W. G., J. Chem. Phys. 46, 4181 (1967).

117. Rice, S. A., Kirkwood, J. G., Ross. J., and Zwanzig, R. W., J. Chem. Phys. 31, 575 (1959).

118. O'Toole, J. T., and Dahler, J. S., J. Chem. Phys., 32, 1487 (1960).

119. Hollinger, H. B., and Curtiss, C. F., J. Chem. Phys., 33, 1386 (1960).

120. Andrews, F. C., J. Chem. Phys., 35, 922 (1961).

121. Dymond, J. H., and Alder, B. J., J. Chem. Phys., 48, 343 (1968).

122. Dymond, J. H., and Alder, B. J., J. Chem. Phys., 52, 923 (1970).

123. Chapman, S., and Cowling. T. G., "The Mathematical Theory of Non-Uniform Gases", Chapter 16, (Cambridge University Press, Cambridge, 1952).